ERDC/CRREL TR-18-12

US Army Corps of Engineers®
Engineer Research and Development Center

ERDC
INNOVATIVE SOLUTIONS for a safer, better world

Ice Forces along the Missouri River Shoreline of the Lower Brule Sioux Tribe Lands

Jeremy Giovando, Robert B. Haehnel, Timothy Baldwin, and Steven F. Daly

July 2018

Cold Regions Research and Engineering Laboratory

The U.S. Army Engineer Research and Development Center (ERDC) solves the nation's toughest engineering and environmental challenges. ERDC develops innovative solutions in civil and military engineering, geospatial sciences, water resources, and environmental sciences for the Army, the Department of Defense, civilian agencies, and our nation's public good. Find out more at www.erdc.usace.army.mil.

To search for other technical reports published by ERDC, visit the ERDC online library at http://acwc.sdp.sirsi.net/client/default.

ERDC/CRREL TR-18-12
July 2018

Ice Forces along the Missouri River Shoreline of the Lower Brule Sioux Tribe Lands

Jeremy Giovando, Robert B. Haehnel, Timothy Baldwin, and Steven F. Daly

U.S. Army Engineer Research and Development Center (ERDC)
Cold Regions Research and Engineering Laboratory (CRREL)
72 Lyme Road
Hanover, NH 03755-1290

Final Report

Prepared for U.S. Army Corps of Engineers, Omaha District
1616 Capitol Ave., Ste. 9000
Omaha, NE 68102

Under Under Civil Works General Investigation funding 3121, “Lower Brule Reservoir Ice Erosion Study”

Abstract

Significant erosion along Lake Sharpe reservoir has occurred since the reservoir was formed in the 1960s. A major contributor to the shoreline erosion is ice shove, which is most severe when thick ice cover on the reservoir is combined with large wind events. One of the areas of highest concern for erosion induced by ice shove is located on the Lower Brule Sioux Reservation in South Dakota. Critical infrastructure is at risk for the Lower Brule Sioux Tribe as continual erosion occurs. This analysis estimates the ice shove forces due to wind and the water current along 10 miles of shoreline adjacent to the reservation. Additionally, this report discusses shoreline erosion mitigation measures.

Contents

Figures and Tables

Figures

Tables

Preface

This study was conducted for the U.S. Army Corps of Engineers (USACE), Omaha District (NWO), under Civil Works General Investigation funding 3121, "Lower Brule Reservoir Ice Erosion Study." The technical monitor was Ms. Gwyn Jarrett, USACE-NWO.

The work was performed by the Terrain and Ice Engineering Group and the Water Resources / Geographic Information System (GIS) Group of the Remote Sensing/GIS Center of Expertise (CEERD-RS) and the Terrestrial and Cryospheric Sciences Branch of the Research and Engineering Division (CEERD-RR), U.S. Army Engineer Research and Development Center, Cold Regions Research and Engineering Laboratory (ERDC-CRREL). At the time of publication, Mr. Stephen D. Newman was lead for the Terrain and Ice Engineering Group; Mr. Bryan E. Baker was lead for the Water Resources/GIS Group; Mr. David C. Finnegan was Chief, CEERD-RS; Dr. John Weatherly was Chief, CEERD-RRG; and Mr. J. D. Horne was Chief, CEERD-RR. The Deputy Director of ERDC-CRREL was Mr. David B. Ringelberg, and the Director was Dr. Joseph L. Corriveau.

COL Ivan P. Beckman was Commander of ERDC, and Dr. David W. Pittman was the Director.

Acronyms and Abbreviations

AASHTO	American Association of State Highway and Transportation Officials
AFDD	Accumulated Freezing Degree-Days
CRREL	Cold Regions Research and Engineering Laboratory
ERDC	U.S. Army Engineer Research and Development Center
FDD	Freezing Degree-Days
GEV	Generalized Extreme Value
GIS	Geographic Information System
GPD	Generalized Pareto Distribution
HEC-DSS	Hydrologic Engineering Center's Data Storage System
HEC-SSP	Hydrologic Engineering Center's Statistical Software Package
LBST	Lower Brule Sioux Tribe
LP3	Log-Pearson III
MRBWM	Missouri River Basin Water Management
NCDC	National Climatic Data Center
NIST	National Institute of Standards and Technology
NWO	USACE Omaha District
POT	Peaks-over-Thresholds
RM	River Mile
TDD	Thawing Degree-Days
USACE	U.S. Army Corps of Engineers

Unit Conversion Factors

Multiply	By	To Obtain
cubic feet	0.02831685	cubic meters
degrees (angle)	0.01745329	radians
degrees Fahrenheit	(F-32)/1.8	degrees Celsius
feet	0.3048	meters
inches	0.0254	meters
kip	4448.2216	newtons
miles (nautical)	1,852	meters
miles (U.S. statute)	1,609.347	meters
miles per hour	0.44704	meters per second
one thousand cubic feet per second	28.31685	cubic meters
pounds (force)	4.448222	newtons
pounds (force) per square foot	47.88026	pascals
pounds (force) per square inch	6.894757	kilopascals

Executive Summary

The combination of wind events and ice conditions for Lake Sharpe can vary drastically from year to year. This is reflected in both the range of wind speed magnitudes and the range of maximum annual ice thickness values. The wind speed frequency analysis indicated that relatively high 1-hour events are possible during the periods of ice cover. January and February wind speeds range from approximately 43 mph for the 10-year return period to approximately 47 mph for the 50-year return period. The wind speed magnitudes do increase in March and April to more than 50 mph for the 50-year return period. This is generally the timeframe for maximum ice thickness, which results in potentially large ice forces on many shoreline locations on Lake Sharpe. The shoreline locations near the treatment ponds for the Lower Brule Sioux Tribe (LBST) community have the compounding issue that both maximum wind speed and water velocity direction in the reservoir are coincident, thus resulting in an increase in potential environmental forces on the ice sheet and even greater erosion potential due to ice shove in these locations.

Because of the relatively low water velocity and small operating range of Lake Sharpe, the heat transfer mechanics are going to be the primary control for ice formation processes. Although there were limited observations for ice thickness at Lake Sharpe, the available information from the LBST did help in the model validation. The average annual maximum ice thickness computed was approximately 18 in. The annual maximum date was between mid-February and mid-March, based on the model results.

The ice thickness estimates indicate that crushing force of the ice is much greater than environmental forces that have been observed. Although the crushing strength of the ice decreases significantly in later winter when the maximum annual ice thickness occurs, the estimated strength is still much greater than the combined environmental forces. This results in the shoreline erosion being only a function of the environmental forces anytime when ice is present. Using the 50-year wind speed values, the combined (wind and water current) force for the Lake Sharpe shoreline ranges from approximately 100 lb_f/ft at River Mile 999.1 to 800 lb_f/ft at River Mile 992.5. The measures considered for Lake Sharpe will need to be evaluated by location based on this large range of ice forces.

Shoreline erosion mitigation measures should consider ice forces. The measures may consist of a combination of riprap and offshore breakwater structures, depending on the estimated ice forces and criticality of the infrastructure near the shoreline. The stone sizing criteria for ice shove are based on laboratory experiments that indicate that a median stone size (D_{50}) of 36–54 in. would result in a 15% chance of failure for the riprap. This design guidance should be combined with any information from current field installations in the region to develop a cost-effective, long-term solution.

1 Introduction

1.1 Background

Shoreline erosion on Lake Sharpe, the reservoir created by Big Bend Dam on the Missouri River in South Dakota, has been an issue since the reservoir was created in the early 1960s. In more recent decades, the rate of shoreline retreat has become alarming with some estimates at approximately 7.5 to 21 ft/year (Louis Berger 2017). The loss of shoreline along the reservoir has both recreational and economic impacts. The recreational impacts include loss of picnic facilities and playground equipment. The economic consequences of the shoreline erosion are even more dramatic, including loss of agricultural land and a constant effort to protect other important infrastructure from erosion.

The area analyzed in this study is part of the Lower Brule Sioux Tribe Reservation and is on the southern shoreline of the "big bend" of the Missouri River (Figure 1). Specifically included in this analysis are river miles (RM) 992.1 through 1001.2 with an additional location at RM 1017.9 requested by the U.S. Army Corps of Engineers (USACE) Omaha District (NWO). One of the locations of most concern is the wastewater treatment facility for the Lower Brule Sioux Tribe, located at RM 992.9. Relocating the treatment facility would be a multi-million dollar project, assuming there is a technically and socially acceptable site for relocation. Understandably, without a functioning wastewater treatment facility, sustaining the Lower Brule community in its present location will be difficult.

Shoreline erosion on Lake Sharpe apparently is a two-step process (Harwood 1993; Thompson 2013). The first step occurs when the wintertime ice cover on Lake Sharp is driven by the wind up onto the shoreline. These ice shoves peel back the sod and lay open the bare soil of the river bank. Then, in the second step, wave action during open water erodes and carries away the exposed soil.

Figure 1. Study location.

The ice shove impacts to Lake Sharpe shoreline are significant and result in shoreline sloughing into the reservoir, which is ultimately eroded by wave action (Figure 2). In addition, in areas where the ice shove does not result in sloughing of material directly into the reservoir, the land becomes unusable for other purposes because of the resulting mounds (Figure 3). Shoreline erosion resulting from ice shove and wind action has reached critical levels. Originally, the town of Lower Brule was approximately 1000 ft from the shoreline; but today, important infrastructure like the wastewater treatment facilities is approximately 100 ft from the shoreline (Louis Berger 2017). Given the current erosion rates of up to 21 ft/year, the viability of this infrastructure is limited without immediate mitigation measures. Shoreline protection structures are required to protect against wave action, but these protection structures will be exposed to ice shoves and need to be designed to resist the applied ice forces.

Figure 2. Ice shoves along the Lake Sharpe shoreline.

Figure 3. Soil layers pushed up by ice.

1.2 Objectives

The goal of this study was to determine the design force levels that ice shoves occurring on Lake Sharpe can exert on shoreline protection structures. We calculated the design force levels for a range of expected return periods, 1.01 to 100 years, for every month that ice normally is in place on the Missouri River (December through April). We then estimated the forces at 37 analysis points along the Lake Sharp shoreline, which equated to one point every 1640.4 ft (500 m) along approximately 10 miles of

shoreline. The shoreline length includes several important locations for the Lower Brule Sioux Tribe Community that are subject to erosion.

1.3 Approach

The ice shove forces are created by the wind blowing over a continuous fetch of ice cover. The river current may also contribute to the force, depending on the alignment of the wind direction and water current direction. However, the ice shove force is not unlimited. It cannot exceed the crushing force developed by the ice cover. Therefore, it is important to estimate the crushing force of the ice cover to determine if the calculated shove force based on wind and water current exceeds the crushing strength of the ice.

We calculated the ice shove force resulting from the wind velocity based on the wind speed, the wind direction, and the ice-cover fetch length aligned with the wind direction. To perform these calculations, we determined the fetch lengths for 16 directions (every 22.5°) at each analysis point starting with north at 0°. The annual return period of the ice shove force was set to the annual return period of the applied wind velocity. We also estimated the ice shove forces resulting from the Lake Sharpe water current acting on the ice cover and assumed that the water current acted parallel to the center line of the channel. The velocity associated with the 95th percentile monthly flow was used to estimate the magnitude of the water current. Based on engineering judgment, reasonable estimates of the ice-cover geometry were assumed to approximate the dimensions and orientations of large ice masses that could collide with the shore. Shoreline locations along the outside of channel bends were the most susceptible to ice shoves caused by water currents.

Next, we combined the ice shove force vectors resulting from the wind and water current to determine the overall ice shove force at each of the 37 analysis points for each month for each direction. At each analysis point, we selected the direction with the maximum ice force for a given annual return period. The result was an ice shove force magnitude and direction for each annual return period for each month at all 37 analysis points. Finally, we compared the magnitude of the ice shove force to the crushing force that the ice cover could apply. To estimate the ice-cover crushing force, we first estimated the ice thickness and effective ice crushing strength. The effective ice crushing strength was estimated based on experience and the climatology of the area. We modeled the daily ice thickness

using 54 years of available air temperature data and then analyzed this data to develop the annual maximum ice thickness frequency distribution.

The annual maximum ice thickness was used along with stone sizing criteria from laboratory experiments to recommend potential riprap sizes for shoreline erosion mitigation measures. This report also presents alternatives to using riprap as the only mitigation measure.

Following this introduction, section 2 summarizes the environmental data that was used as inputs to the analysis. Note that while all calculations were made using metric units, we report many of the measurements in U.S. customary units for ease. Subsequent sections discuss the ice thickness model formulation and results. Finally, the report concludes by discussing the ice shove force calculation methods and results. Several appendices provide supporting material, including details of the results from the wind, ice thickness, and ice shove force calculations.

2 Environmental Data

The data used for this study came from two primary sources. NWO provided the reservoir and streamflow data, and the climate information (i.e., wind and air temperature) was sourced from the National Climatic Data Center (NCDC). NWO engineers reviewed the wind data from NCDC for outlier values, and the wind analysis presented in this report incorporates their results. Figure 4 summarizes the stations and data periods used for analysis in this study.

Figure 4. Summary of study data.

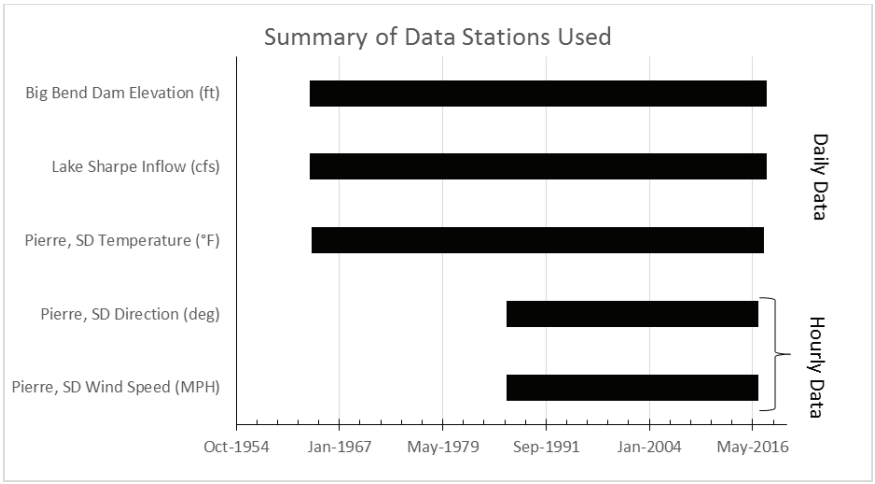

2.1 Water levels and flow data

The monthly average inflow to Lake Sharpe typically ranges from approximately 15 kcfs* to 30 kcfs during the December through April period (Figure 5). On a daily basis, the inflow can be quite variable due to power-peaking releases from the Oahe Dam upstream. It should be noted for this analysis that the water velocity is most important and that, due to the backwater conditions creation by Big Bend Dam, the variability in discharge translates to only minor velocity variations (Appendix F).

The thickness of ice and location can depend on the water velocity and depth of water. For Lake Sharpe the normal operating range is approximately 1–2 ft (Figure 6). For this study, we assumed that differences in water depth would not significantly impact the ice formation on the reser-

* Thousand cubic feet per second

voir. The upstream Oahe Dam, has a power plant release capacity of approximately 60 kcfs. At this discharge, the average velocities in Lake Sharpe range from 0.2 to 0.3 ft/s (Appendix F).

Figure 5. Lake Sharpe monthly summary hydrograph.

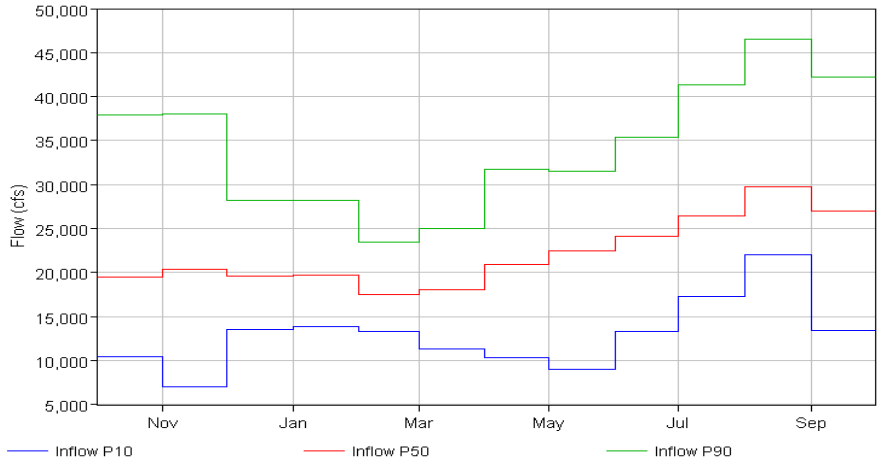

Figure 6. Lake Sharpe daily elevation summary.

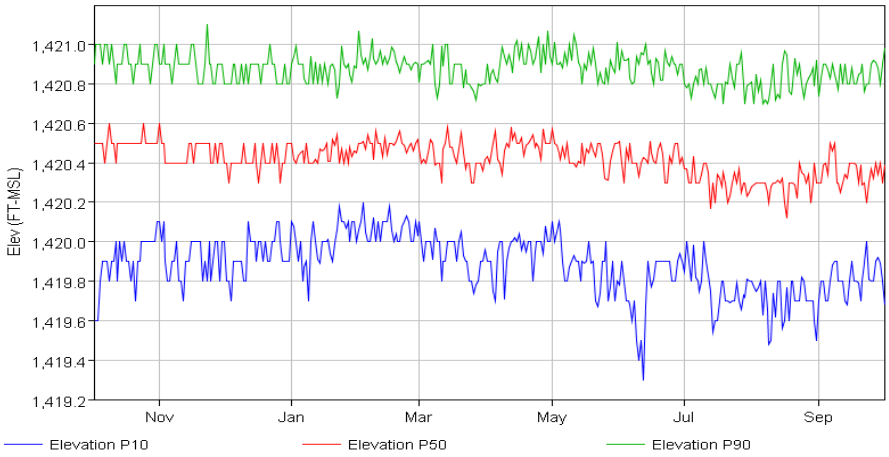

2.2 Air temperature data

This analysis used the Pierre, South Dakota, Regional Airport temperature data. The dataset was downloaded from the NCDC for the period of October 1962 through September 2017. We computed the average daily temperature from the simple average of the minimum and maximum temperature values in the dataset. Figure 7 provides a summary plot of the temperature cycle.

Note that we did not use discharge temperature from Oahe Dam in the ice analysis and instead assumed that the reach between Oahe Dam and the

current study location (approximately 70 river miles) is sufficiently long enough that air temperature would be the primary control on ice growth.

Figure 7. Pierre, South Dakota, Regional Airport daily average temperature summary

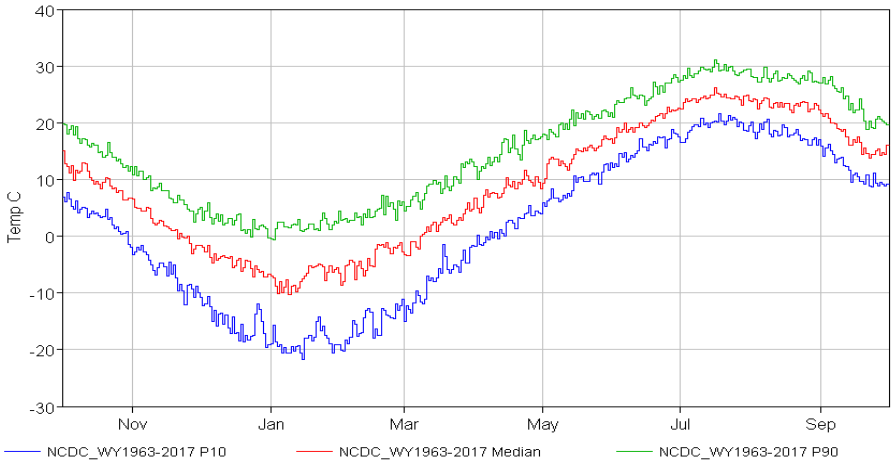

2.3 Ice data

There were limited ice thickness observations available for Lake Sharpe. However, there is a nearly complete record of annual ice-cover duration for the reservoir. This record consists of the freeze-up and breakup dates from water year 1963 through 2017. There are actually two ice-cover duration records, one that is kept by the USACE Missouri River Basin Water Management (MRBWM) staff and the other by the Lower Brule Sioux Tribe (LBST). The LBST dataset consists of observations from water year 2001 through 2016. Both of these observed datasets were used to calibrate the ice model for the reservoir and are provided in Appendix A.

In addition to ice-duration information, the LBST provided some thickness information that was based on records from local ice fishermen. Although the data collection methods used for this information cannot be verified, the local source is considered reliable and proved consistent with the model calibration using the ice-cover duration information. The most important ice thickness information is the average annual maximum values, which we used in the model validation. LBST estimated that the average annual maximum thickness for the last 8–10 years was approximately 18 in. The maximum annual thickness was approximately 42 in. in 1977. Appendix B provides the full context of the information from the LBST.

2.4 Wind data

This analysis used the hourly wind speed and direction data for the Pierre, South Dakota, Regional Airport, which were retrieved from the NCDC. The dataset initially contained irregular time steps (i.e., multiple readings per hour or inconsistent time intervals for hourly values). To facilitate analysis of the data, the "irregular" time series was converted to "regular" in HEC-DSS (the USACE Hydrologic Engineering Center's Data Storage System) and snapped to the nearest hour. There are several advantages of going through this process, but the most apparent is that only one value of wind speed and direction is assigned to an individual date and hour for the period analyzed. Although small amounts of data are lost with this processing strategy, the overall impacts to the results are minimal since sub-hourly wind speed variations would not have a significant impact on ice run-up on the shoreline.

Before beginning any ice force analysis, it is often helpful to review the wind speed data. To facilitate this review, we derived the daily wind speed from the hourly information. Figure 8 summarizes the median daily wind speed magnitude. The median wind speed values generally increase in the spring season compared to the rest of the year. However, during the ice-cover months (December through April), there can be relatively high magnitudes of wind speed based on the 90th percentile values. Evaluating the maximum daily wind speed values reinforces this conclusion (Figure 9). During ice-cover months, the maximum daily wind speed values are considerably greater when compared to the summer and fall seasons. The wind speed data summary provides empirical evidence that wind forces are certainly a contributing factor to the ice shove observed on Lake Sharpe.

Figure 8. Pierre, South Dakota, Regional Airport daily median wind speed summary.

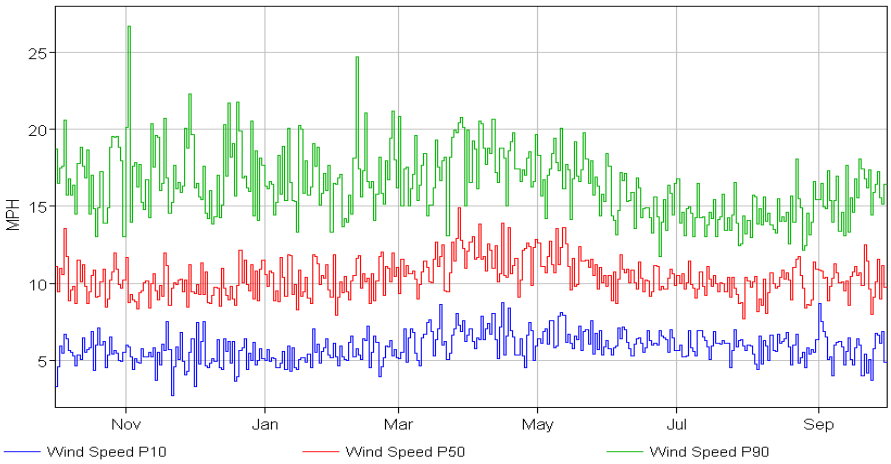

Figure 9. Pierre, South Dakota, Regional Airport maximum daily wind speed summary.

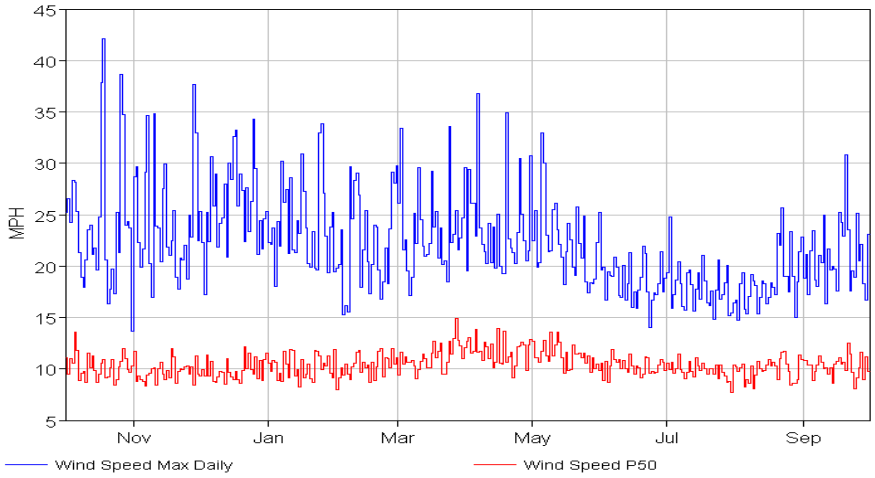

3 Ice Shove Force Analysis

The ice shove forces are created by the environmental forces, specifically wind and water drag, acting on the ice cover. The wind and water flow vary from month to month during the period when the ice cover is in place. We therefore decided to calculate the ice shove forces separately for each month. As the goal was to determine the design forces to be used in the development of shoreline protection, we calculated the ice shove forces over a range of annual return periods for December through April. The design ice shove forces were calculated by

$$f_{shove}(m, x, R),$$

where $f_{shove}(m, x, R)$ is the design ice shove force for month m, at analysis point x, and with annual return period R.

The ice shove forces created by the wind and water current are necessary to estimate f_{shove}. The force per unit width created by the wind drag is

$$f_{wind}(m, x, \emptyset, \mathrm{R}) = C_{D-wind}\rho_{air}U^2_{wind}(m, x, \phi, R)L(x, \phi), \quad (1)$$

where

$f_{wind}(m, x, \phi, R)$ = the ice shove force due to the wind per unit width acting during the month m, at analysis point x, with a direction angle ϕ, and an annual return period of R;
$C_{D\text{-}wind}$ = the drag coefficient for the air over the ice surface;
ρ_{air} = air density;
$U_{wind}(\mathrm{m,x},\phi, R)$ = wind velocity magnitude with a direction angle ϕ and an annual return period R; and
$L(x, \phi)$ = fetch length with a direction angle ϕ from analysis point x over which the wind blows.

The force created by the water drag is

$$f_{water}(m, x, \gamma) = C_{D-water}\rho_{water}U^2_{water}(m, \theta)L(x, \gamma), \quad (2)$$

where

$f_{water}(m, x, \gamma)$ = the per unit width ice shove force due to the current during month m, at analysis point x, and with a direction angle γ;
$C_{D\text{-}water}$ = the drag coefficient for the water flowing under the ice cover;
ρ_{water} = water density;
$U_{water}(m, \gamma)$ = water velocity magnitude with a direction angle γ; and
$L(x, \gamma)$ = fetch length with a direction angle θ from analysis point x over which the water acts.

(Note that both ϕ and γ are angles relative to north [0°] with positive angles in a clockwise direction.)

The ice shove force due to the wind, f_{wind}, was assigned the same return period as the wind; but f_{water}, the ice shove force due to the water current, was not assigned a return period. This was due to the relatively small variation in the water flow during the months that the ice cover was in place, as shown in Figure 5. The location of this reservoir section of Lake Sharpe is immediately upstream of Big Bend Dam and downstream of Oahe Dam, which provides a relatively stable flow and stage regime. The analysis included the variation of the Missouri River flow from month to month, but the return period of design ice shove forces was determined only by the return period of the wind velocity magnitude along each direction angle.

The total ice shove force was then found at each analysis point x, for each month m, for each direction angle ϕ, and for each annual return period R, as

$$f_{shove-\phi}(m, x, \phi, R) = sum\{f_{wind}(m, x, \phi, R), f_{water}(m, x, \gamma)\},$$

where the brackets, {}, imply vector addition. Given that the wind can blow from any direction but that the water current must always be parallel to the channel centerline, ϕ and γ may or may not be equal. The vector addition process is described in section 3.4.3.

The final ice shove force value was then found as the maximum force over all the direction angles as

$$f_{shove}(m, x, R) = max\left|f_{shove-\phi}(m, x, \phi, R)\right| \text{ for } 0° \leq \phi \leq 360°.$$

Finally, we checked the above equation to determine that $f_{shove}(m, x, R)$ does not exceed the strength of the ice cover. The ice strength is determined by the force level required to crush the ice cover, f_{crush}:

$$f_{shove}(m, x, R) < f_{crush} \cong tS,$$

where S is the effective crushing strength of the ice and t is the ice thickness. The crushing strength may depend on other factors such as the relative width of the structure being impacted. The effective crushing strength of the ice, S, can vary throughout the winter. It generally tends to decline near the end of the ice season as the ice cover deteriorates from sunlight and through other forms of melting.

The subsequent sections describe the data inputs, methods, and final results for the ice shove force calculations.

3.1 Fetch length analysis

We applied the above equations to the shoreline along Lake Sharp by first creating a series of analysis points 1640.4 ft (500 m) apart along the shoreline, starting near RM 992, in the vicinity of the Lower Brule Sioux Tribe community. The shoreline was digitized based on recent aerial imagery (USGS 2013). The analysis points started at RM 992.1 and extended upstream to RM 1001.2 for a total of 36 points, which were labeled with the closest river mile. One additional shore point was located upstream of the main study area at RM 1017.9 because an existing erosion mitigation structure is located in that area. Therefore, NWO was interested in getting ice shove forces in a location where shoreline measures have already been implemented.

We then calculated fetch lengths for each analysis point by extending a fetch line every 22.5° between 0° (north) and 337.5°. The fetch lengths were calculated as the distance from the analysis point origin to the position where the fetch line first intersected either bank of the digitized shoreline (Seers 2017). Any fetch lengths less than 2 m were set to 0. Figure 10 shows an example of calculated fetch lengths for a single analysis point.

Figure 10. Fetch lengths calculated at Analysis Point 992.9.

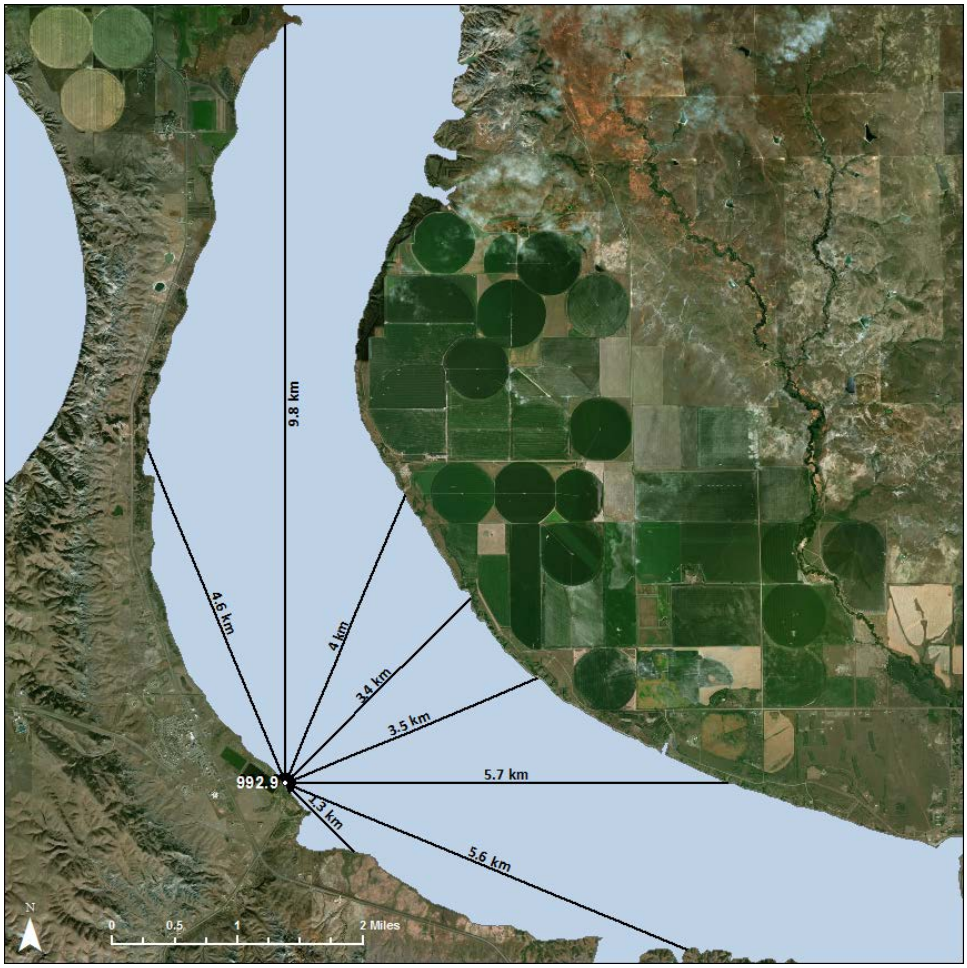

3.2 Wind analysis

As shown in previous sections, the primary force exerted on the Lake Sharpe ice cover is from wind. Based on this information, it was important to understand the current wind speed magnitudes for various return periods. The results of this analysis will be used in subsequent sections to compute the wind drag force on the ice cover, which will then allow estimation of the ice shove forces.

3.2.1 Wind direction

We created monthly and annual wind rose plots by using the Pierre Regional Airport data and 22.5 directional degree bin sizes. The bin size of 22.5° resulted in sixteen (360/22.5) directional ordinates, which is consistent with the previously published wind speed and direction analysis for Lake Sharpe (Nelson 1988). Since NCDC specifies wind direction using compass directions (e.g., 360 = true north, 180 = south, 270 = east, etc.),

each bin was populated using the reported directions from the Pierre dataset. For this analysis, the bins are populated with all observations within the specified range, including data equal to the upper bounding value. This results in values greater than the lower bound up to the upper bound being grouped together. The only exception to how observations were grouped was the first and last bins, which ranged from 0° to 360° and 337.5° to 360°, respectively. In polar coordinates, 360° and 0° are the same direction; therefore, analyzing wind data from the north takes special consideration. We assumed that any reported wind direction of 360° would be included in the first bin (0°–22.5°). It is important that these values (0° and 360°) are grouped consistently, otherwise there may be a bias introduced when determining the block maxima values used for the frequency analysis.

In general in this study, the highest frequency directions are from the northwest and southeast. The large-magnitude wind events do vary by month and have been observed coming from the northerly direction during the period of maximum ice thickness (March). This is important since the longest fetch length for the shoreline near the treatment ponds is along a north to south axis. Figures 11–16 show the wind rose plots for the annual tally and for December through April. These plots were generated using the "openair" R package (Carslaw 2018).

Figure 11. Pierre, South Dakota, Regional Airport annual wind rose.

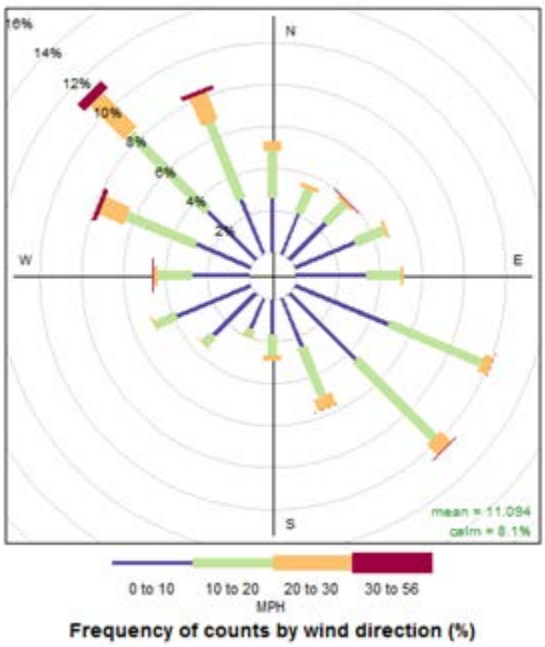

Figure 12. Pierre, South Dakota, Regional Airport December wind rose.

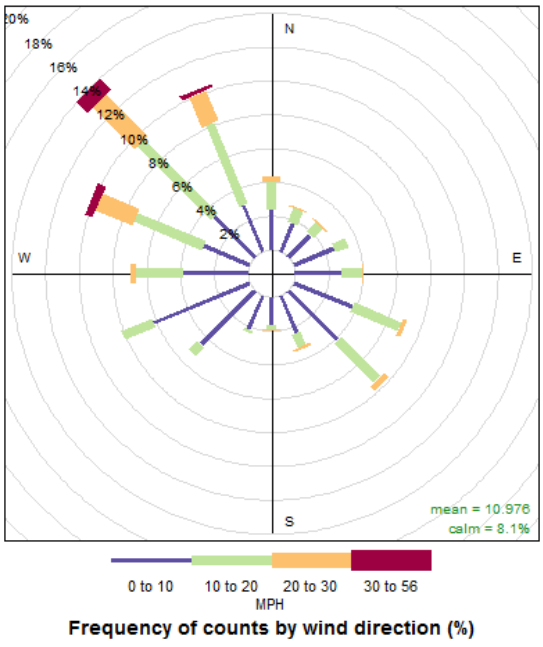

Figure 13. Pierre, South Dakota, Regional Airport January wind rose.

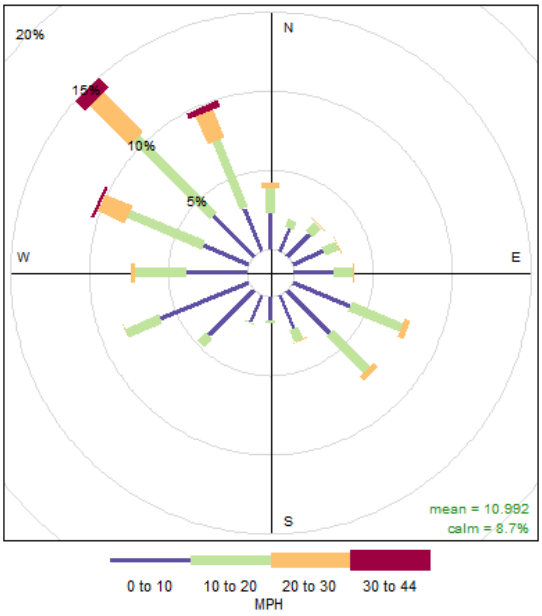

Figure 14. Pierre, South Dakota, Regional Airport February wind rose.

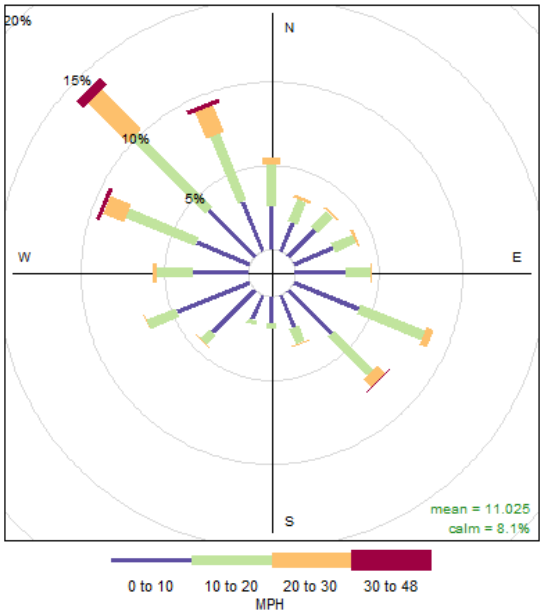

Figure 15. Pierre, South Dakota, Regional Airport March wind rose.

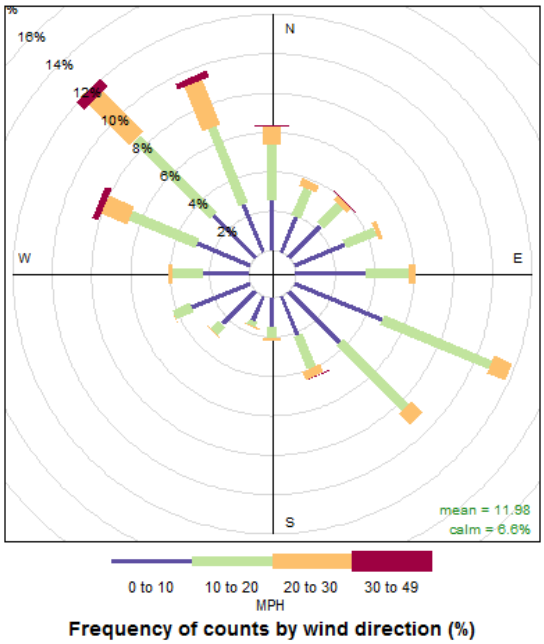

Figure 16. Pierre, South Dakota, Regional Airport April wind rose.

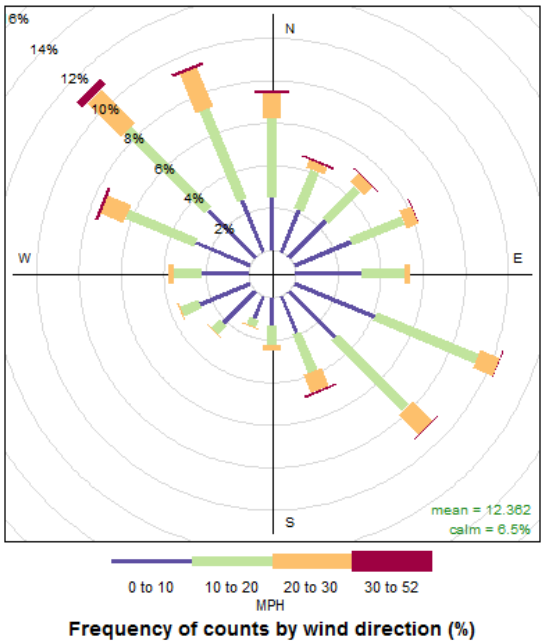

3.2.1 Wind magnitude

We calculated the return period for both monthly and annual block maxima (i.e., maximum 1-hour wind speed for each time block). As previously mentioned, the monthly data were subdivided by wind direction (16 bins); and the block maxima for each of these groups was also used in the frequency analysis (i.e., maximum 1-hour wind speed for each time block and direction). This allowed calculations to be performed for coincident wind speed and fetch lengths by direction ordinates since the fetch directions were also based on a bin size of 22.5°.

Performing a frequency analysis of any variable is generally based on fitting an assumed distribution to the observations. This is certainly the same for frequency analysis of wind speed data; however, the guidance on which statistical distribution to use is much less prescribed when compared to streamflow. Therefore, a literature search and statistical distribution analysis was performed using the Pierre wind speed data.

Literature has shown that using a two-parameter Weibull distribution of mean wind speed value produces the lowest error model (Justus et al. 1977). In our analysis, the mean wind speed values were not of primary concern because the less frequent wind events coinciding with ice cover on Lake Sharpe are going to maximize the ice shove forces along the shoreline. Focusing on fitting distributions to extreme wind speeds resulted in a much larger range of potential statistical distribution families in the literature. Palutikof et al. (1999) compared results using the Generalized Extreme Value (GEV) distribution and the generalized Pareto distribution (GPD) with a peaks-over-thresholds (POT) data-filtering technique. They state that using a GEV Type I (Gumbel) distribution with wind extremes is the most common approach. However, Palutikof et al. (1999) demonstrated that using a POT with GPD can be advantageous because more of the data is used since block maxima are based on events and not calendar periods. Another study by the National Institute of Standards and Technology (NIST) compares several statistical distributions using POT data filtering. The NIST report concluded that the reverse Weibull distribution (often referred to as the inverse Weibull) was the best choice when evaluating climate data from several locations across the United States (Simiu and Heckert 1995).

To determine which statistical distribution would best fit the Pierre Regional Airport wind speed data, we performed an analysis using the 1987–

2016 hourly data. The results of this analysis show that both the inverse Weibull and the 3-parameter Gamma distributions adequately represent the Pierre wind speed data using both a 20 and 30 mph threshold (Figure 17 and Figure 18). The inverse Weibull performed as expected based on the information from the literature review. In contrast, the 3-parameter Gamma, also known as the Pearson Type III distribution, was not often mentioned in the literature and was not one of the distributions evaluated in the NIST study. However, from these results we decided that using the 3-parameter Gamma or Pearson Type III distribution would have several advantages, including well-documented quantiles and published software that can be used to compute the suite of return periods for the wind speed data.

Pearson Type III distribution can also be used with log-transformation of the independent variable to model the frequency. This is referred to as a log-Pearson III (LP3) distribution and is commonly used in water resources engineering for frequency analysis of peak streamflow values. Another advantage of using the LP3 distribution is this analysis will be consistent with Nelson (1988). Several return periods (i.e., 1.01, 2, 10, 20, 50, and 100 years) were estimated for wind speed by using the LP3 fitted distribution. Return periods of greater than the 100-year wind speed event were not considered because more frequent and lower-magnitude wind speeds are most important for assessing incremental shoreline erosion. Also, we assumed that aggregating wind speeds to durations longer than 1-hour would potentially mask the effects on the shoreline since time-averaged wind speed would be lower in magnitude.

The LP3 analysis was completed using scripts developed in the R statistical software. No specific R package was used; all the computations were completed using stepwise calculations of variables for parameter and quantile estimation based on 3-parameter Gamma distribution tables. The purpose of using R scripts to perform the LP3 analysis was that calculations for several datasets can be batched to a single script.

Figure 17. Evaluation of distributions for March wind speed using a 20 mph threshold.

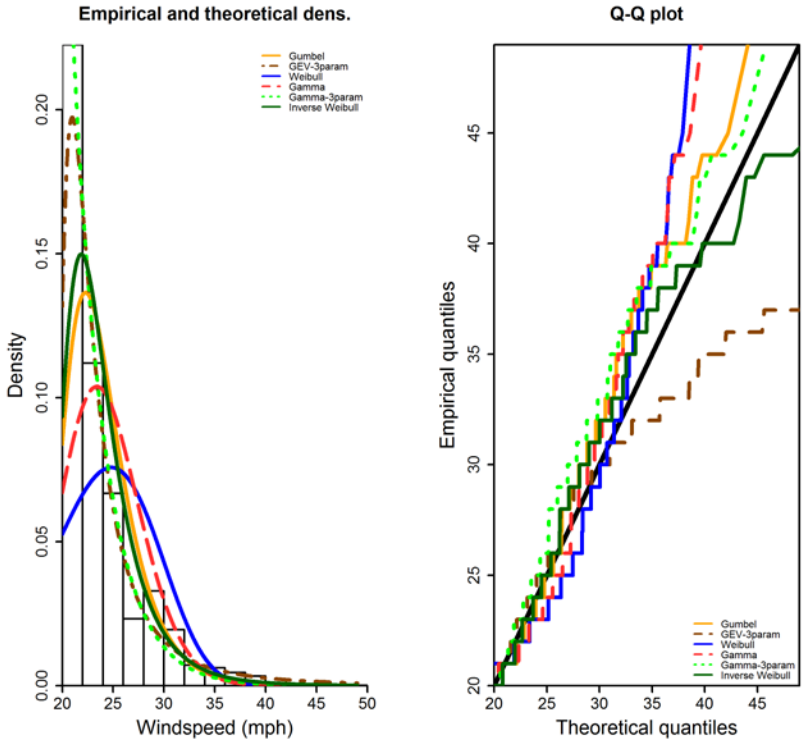

Figure 18. Evaluation of distributions for March wind speed using a 30 mph threshold.

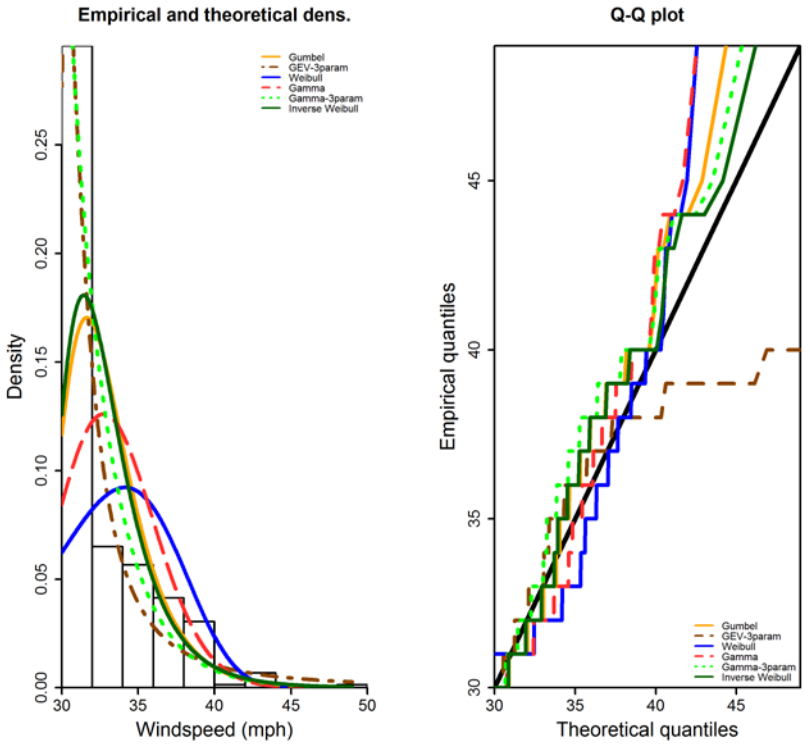

A validation of the R scripts was performed using HEC-SSP (the Hydrologic Engineering Center's Statistical Software Package). Table 1 shows the results of this validation for maximum wind speed in January from any direction. There is minimal difference between the magnitudes from the R script when compared to HEC-SSP results. Based on the assumptions of zero regional skew and no upper or lower thresholds, there are no differences using three significant figures. Assuming differences are only beyond this precision, the values produced by the R script were considered reasonable and were used for all subsequent frequency analyses.

Table 1. LP3 validation of the R script.

Return Period	Percent Chance Exceedance	R script (mph)	SSP v2.1.1 (mph)
1.01	99	23.3	23.3
2	50	36.7	36.7
5	20	41.2	41.2
10	10	43.3	43.3
20	5	45.0	45.0
50	2	46.7	46.7
100	1	47.8	47.8
200	0.5	48.7	48.7
500	0.2	49.6	49.7

3.2.1 Wind magnitude results

Tables 2 through 4 summarize the results of the wind speed frequency analysis. Table 2 summarizes the monthly wind speed quantiles for all directions. These values may be helpful for any design criteria that are dependent on only wind speed and not the combination of wind speed and fetch length. Figure 19 plots the annual wind speed column from Table 2 using the general frequency analysis. This plot again shows a good fit for the Pierre Regional Airport data with the LP3 distribution. Table 3 and Table 4 summarize the 10-year and 50-year return periods for each month and direction. Appendix C contains all of the summary tables for wind speed used in this study.

Figures 20 and 21 compare results with Nelson (1988). These represent the wind speed magnitudes for the 10-year and 50-year return periods across all directions. The current study directional patterns match except

there is a slight bias for lower-magnitude wind speed values from the easterly to southerly directions (Figures 20 and 21). This is likely because Nelson (1988) used both Pierre and Huron, South Dakota, data to generate the wind speed quantiles. The Huron data is generally higher in magnitude based on preliminary analysis; and we decided in consultation with NWO to use only the Pierre data for the current study.

In summary, this analysis indicates that relatively high magnitude wind speeds do occur at Lake Sharpe during periods of ice cover, which will likely result in movement of ice. These wind speed results are combined with the water current force estimates to calculate the total ice shove force.

Table 2. Monthly summary table for Pierre, South Dakota, wind speeds (miles per hour).

Return Period	Jan	Feb	Mar	Apr	May	Jun	Jul	Aug	Sep	Oct	Nov	Dec	Annual
1.01-year, 1-hour	23.3	21.3	24.2	24.3	22.6	21.3	21.8	21.1	24.1	25.4	24.1	24.0	32.7
2-year, 1-hour	36.7	34.9	36.1	35.6	33.9	32.3	29.7	30.9	32.6	37.4	35.7	37.3	43.8
10-year, 1-hour	43.3	42.9	44.3	44.7	39.6	38.5	36.2	39.8	39.4	46.3	43.3	46.0	50.8
20-year, 1-hour	45.0	45.1	46.8	47.8	41.1	40.3	38.4	42.9	41.8	49.3	45.5	48.7	52.9
50-year, 1-hour	46.7	47.5	49.8	51.6	42.7	42.2	41.1	47.0	44.6	52.8	48.1	51.7	55.3
100-year, 1-hour	47.8	49.0	51.9	54.3	43.7	43.4	43.1	49.9	46.7	55.3	49.9	53.8	56.9

Table 3. Summary table for Pierre, South Dakota, wind speeds for a 10-year return period (miles per hour).

Direction	Jan	Feb	Mar	Apr	May	Jun	Jul	Aug	Sep	Oct	Nov	Dec	Annual
N	29.4	27.8	29.2	35.6	29.3	29.5	30.3	31.9	27.7	31.7	27.1	29.1	38.9
NNE	22.8	22.6	30.2	33.5	30.1	28.9	24.2	26.9	24.2	26.9	21.9	24.4	37.9
NE	21.3	23.9	27.1	32.6	30.9	27.8	25.1	25.1	22.0	25.5	20.8	22.4	36.0
ENE	23.1	23.5	25.6	28.5	27.9	27.1	25.6	22.9	22.4	21.3	22.1	22.0	31.3
E	25.0	24.1	28.2	27.9	28.1	27.0	26.4	23.5	25.6	25.5	22.6	23.6	32.8
ESE	26.2	27.5	28.8	31.4	29.8	28.1	28.1	27.6	28.5	27.2	26.1	26.6	35.6
SE	26.3	27.2	29.7	33.8	30.1	29.5	27.8	28.9	31.0	31.6	26.5	26.6	36.5
SSE	21.2	21.7	31.2	34.2	31.4	28.4	27.9	30.1	32.4	31.3	26.2	23.7	37.0
S	14.7	16.7	22.5	24.5	25.9	24.4	25.9	27.0	28.8	22.2	19.3	18.8	33.6
SSW	15.0	18.5	21.7	21.8	24.2	21.2	18.3	22.2	21.3	22.1	18.4	15.6	28.4
SW	19.6	20.3	21.8	22.5	21.3	24.6	22.1	20.6	18.8	22.9	19.3	19.4	30.7
WSW	23.4	26.2	26.5	28.8	29.7	30.5	28.2	23.2	26.7	25.6	26.2	25.3	38.1
W	30.8	36.7	37.4	35.8	35.0	31.7	30.6	29.9	33.1	38.0	33.6	36.3	42.9
WNW	39.8	41.9	42.1	40.0	37.3	34.7	29.8	33.6	35.4	45.7	42.2	45.5	50.6
NW	41.8	40.5	40.8	38.1	35.8	33.0	30.7	33.9	35.8	43.2	40.6	40.7	46.5
NNW	37.3	33.5	37.2	34.7	32.9	31.8	32.6	29.3	29.7	32.5	33.5	32.9	41.6
All	43.3	42.9	44.3	44.7	39.6	38.5	36.2	39.8	39.4	46.3	43.3	46.0	50.8

Table 4. Summary table for Pierre, South Dakota, wind speeds for a 50-year return period (miles per hour).

Direction	Jan	Feb	Mar	Apr	May	Jun	Jul	Aug	Sep	Oct	Nov	Dec	Annual
N	38.6	31.2	31.7	41.8	35.4	34.8	36.6	39.0	31.0	40.3	33.6	36.1	44.7
NNE	32.1	23.4	35.1	42.9	38.1	35.7	27.8	32.0	28.1	33.8	26.0	32.6	43.1
NE	24.8	29.6	30.3	39.8	39.0	34.2	29.0	30.4	25.6	33.8	25.8	28.6	42.5
ENE	26.2	25.9	29.1	33.3	34.0	31.7	31.2	24.8	26.8	23.7	27.3	26.6	34.2
E	27.2	24.8	32.4	33.0	33.6	30.7	29.7	25.4	32.0	31.0	27.3	27.7	36.0
ESE	30.0	32.0	36.1	35.8	35.7	33.0	31.0	31.5	34.4	30.3	30.1	30.6	40.0
SE	30.3	30.1	34.8	39.5	34.3	33.0	31.6	32.0	36.7	37.1	31.1	29.5	42.0
SSE	24.9	24.3	38.9	41.0	34.3	32.0	30.5	34.5	37.2	38.4	28.5	31.2	41.6
S	21.2	21.3	27.5	28.7	31.7	32.5	33.2	33.3	39.5	25.9	25.3	26.2	39.6
SSW	18.5	25.1	29.7	26.2	29.6	26.7	20.0	26.8	23.8	29.0	22.6	18.5	33.0
SW	20.9	21.9	27.7	28.1	25.8	32.8	28.6	25.4	21.6	31.7	20.6	23.5	36.6
WSW	26.0	33.4	33.8	35.2	36.1	39.1	41.1	25.9	31.6	31.5	34.2	30.0	43.5
W	34.7	45.9	45.3	44.7	41.8	38.4	37.9	37.8	40.7	45.1	37.7	45.0	48.7
WNW	45.3	47.5	45.5	50.7	42.0	42.2	34.2	42.2	42.1	52.8	48.1	51.7	55.9
NW	46.2	44.2	47.0	42.9	40.2	39.9	36.4	45.0	39.5	49.1	45.5	47.0	51.2
NNW	44.9	40.2	41.1	39.7	38.3	38.8	39.1	38.7	32.4	36.4	36.1	34.8	45.8
All	46.7	47.5	49.8	51.6	42.7	42.2	41.1	47.0	44.6	52.8	48.1	51.7	55.3

Figure 19. General frequency analysis plot for the maximum annual wind speed from all directions.

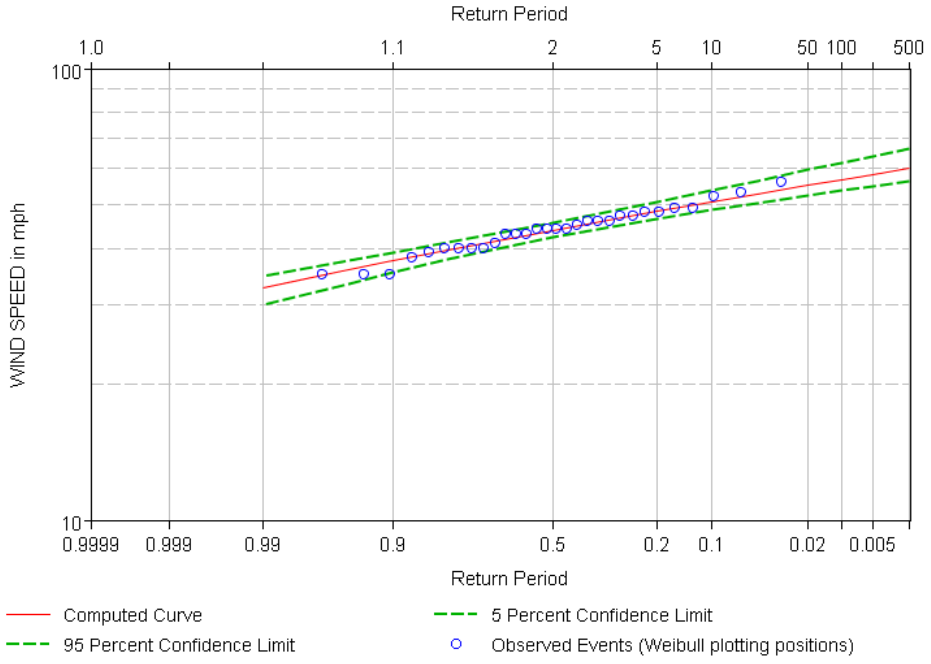

Figure 20. Comparison of current and 1988 study results for a 10-year return period.

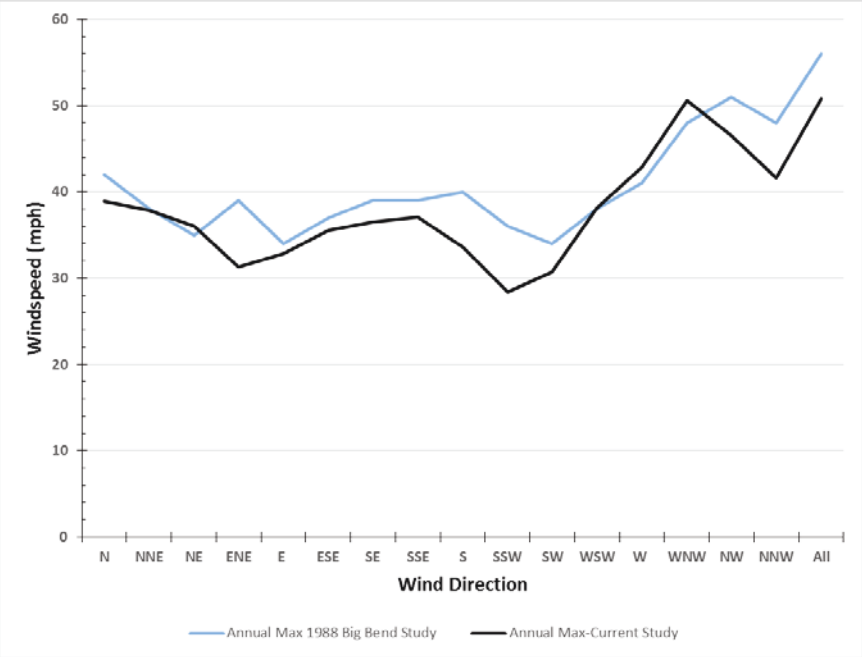

Figure 21. Comparison of current and 1988 study results for a 50-year return period.

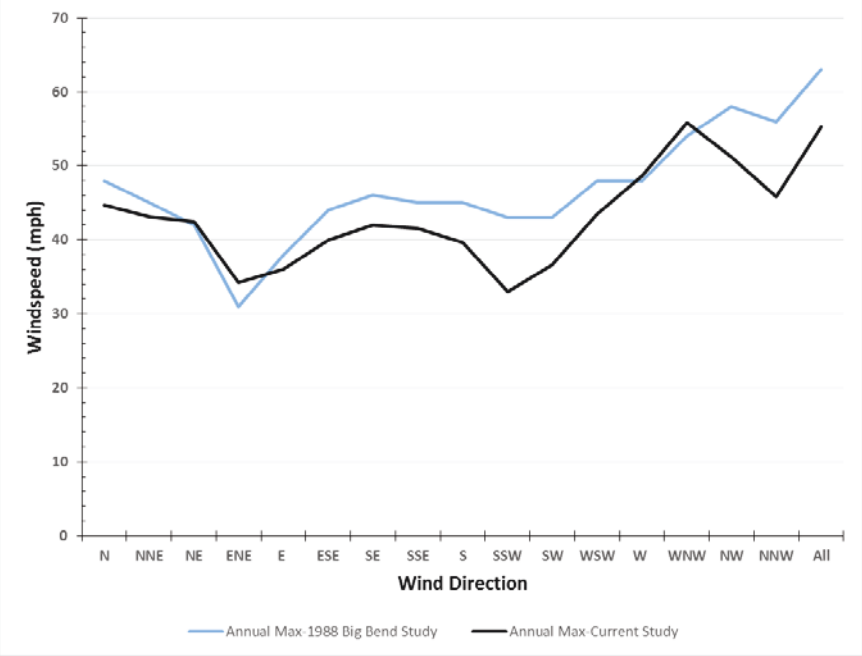

3.3 Ice thickness

We used the ICETHK model to model the ice growth and melt for Lake Sharpe (USACE 2006). This model uses heat conduction principles to develop a relationship between the accumulated freezing degree-days, accumulated thawing degree-days, and ice thickness. One of the primary advantages of using this model is that ice thickness can be estimated using only air temperature data. Validation of results can be difficult without any observed ice thickness measurements. However, ice-cover duration and limited thickness information were available for this study. This information was used to parameterize the ICETHK model for Lake Sharpe.

3.3.1 Ice-model formulation

The formula for heat conduction through the ice cover is

$$\rho_i C_p \frac{\partial T_i}{\partial t} = \frac{\partial}{\partial z}\left[k_i \frac{\partial T_i}{\partial z} \right] + \frac{\partial Q_{sw\,z}}{\partial z}, \tag{3}$$

where

T_i = temperature of the ith snow or ice layer,
z = depth,
t = time,
ρ_i = density of the ith snow or ice layer,
C_p = specific heat,
k_i = thermal conductivity, and
Q_{sw} = solar radiative flux.

The bottom boundary condition is a known temperature, the ice/water interface temperature:

$$T_B = T_m \tag{4}$$

And the change in ice thickness is

$$\frac{d\eta}{dt} = \frac{k}{\rho\lambda}\frac{dT}{dz}_B, \tag{5}$$

where the temperature gradient is evaluated at the bottom of the ice cover (B). Given the steady-state assumption, equation (3) can be stated as

$$\frac{\partial T_i}{\partial z} = \frac{\left(T_m - T_{si}\right)}{\eta}, \tag{6}$$

where T_{si} is the ice surface temperature. This equation represents the change in temperature through the depth of the ice layer.

The growth rate of the ice cover is then

$$\frac{d\eta}{dt} = \frac{k_i}{\rho\lambda}\frac{\left(T_m - T_a\right)}{\eta}. \tag{7}$$

Integrating this equation to solve for η and assuming that the ice surface temperature is equal to the air temperature, T_a,

$$\eta_j = \sqrt{\eta_0^2 + \frac{2k_i}{\rho\lambda}\int_1^j \left(T_m - T_a\right) dt} = \sqrt{\eta_0^2 + \alpha^2 AFDD_j}\,, \tag{8}$$

where

$AFDD_j$ = the accumulated freezing degree-days on day j and
η_o = the ice thickness at the start of the AFDD period. (Usually this is set to zero.)

Note that this equation applies to thermal ice sheet growth only. It assumes that the heat transfer rate is limited by heat conduction through the ice. The heat transfer coefficient (α) is defined as

$$\alpha = \sqrt{\frac{2k_i}{\rho\lambda}}\,. \tag{9}$$

Equation (8) requires knowledge of the thermal conductivity of the ice.

During melt, the surface of the ice cover will be at T_m; the base of the ice cover will be at T_m; and according to our steady-state assumption, the temperature throughout the ice cover will be at T_m. There can, therefore, be no heat transfer through the ice cover occurring, and the Stefan equation cannot apply during melt.

During melt, the heat transfer into the ice cover and the subsequent melt can be written as

$$\frac{d\eta}{dt} = \frac{H_{ia}}{\rho\lambda}\left(T_m - T_a\right), \tag{10}$$

where H_{ia} is the ice/air heat transfer coefficient. Integrating this equation results in

$$\eta_j = \eta_0 - \frac{H_{ia}}{\rho\lambda}\int_1^j \left(T_m - T_a\right) dt = \eta_0 - \beta ATDD_j, \tag{11}$$

where

$ATDD_j$ = the accumulated thawing degree-days on day j and
η_o = the ice thickness at the start of the melt period.

Ice growth and melt can be estimate using the two-step ice model. The inputs for the model consist of freezing degree-days (FDD) and thawing degree-days (TDD), which are derived from the daily temperature data. These variables are monotonically increasing over an annual period. Another important variable that has to be estimated is AFDD minimum value, which is used to transition from the cooldown period to actual ice formation. This variable can be estimated from a variety of data sources. The most accurate method is to use ice-cover information; however, qualitative information from newspapers, fishing reports, etc., may also be helpful in determining this value.

3.3.2 Ice model

The ICETHK is a physically based model for remote estimation of thermally grown ice thickness. The model accounts for three distinct periods during the ice formation process. Those are the initial cooldown when the reservoir is losing energy to the colder air above the water surface, next is the period of ice formation when water surface is frozen and additional energy transfer to the atmosphere results in increased ice thickness, and finally the melt period when the ice cover on the water surface is gaining energy from the warmer (above freezing) air. Details of these processes are described below.

3.3.3 Initial cooldown period

During the cooldown period, the water temperature drops from a temperature > T_m to T_m, when ice formation can start. To begin ice formation, a minimum AFDD value has to be estimated. This represents the energy removed from the water during the cooldown period. This value will be site specific:

$$\eta_j = 0,$$

where $AFDD_j < AFDD_{min}$.

3.3.4 Ice formation and melt period

When the AFDD value is greater than the minimum value, ice begins to form on the water surface. The ice thickness will continue to increase along with AFDD values. Following the transition from cold to persistent warmer conditions, the ice thickness will begin to melt as the TDD values get larger. This is represented by the equation

$$\eta_j = \left(\left(\eta_{j-1}\right)^2 + \alpha^{*2} FDD_j\right)^{1/2} - \beta TDD_j ,$$

where $\eta_j \geq 0$ and $AFDD_j \geq AFDD_{min.}$

Parameterization of the ice model can be challenging without any observed data for ice cover duration or ice thickness. However, there is guidance based on the waterbody type that generally provides responsible results (USACE 2006). For our, there was some observed ice-cover data along with information related to ice thickness, which allow for better estimates of the model parameters. The thermal conductivity of the ice (α) is a fixed value based on material properties. However, in natural environments, unknown conditions may changes this value; therefore, α is generally modified to account for various influences that reduce the ice thickness. This is represented by

$$\alpha^* = C_1 C_2 \alpha ,$$

where C_1, C_2, are constants to account for the factors that reduce the ice growth. Table 5 shows values of α^* for various field conditions.

Table 5. Ice-model parameters.

Condition	α*
Windy Lake No snow	2.7
Average Lake with Snow	1.7–2.4
Average River with Snow	1.4–1.7
Sheltered River with Snow	0.7–1.4

3.3.5 Lake Sharpe ice thickness analysis results

The ice model developed for Lake Sharpe used daily average air temperature data for Pierre. This site was selected because we considered it most representative for Lake Sharpe temperature, and it also provided consistency of climate stations between the ice and wind analysis. We used the ice-duration information directly to parameterize the ice mode and estimated the $AFDD_{min}$ value by using the observed freeze-up dates provided by MRBWM. A test for outliers in the $AFDD_{min}$ values was performed using Rosner's Test for outliers within the R package "EnvStats" (Millard 2017). Rosner's Test indicates that two years are outliers (at the 95% confidence interval). These years are water years 2000 and 2015, which had AFDD values of 348°C-days and 290°C-days, respectively. Another quick check for outliers can also be performed by plotting each point against the two standard deviation bounds. Figure 22 shows the results of this method, and again these two water years plot beyond the boundary lines. Appendix D shows the detailed output from the R script Rosner's Test.

Figure 22. Test for outliers in minimum AFDD analysis.

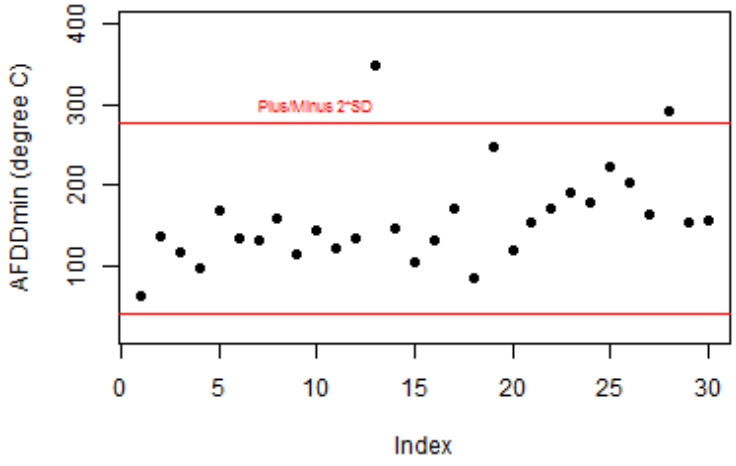

After determining the $AFDD_{min}$ value for this reservoir, we determined the coefficients α^* and β. A value of β =0.45 cm (°C-day)$^{-1}$ is generally recommended (Ashton 1989). Using this value for β, α^* can be determined. The adjustment to α^* was performed using numerical methods to minimize the mean absolute error for ice cover duration between the model and observations. Table 6 summarizes parameters for the Lake Sharpe ICETHK model.

Table 6. Lake Sharpe ICETHK model parameters.

$AFDD_{min}$(°C)	151.86
α^* (cm(°C-day)$^{-1/2}$)	2.3
β (cm(°C-day)$^{-1}$)	0.45

The two primary comparisons used in the validation of the Lake Sharpe ice model were the ice-cover duration data from MRBWM and the average ice thickness for water years 2007–2017 from the LBST. As discussed previously, the observation data for ice cover is relatively complete and was used directly for the parameterization of the model. Table 7 below summarizes the average annual ice-cover duration between the model and the observation data. The model does represent the average annual ice-duration reasonably well and appears to be insensitive to the averaging period (e.g., 2007–2017 or 1963–2017). Overall, the Lake Sharpe model provides a slight bias to longer ice cover duration; however, this bias is only approximately 4% (102 days vs. 98 days) for the 2007–2017 period when compared to observations.

Table 7. Lake Sharpe ice-cover duration comparison.

	Freeze-Up Date	Break-Up Date	Duration
Model Avg. 1963–2016	20-Dec	31-Mar	101
Model 2007–2016	19-Dec	31-Mar	102
Tribal Avg. 2001–2016	19-Dec	28-Mar	99
District Avg. 1963–2016	21-Dec	28-Mar	97
District Avg. 2007–2016	21-Dec	29-Mar	98

Another visualization of the model performance is to compare the annual modeled and observed freeze-up and breakup dates, shown in Figure 23 and Figure 24, respectively. A perfect model fit is represented by the 1:1 response (black) line. If the modeled values are above this line, then the freeze-up (breakup) is after the observed date. The converse is true if the modeled values are below the black line. Overall, the model results fit the observed ice-cover information. A contributing factor in the difference for

ice-cover duration is generally due to later breakup estimates from the model. One of the uncertainties with the ice-cover observations is the definitions used for breakup. The model assumes a one-dimensional continuous ice cover, and the breakup date is when the ice thickness goes to zero. In contrast, observers may consider any open water the date for annual breakup, or the observer may not happen to be in the specific location of where the last ice cover is on the reservoir. These observations will be spatially variable and thickness of the ice may have minimal influence on the date designation.

Figure 23. Ice-model comparison of freeze-up dates.

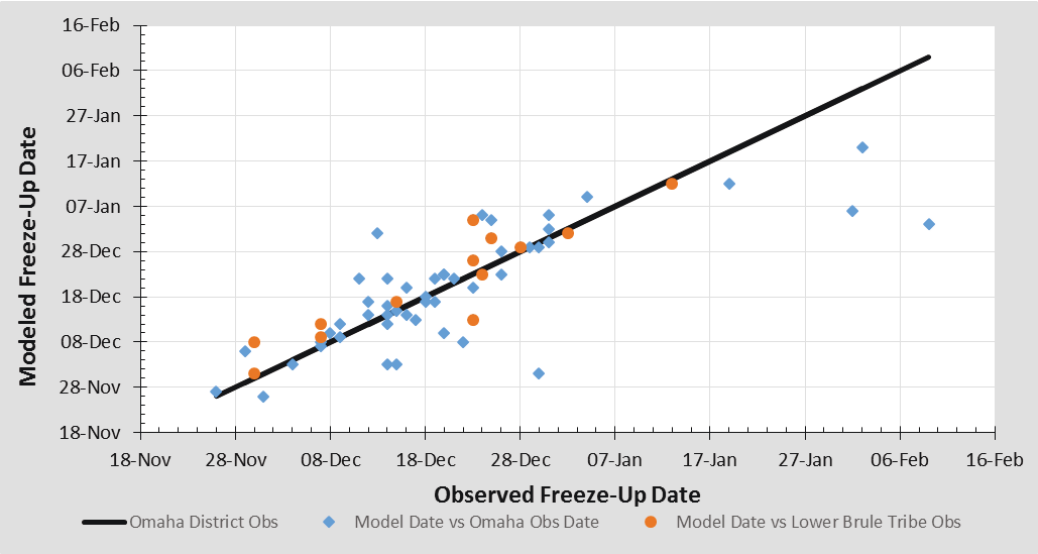

Figure 24. Ice-model comparison of breakup dates.

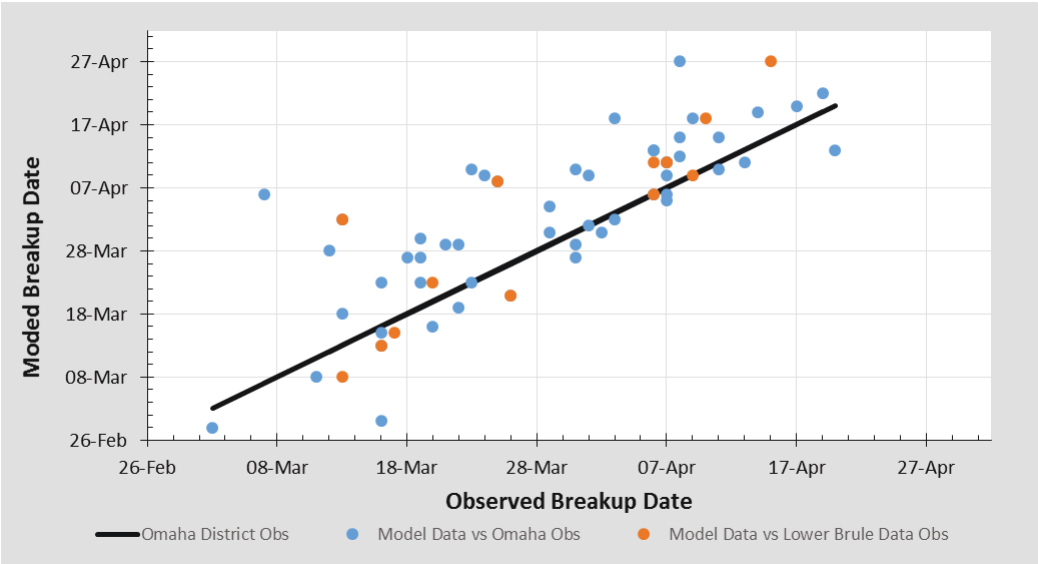

The important output from the model is the estimated ice thickness, specifically the annual maximum thickness. This will be used in the ice shove force calculations and the stone-sizing criteria for shoreline erosion mitigation. The results of the model match the qualitative ice thickness information provided by the LBST for average thickness over the last 8–10 years. If we assume that 18 in. for the average annual maximum ice thickness described by the LBST information is representative of water years 2007–2017, then the model appears to be very well calibrated (Figure 25). Another output from the ice model is the average monthly maximum ice thickness. The peak monthly value is in February, closely followed by the March thickness (Figure 26). This is important because March and April can have higher-magnitude wind speeds, which would result in increased forces due to ice shove.

The final step in this analysis was to determine the ice thickness frequency based on the modeled historical maximum ice thickness (Figure 27). We determined the ice thickness frequency by using the Pearson Type III distribution for generalized frequency in the HEC-SSP software. When comparing the fitted and observed values, the Pearson Type III distribution appears reasonable to use with this data. We should note that the values for the ice thickness model results and the general frequency analysis were computed in centimeters and then converted to inches for convenience of design calculations. Table 8 summarizes the frequency analysis for annual maximum ice thickness. Appendix E lists the individual monthly tables for ice thickness probabilities. We recommend for this analysis not using an ice thickness return period of more than 100 years. This is because of the limited calibration and validation data that was available for the Lake Sharpe ICETHK model.

Figure 25. Modeled annual maximum ice thickness for 2007–2017.

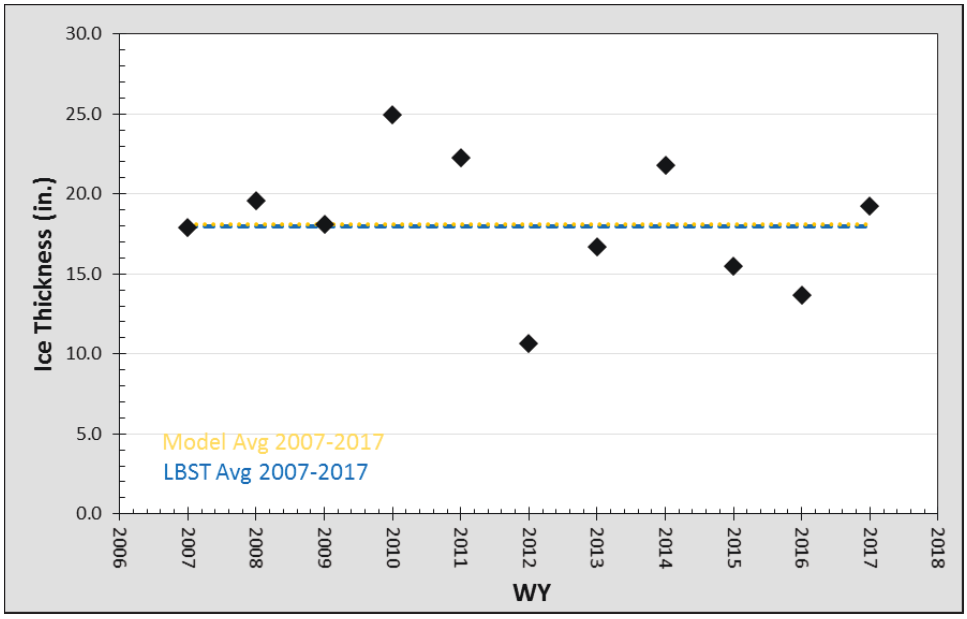

Figure 26. Modeled average monthly maximum ice thickness for 2007–2017.

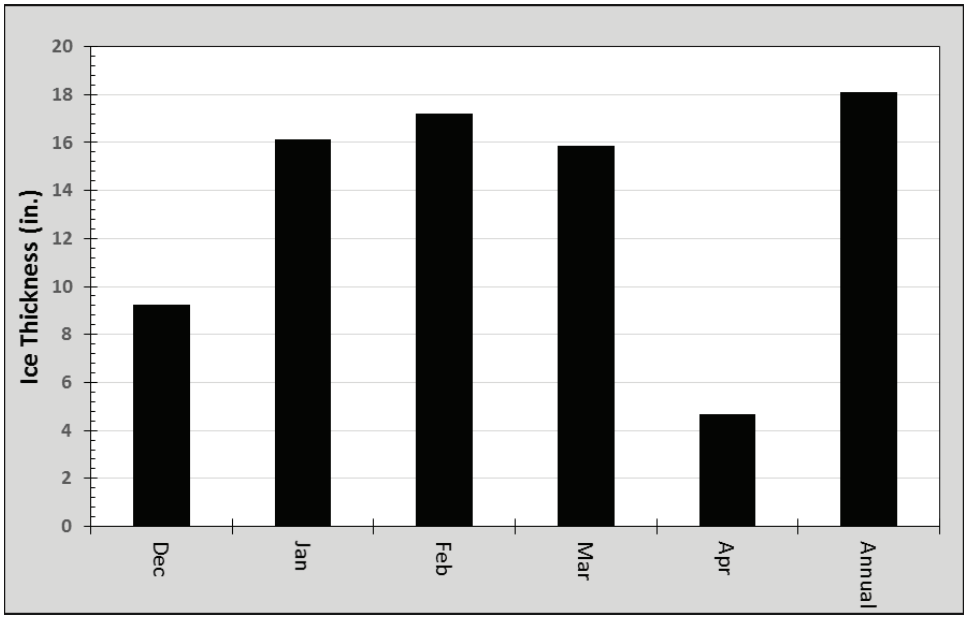

Figure 27. General frequency analysis results for modeled annual maximum ice thickness (1963–2017).

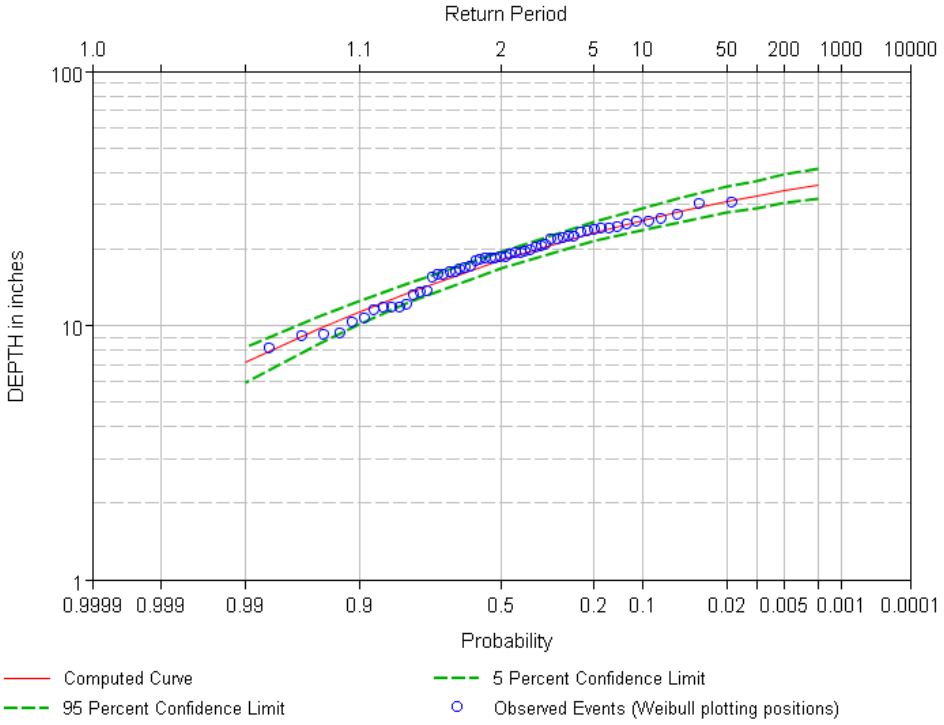

Table 8. Modeled maximum annual ice thickness (inches) quantiles (1963–2017).

Percent Chance Exceedance	Computed Curve	Confidence Limits	
		0.05	0.95
0.2	35.5	41.5	31.6
0.5	33.8	39.1	30.2
1	32.4	37.2	29.1
2	30.7	35.0	27.7
5	28.2	31.8	25.7
10	25.9	28.9	23.8
20	23.2	25.5	21.4
50	18.1	19.5	16.9
80	13.5	14.6	12.3
90	11.4	12.4	10.1
95	9.7	10.8	8.5
99	7.1	8.2	5.9

3.4 Ice shove forces estimates

3.4.1 Ice strength estimation

The American Association of State Highway and Transportation Officials (AASHTO 2012) provides guidance on computing ice forces on structures, most particularly bridge piers. However, the guidance is also applicable to wide structures (i.e., reservoir walls or dam gates) and can be applied to shorelines, also. AASHTO (2012) considers vertical- and sloped-face structures and how this affects ice failure in crushing and bending. The ice force used to determine the ice shove force along the shoreline is the minimum of either the crushing or bending force represented by equation (12):

$$F_i = K\min(F_c, F_b), \tag{12}$$

where the subscripts c and b refer to the crushing and bending forces and K is a force reduction factor that takes into account the size of the ice floe in comparison to the width of a structure.

For ice floes that are large in comparison to structure width, $K = 1$ can be assumed while, for floes that have similar size to the structure width, the minimum value of $K = 0.5$ is used. In this study, we assume that the ice floes and shoreline interaction are of similar size and assume $K = 0.5$ is appropriate.

The force associated with ice failing by crushing is computed from

$$F_c = C_a S t w, \tag{13}$$

where

t = the ice thickness;
S = the effective crushing strength of the ice;
w = the width of the structure;
C_a = sqrt($5/a$ +1), a factor that adjusts for the aspect ratio between the ice thickness and structure width; and
a = w/t, the aspect ratio of structure width to ice thickness.

For wide structures, $a \geq 6$; and in this study, $a = 6$ is used in equation (13).

For ice failing in bending, the force is computed from

$$F_b = C_n S t^2, \tag{14}$$

where

C_n = 0.5/tan(α – 15),
α = slope (in degrees) of the structure face measured from vertical,
t = the ice thickness, and
S = the effective crushing strength of the ice.

Equation (14) applies only for structures that have a slope greater than 15°; otherwise it is assumed that ice fails in crushing, and equation (13) is used. Furthermore, for a wide structure ($a \geq 6$), regardless of face slope, it is assumed that ice fails in crushing. Therefore, for ice interacting directly with the shoreline, we consider this ice impacting a wide structure; and equation (14) cannot be used to estimate ice forces. However, if the ice is interacting with smaller offshore, sloped, island-like structures, it is possible that bending failure may dominate. The geometry of such features would need to be reviewed to determine if the structures are narrow enough for equation (14) to apply.

For the purposes of this study, the ice forces based on ice strength will generally be determined from equation (13). Normalizing this by unit width of the ice sheet, the force is then

$$f_c = K C_a S t. \tag{15}$$

The ice thickness used in equation (15) varies by month and chance exceedance (Table 8; Appendix E). The ice strength varies through the winter season with it being at a maximum strength of 400 psi when the ice is cold (e.g., late December to early January) and then declines as the ice warms into the spring. Based on observations (Appendix B), it appears that the ice can be quite weak by mid-February. Using this limited anecdotal evidence, we estimate that the ice strength varies by month as provided in the below Table 9.

Figure 28 provides a summary of the range in ice forces possible if limited by the crushing strength of the ice. The December crushing strength is typically much higher compared to the later-season ice strength. Therefore, early season crushing forces will be higher in comparison given the same

ice thickness. The range in ice thickness for each month is taken from the ice thickness probability calculations.

Table 9. Estimate of variation in ice strength by month.

Month	Ice Strength (psi)
December	400
January	350
February	200
March	150
April	100

Figure 28. Summary of estimated ice forces limited by the crushing strength of the ice.

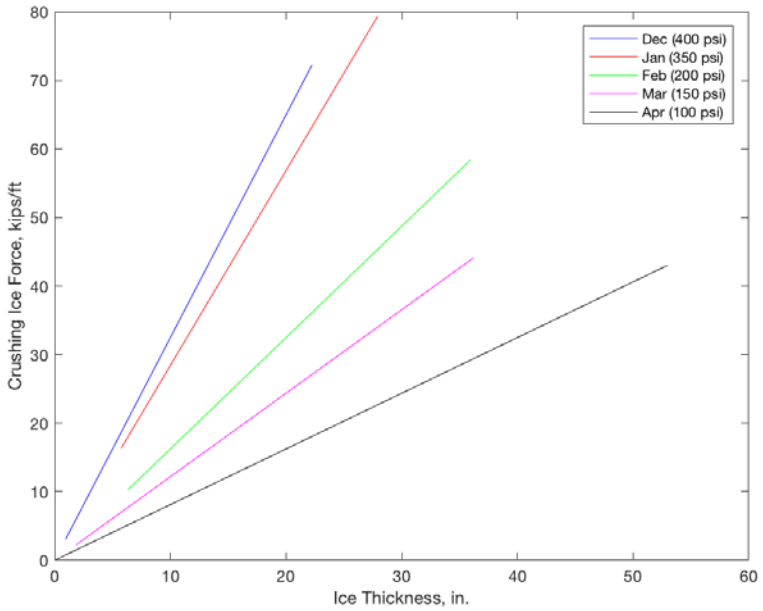

3.4.1 Water current force on the ice sheet

Large ice floes can be driven into the shoreline by the river current. We estimated the likely dimensions of two large ice floes based on the channel geometry, assuming the floes to be roughly rectangular. The forces on the shoreline were estimated as follows.

We use equation (16) to calculate the total force acting on a floe in the direction to cause it to impinge on the channel bank. This equation uses the spatially integrated velocity direction vector $(\overline{\beta})$, which is needed to determine the force on the ice from the water. The water velocity direction acting on the ice floe varies due to the sinuous geometry of the reservoir

shoreline. Therefore, the velocity has to be descritized and integrated for the area of each individual floe. Equation (17) details the information requred for this calculation.

$$F_{water} = C_{D-water}\rho_{water}AU_{water}^2\cos(\delta - \bar{\beta}), \tag{16}$$

where

F = the total force (N),
ρ_{water} = the water density (kgm^{-3}),
$C_{D\text{-}w}$ = the drag coefficient,
U = the water velocity (ms^{-1}),
δ = the direction of application of the floe (parallel to the long sides of the floe), and
$\bar{\beta}$ = the spatially integrated velocity direction (assumed to act parallel to the channel centerline).

$$\bar{\beta} = \frac{1}{L}\int_0^L \beta(l)\,dl = \frac{1}{L}\sum_{j=1}^{n}\beta(j)l(j), \tag{17}$$

where

L = the length of the channel centerline through the floe (m),
$\beta(l)$ = the current direction along the channel centerline at a distance l from the upstream limit of the floe,
n = the number of straight lines used to approximate the channel centerline,
$\beta(j)$ = the direction of each segments, and
$l(j)$ = the length of each segment (m).

The force per unit width that the floe can apply, f_w (Nm^{-1}), is

$$f_{water} = \frac{F_{water}}{w}, \tag{18}$$

where w is the width of the floe normal to its direction of application (m).

The force from water that is perpendicular to the shoreline at each location, $f_{water\perp}$ (Nm^{-1}), is then

$$f_{water\perp} = f_{water} \left|\sin(\delta - \psi)\right|, \quad (19)$$

where ψ is the direction parallel to the shoreline at each location.

Abdelnour (2012) provides estimates of the drag coefficient for the water–ice interface for a rough to smooth ice cover as $C_{D\text{-}water}$ = 0.05 (rough), 0.035 (medium), and 0.02 (smooth). A rough ice cover would be associated with a broken and refrozen ice mass. It is most likely that the ice on Lake Sharpe can be classified as smooth. However, we use $C_{D\text{-}water}$ = 0.035 as a conservative upper limit on the drag for the ice on Lake Sharpe. The water density was assumed as constant at 1000 kg/m^3. The water velocity was estimated using the 90th percentile flows during a given month. We derived estimates of water velocity from relating these discharge values to the information in Table 10.

Table 10. Estimates of average water velocity in Lake Sharpe by month.

Month	Average water velocity (ft/s)
December	0.16
January	0.17
February	0.12
March	0.13
April	0.15

Figure 29 illustrates how the water current force is calculated. The frame of reference for the vector angles is important to understand. The direction of application for the Ice Block 1 force vector is shown by the solid red arrow line. The angle associated with the direction of application (δ) is the azimuthal direction. This vector has two force components, one parallel to the shoreline and the other perpendicular (dashed blue lines). For this analysis, only the perpendicular component is assumed to be causing erosion. Although shear stress along the shoreline may cause erosion, based on the evidence available it does not appear to be the primary source for most of the observed erosion. The perpendicular force component of the floe (equation [19]) is calculated by subtracting the shoreline angle (ψ), referenced from the Floe 1 force vector, which is shown by the dashed red line, from the direction of application angle. This result represents the forces from the Floe 1, which are perpendicular to the shoreline at RM 993.6.

Figure 29. Illustration of how the water force is derived from floe information.

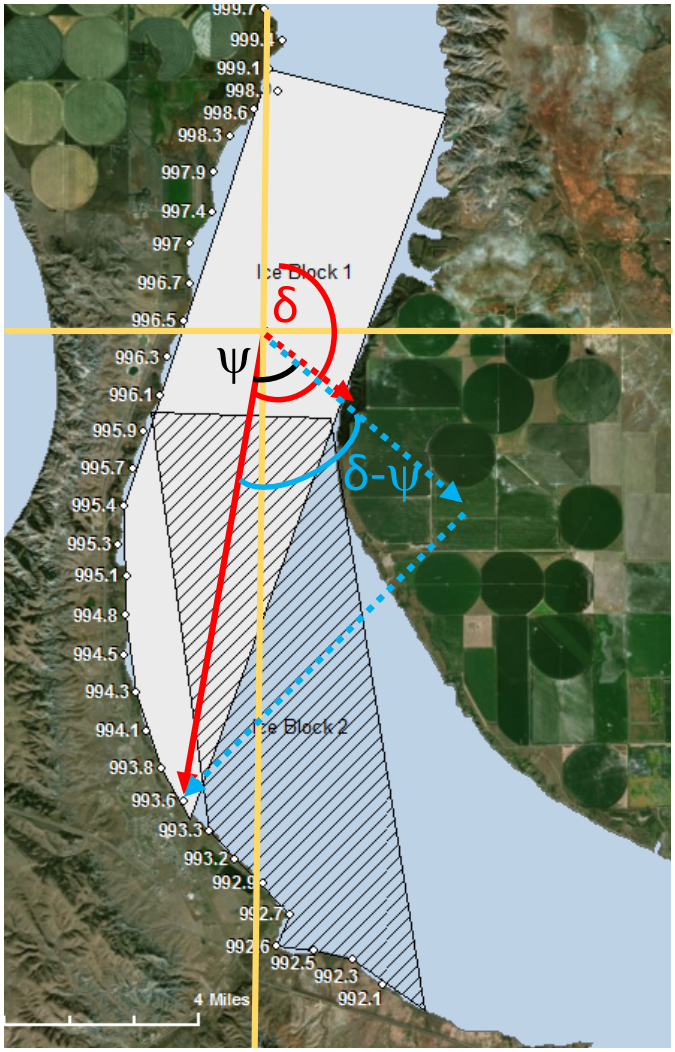

Table 11 summarizes the information about each floe size and applied velocity direction for the study reach. Table 12 and Table 13 show the angle for each perpendicular force component for both Floe 1 and 2, respectively. All of this information was used to compute the force per width on the ice sheet due to the water current.

Table 11. Estimated floe dimensions and orientation.

Floe	Area, A (m²)	Direction of Application (°)	Width, w (m)	Stations Impacted	Integrated Velocity Direction, $\bar{\beta}$	$\cos(\delta - \bar{\beta})$
1	17,074,992	199.05	2189	995.4-993.6	190.3473	0.988
2	14,529,763	172.5	2250	993.3-992.1	160.3965	0.978

Table 12. Floe 1 angle of applied force vector by shoreline location.

Location	Direction Parallel to Shore, ψ	Force Direction, $\lvert\sin(\delta - \psi)\rvert$
995.4	8.787	0.178
995.3	−0.741	0.339
995.1	−0.741	0.339
994.8	−4.599	0.401
994.5	−8.457	0.462
994.3	−13.380	0.536
994.1	−18.303	0.607
993.8	−23.963	0.682
993.6	−29.623	0.751

Table 13. Floe 2 angle of applied force vector by shoreline location.

Location	Direction Parallel Shore, ψ	Force Direction, $\lvert\sin(\delta - \psi)\rvert$
993.3	−26.054	0.318
993.2	−44.082	0.596
992.9	−44.082	0.596
992.6	−54.143	0.727
992.7	−44.082	0.596
992.5	−80.565	0.957
992.3	−65.905	0.852
992.1	−54.143	0.727

3.4.2 Wind force on ice sheet

The wind or water force is computed from equation (1) as

$$f_{wind}(m, x, \phi, R) = C_{D-wind}\rho_{air}U_{wind}^2(m, x, \phi, R)L(x, \phi),$$

where

f_{wind} = an environmental force from wind as a force per unit width,
$C_{D\text{-}wind}$ = coefficient of drag for the air–ice interface,
ρ_{air} = air density,
U_{wind} = flow velocity, and
L = fetch length.

The wind, like the water current, acts on the entire ice sheet. However, equation (8) has already assumed that the area of the ice sheet has been divided by the width, thus making a force per unit width equation. The fetch length, L, is based on the length of the ice from shore to shore, which is concurrent with the wind direction. The fetch length for the point on the shore where the force is expected to act was computed for each azimuthal direction in 22.5° increments and tabulated for the 37 locations identified in the study reach.

Past research has explored the development of the coefficient of drag for wind on ice sheets. Banke and Smith (1973), Foltyn and Tuthill (1996), and Abdelnour (2012) provide estimates for the coefficient of drag for the air–ice interface, $C_{D\text{-}wind}$, with a range of 0.0017 to 0.0022 for a smooth ice cover and as high as 0.005 for a rough ice cover. For this analysis, we considered the ice a smooth surface and estimated the coefficient of drag by a two-step process. First, we used the expression for fully developed flow over a flat plate (Schlichting 1979), $C_{D\text{-}wind} = 0.455/\log(Re)^{2.58}$, where $Re = UL/\nu$ (Reynolds Number), and ν is kinematic viscosity. This method captured any potential increase in $C_{D\text{-}wind}$ over the published range values due to changes in flow conditions or fetch length. In addition, this method allowed for the coefficient of drag to be estimated using variations of air density and kinematic viscosity that result from monthly air temperature differences. Although the first estimate of the coefficient of drag is a more physically based method, the uncertainty associated with the ice roughness is relatively high. Therefore, the second step in the processes ensured that a minimum value of $C_{D\text{-}wind} = 0.0022$ was used for all calculations. This process provided a relatively conservative estimate for the air–ice interface coefficient of drag.

The result of the wind speed frequency analysis (e.g., Table 3) was used for wind force calculations. This along with the tabulated fetch lengths for each location were used to compute the wind force for each combination of

month and direction. The maximum wind force vector was combined with the water velocity vector to determine the maximum direction for each location along the shoreline.

3.4.3 Combination of forces

To determine the total environmental load on the shoreline, we computed the vector sum of the wind and water forces. Since the wind direction is reported as increasing clockwise from north, the water force vector is also referenced from north. The included angle between the water and wind force, θ, is the difference between the two azimuthal angles δ and γ, where γ is the azimuthal angle of the wind force vector and δ is the azimuthal direction of the water force vector. Figure 30 demonstrates how the angles relate to one another. The sum of the forces acting along the wind force vector is

$$fc_{||} = f_{wind} + f_{water} \cos\theta, \tag{20}$$

and perpendicular to the wind force direction is

$$fc_{\perp} = f_{water}\mathrm{Sin}\theta = f_{water}\,|\sin(\delta - \gamma)|. \tag{21}$$

The vector magnitude of the environmental force is

$$f_c = \sqrt{\left(f_{c\perp}^2 + f_{c\|}^2\right)}, \tag{22}$$

and the resultant direction relative to north, ϕ, is

$$\phi = \gamma + \sin^{-1}(f_{c\perp}/f_c). \tag{23}$$

Comparison of the environmental forces to the potential forces limited by the strength of the ice show that the environmental forces are several orders of magnitude lower and will govern the forces for the ice interacting with the shoreline. Table 14 summarizes the resulting forces for each location along the shoreline. Appendix G individually summarizes all of the variable values used in computing the ice forces. We should note that the calculations in the appendix are in metric while for convenience they have been converted to standard units for the tables in the next section.

Figure 30. Combination of wind and water force vectors.

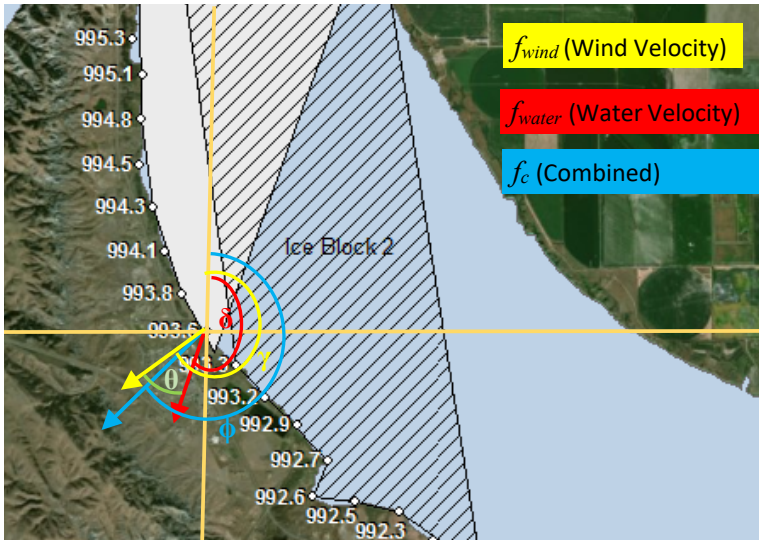

3.5 Ice shove force results

Table 14 summarizes the ice shove force results. Visualization of these results can be helpful when considering the spatial patterns along the Lake Sharpe shoreline. Appendix H provides a series of maps showing the maximum resulting ice force vectors for each month and wind speed return period. These maps provide ice force magnitude ranges (indicated by color) and direction (arrow orientation). For illustration purposes, Figure 31 and Figure 32 present the March ice force vectors for the 10-year and 50-year return periods, respectively.

The maps indicate quantitatively what previous sections related to observed ice shove have already referenced. For example, the area near the wastewater treatment facility (RM 992.5 through 993.3) consistently has ice forces that fall in the higher magnitude categories. Moreover, the direction orientation from the wind speed analysis indicates that wind and water current drag on the ice sheet will be coincident in these areas. Therefore, the water force vector will often be additive to the wind speed force during ice-cover periods on the reservoir. Other areas have wind directions that would be opposite in direction from the water current (e.g., RM 997.9 through 998.6), which would result in slightly reduced ice force magnitudes when compared to those produced by only wind drag on the ice sheet.

Table 14. Summary of ice forces by shoreline location (lbf/ft).

Lake Sharpe Ice Forces (lbf/ft)

	December						January						February						March						April					
Return Period	**1.01-yr**	**2-yr**	**10-yr**	**20-yr**	**50-yr**	**100-yr**	**1.01-yr**	**2-yr**	**10-yr**	**20-yr**	**50-yr**	**100-yr**	**1.01-yr**	**2-yr**	**10-yr**	**20-yr**	**50-yr**	**100-yr**	**1.01-yr**	**2-yr**	**10-yr**	**20-yr**	**50-yr**	**100-yr**	**1.01-yr**	**2-yr**	**10-yr**	**20-yr**	**50-yr**	**100-yr**
Percent Chance Exceedance	**0.9901**	**0.5**	**0.1**	**0.05**	**0.02**	**0.01**	**0.9901**	**0.5**	**0.1**	**0.05**	**0.02**	**0.01**	**0.9901**	**0.5**	**0.1**	**0.05**	**0.02**	**0.01**	**0.9901**	**0.5**	**0.1**	**0.05**	**0.02**	**0.01**	**0.9901**	**0.5**	**0.1**	**0.05**	**0.02**	**0.01**
RM992.1	97.5	248.1	351.8	372.3	389.9	400.6	127.5	268.9	452.4	531.8	642.5	722.8	80.7	201.8	353.5	416.5	502.3	569.8	95.3	280.9	427.0	469.7	516.7	546.9	125.4	246.3	370.2	417.1	477.9	523.8
RM992.3	90.6	231.5	325.6	344.1	360.1	368.0	123.0	251.2	417.6	489.6	590.0	662.9	77.3	187.1	324.7	381.9	459.7	520.9	91.1	259.4	392.0	430.7	473.3	500.7	119.6	229.2	341.6	384.1	439.3	480.9
RM992.5	79.0	262.1	529.4	642.7	795.9	915.0	132.7	279.5	549.6	692.7	918.0	1121.9	93.8	294.7	472.3	527.6	590.4	632.2	173.9	372.9	513.2	554.4	600.7	631.3	143.9	423.7	737.5	855.7	1006.4	1117.8
RM992.6	30.0	92.9	176.6	207.0	244.3	270.8	32.7	119.4	199.9	219.1	237.3	253.2	34.5	136.8	183.6	190.1	194.6	196.4	68.1	155.9	247.3	281.8	326.5	360.0	79.5	145.9	235.7	275.6	332.0	378.4
RM992.7	67.4	253.8	525.6	640.8	796.6	917.7	120.4	269.7	544.4	690.0	919.1	1126.5	87.3	291.6	472.2	528.5	592.3	634.8	167.7	370.1	512.7	554.7	601.7	632.8	134.8	419.3	738.5	858.7	1012.0	1125.2
RM992.9	50.9	171.7	347.9	422.6	523.6	602.1	86.1	182.9	361.0	455.4	604.0	738.4	61.1	193.6	310.7	347.1	388.6	416.1	113.8	245.0	337.5	364.7	395.2	415.4	93.8	278.3	485.3	563.2	662.6	736.0
RM993.2	48.7	161.1	325.1	394.5	488.5	561.6	81.7	171.8	337.5	425.3	563.5	688.5	57.7	181.0	289.9	323.8	362.4	388.0	106.9	229.0	315.0	340.3	368.7	387.5	88.5	260.2	452.7	525.2	617.6	685.9
RM993.3	44.3	139.0	277.1	335.7	414.9	476.4	72.5	148.4	288.0	362.0	478.5	583.9	55.6	154.5	246.3	274.9	307.4	341.0	109.4	195.2	267.8	293.9	381.8	463.6	86.8	222.1	384.4	445.5	523.4	580.9
RM993.6	63.8	155.4	251.4	286.7	337.4	385.4	82.0	160.6	245.9	298.1	388.8	470.9	72.7	164.3	267.2	307.9	361.9	403.6	135.7	177.1	287.3	349.8	451.9	547.1	112.2	221.6	334.6	377.6	433.6	476.2
RM993.8	78.2	200.4	325.9	371.8	429.8	497.6	102.1	206.8	318.4	361.5	417.9	515.3	93.1	213.0	347.0	399.9	470.1	524.3	175.5	229.6	373.0	454.3	587.0	710.7	144.0	287.3	434.3	517.4	666.5	734.5
RM994.1	78.5	203.5	331.3	378.1	437.0	510.3	102.8	209.9	323.6	367.5	424.9	528.0	94.4	216.5	352.8	406.7	478.1	533.2	178.4	233.4	379.3	462.0	597.0	722.8	146.1	292.0	441.7	531.1	685.2	755.5
RM994.3	76.1	198.7	323.6	369.3	426.9	512.5	99.9	204.9	316.1	358.9	420.2	530.0	92.0	211.5	344.7	397.3	467.1	520.9	174.2	228.0	370.5	451.4	583.2	706.1	142.5	285.3	431.5	533.9	689.7	760.7
RM994.5	73.8	194.0	316.2	360.9	420.6	506.4	97.1	200.0	308.8	350.7	414.3	523.4	89.8	206.7	336.9	388.3	456.4	509.1	170.2	222.8	362.1	441.1	570.0	690.1	139.1	278.7	424.0	528.0	682.8	753.4
RM994.8	38.4	114.8	235.4	305.9	408.0	491.7	49.8	111.2	212.6	285.0	401.6	508.0	44.8	137.6	216.6	241.2	267.7	284.4	84.0	188.1	341.8	394.0	455.7	498.2	75.6	203.3	411.6	512.9	663.9	732.7
RM995.1	31.5	134.3	239.9	295.0	394.2	475.5	40.7	130.3	235.8	274.5	387.7	491.1	36.5	152.3	251.5	279.9	310.5	329.9	68.3	181.3	330.5	381.2	441.2	482.5	88.7	222.3	397.9	496.3	643.0	709.8
RM995.3	30.5	139.0	248.2	293.4	391.9	472.8	39.4	135.0	244.1	281.1	385.5	488.2	39.9	157.6	260.2	289.6	321.3	341.3	65.9	180.2	328.6	379.0	438.6	479.7	91.9	230.0	395.6	493.4	639.2	705.7
RM995.4	25.5	152.2	269.6	300.6	369.8	447.4	33.6	148.1	265.5	305.2	362.8	461.4	38.7	171.2	281.4	312.9	346.9	368.4	71.6	193.3	329.6	382.8	452.9	506.2	101.1	249.7	417.6	484.1	607.7	671.4
RM995.7	24.1	165.8	291.3	324.3	357.7	377.2	38.9	161.8	287.3	329.8	380.3	415.4	43.3	184.9	302.6	336.2	372.6	395.5	78.7	208.8	354.4	411.2	486.1	543.0	110.9	269.7	449.0	520.0	614.3	687.1
RM995.9	26.0	178.9	314.2	349.9	385.9	406.9	42.0	174.6	309.9	355.8	410.3	448.2	46.7	199.5	326.5	362.8	402.0	426.7	84.9	225.3	382.3	443.7	524.4	585.8	119.6	291.0	484.4	561.0	662.8	741.3
RM996.1	15.2	78.9	183.0	237.7	316.9	382.1	20.1	77.1	151.2	207.8	298.8	382.0	31.0	99.2	153.5	172.3	192.4	205.1	49.1	154.3	309.8	380.7	482.4	566.6	52.8	189.7	363.9	433.1	524.0	583.5
RM996.3	14.7	75.0	197.8	257.0	342.6	413.0	19.5	81.2	159.9	187.1	219.4	241.7	30.3	95.8	166.0	186.2	208.0	221.7	53.1	166.8	334.9	411.6	521.5	612.5	53.9	205.1	393.4	468.2	566.4	630.8
RM996.5	14.1	80.7	212.9	276.6	368.7	444.5	18.7	87.4	172.0	201.3	236.1	260.2	28.8	103.1	178.6	200.4	223.9	238.6	57.1	179.5	360.4	442.9	561.2	659.1	58.0	220.7	423.3	503.9	609.6	678.8
RM996.7	14.8	85.3	224.9	292.2	389.5	469.7	19.6	92.3	181.8	212.7	249.5	274.9	27.9	108.9	188.7	211.7	236.5	252.1	60.3	189.7	380.8	468.0	593.0	696.4	61.3	233.2	447.3	532.4	644.1	717.2
RM997.4	15.5	94.9	250.3	325.2	433.4	522.6	20.5	102.7	202.3	236.7	277.6	305.9	24.5	121.2	210.0	235.6	263.2	280.5	67.2	211.1	423.7	520.8	659.9	775.0	68.2	259.5	497.7	592.4	716.7	798.1
RM997.9	16.8	45.0	89.0	115.6	154.1	185.8	22.2	46.4	75.7	86.9	100.2	109.5	23.1	48.7	84.2	102.1	128.8	151.8	39.5	75.0	150.6	185.1	234.6	275.5	32.2	92.2	177.0	210.6	254.8	283.8
RM997	15.7	90.9	239.8	311.6	415.4	500.9	20.8	98.5	193.8	226.9	266.1	293.1	26.7	116.2	201.2	225.8	252.3	268.8	64.4	202.3	406.0	499.1	632.4	742.7	65.4	248.6	477.0	567.7	686.8	764.9
RM998.3	16.2	44.5	125.9	171.6	243.3	306.9	21.5	44.8	77.1	106.7	160.6	216.0	20.1	49.7	99.1	124.7	160.9	190.2	38.2	68.1	174.9	214.7	261.4	292.5	31.1	102.9	203.6	238.5	279.9	308.5
RM998.6	16.7	49.6	133.9	182.5	258.8	326.5	22.1	48.5	86.0	113.5	170.8	229.7	20.7	55.4	105.4	132.7	171.2	202.3	39.3	69.5	186.0	228.4	278.0	311.0	33.2	109.4	216.6	253.7	297.7	328.1
RM998.9	13.9	37.2	76.2	100.7	136.3	165.5	18.4	38.3	67.4	92.7	133.3	170.4	17.2	44.2	65.3	74.4	88.0	103.6	32.6	61.4	114.9	133.1	154.6	169.4	26.6	65.6	138.1	173.4	226.0	250.0
RM999.1	15.8	42.5	73.4	81.8	91.5	100.6	21.0	43.8	72.4	83.1	95.9	104.7	19.6	46.6	76.3	85.1	100.1	111.6	37.3	52.6	89.4	103.7	125.0	151.3	30.5	68.0	113.2	131.1	154.9	176.1
RM999.4	14.1	65.4	141.5	173.7	217.3	251.2	27.3	69.1	146.0	186.7	250.9	308.9	20.8	78.1	128.6	144.3	162.2	174.1	42.9	99.5	139.5	151.2	164.4	173.1	32.6	112.3	201.6	235.3	278.2	309.9
RM999.7	15.6	59.2	128.2	157.4	196.9	227.6	24.7	62.6	132.3	169.2	227.3	279.9	19.3	70.7	116.5	130.8	147.0	157.8	38.9	90.2	126.4	137.0	152.2	170.1	34.7	101.7	182.7	213.2	252.1	280.8
RM1000.1	16.1	52.0	91.3	101.7	112.1	118.2	21.4	50.7	90.1	103.4	119.2	130.2	20.0	58.0	94.9	105.4	116.8	124.0	37.9	65.4	111.1	128.9	152.4	170.2	34.8	84.6	140.7	163.0	192.6	215.4
RM1000.5	16.1	54.3	104.5	135.8	181.0	218.2	21.3	53.0	95.2	121.7	163.5	201.4	20.0	60.5	99.0	110.1	121.9	129.5	37.9	88.1	176.9	217.4	275.5	323.6	36.3	108.3	207.8	247.4	299.3	333.3
RM1000.8	107.2	228.5	360.4	412.3	480.9	533.9	88.9	253.7	384.0	423.7	468.8	498.8	77.4	240.0	357.1	389.7	424.7	446.7	100.6	223.1	353.9	404.4	470.7	521.3	87.5	200.1	302.5	338.4	382.7	414.7
RM1001.2	102.6	218.7	345.0	394.7	460.4	511.1	85.1	242.9	367.6	405.6	448.7	477.5	74.1	229.8	341.8	373.0	406.5	427.7	96.3	213.6	338.7	387.1	450.6	499.1	83.7	191.5	289.6	323.9	366.4	397.0
RM1017.9	128.1	348.5	576.2	659.7	744.6	805.1	153.2	299.2	445.0	501.7	576.3	633.6	90.2	293.0	488.1	554.8	625.8	667.6	51.3	300.3	482.1	524.3	563.8	585.3	118.5	229.7	426.1	527.2	684.1	785.6

Figure 31. Ice force vectors for March (10-year return period).

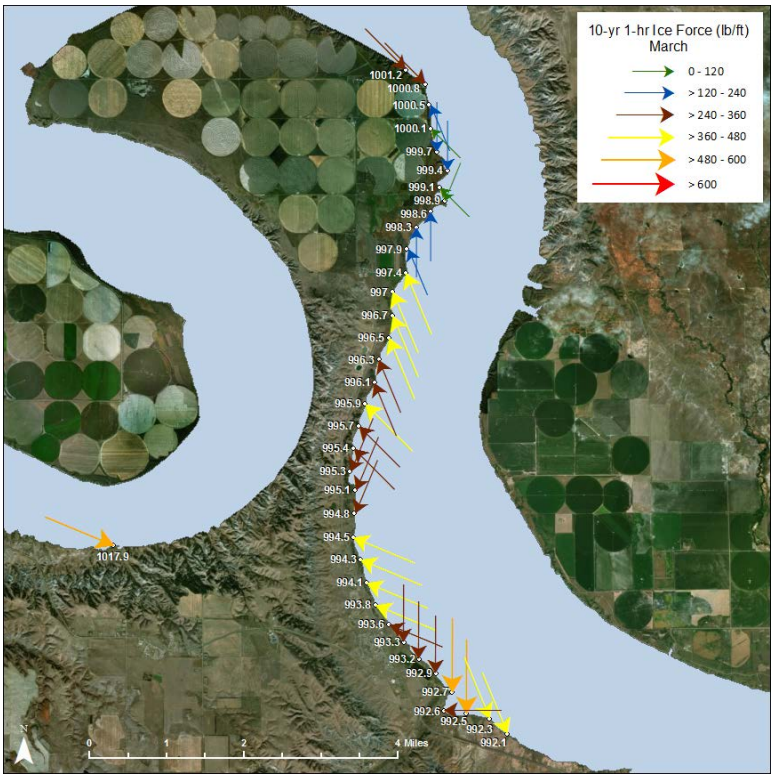

Figure 32. Ice force vectors for March (50-year return period).

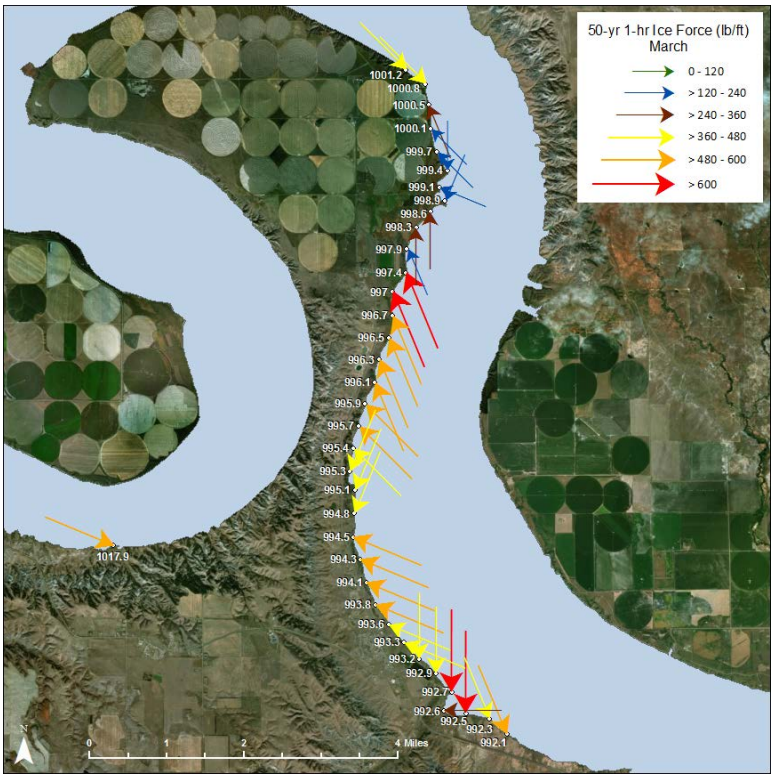

4 Shoreline Ice Erosion Mitigation

Design of measures to reduce shoreline erosion often considers only wave action for open-water conditions. In this instance, ice shove must also be considered as a primary mechanism for significant erosion. Often, the first consideration for mitigating shoreline erosion is to randomly place riprap in areas of highest erosion rates or where other critical infrastructure are located. Generally, this solution is adequate and cost effective, especially when open-water forces are causing the shoreline erosion. However, in situations where ice is a contributor to shoreline erosion, randomly placed riprap may not significantly reduce shoreline erosion rates. This is because ice will often "pluck" the stones and move them upslope, resulting in exposure of the underlying erosion-prone material.

Laboratory experiments at CRREL have been conducted to measure the impact of ice on various size and placement methods for riprap.* The sizing of the stone is generally the first consideration for shoreline erosion mitigation. Figure 33 shows the general sizing criteria for stone riprap where ice forces are present. The level of risk for failure can be determined from ice thickness (h), median stone size (D_{50}) and shoreline slope. The general recommendation for riprap stone size is to be two to three times the ice thickness while accepting a 15% probability of failure. If the annual average ice thickness is estimated to be 18 in., then the D_{50} stone size would for a 15% probability of failure would be 36–54 in. Slight variation of this range would occur based on the shoreline slope.

Stone placement is another factor that will contribute to the effectiveness of shoreline erosion mitigation. Sodhi and Donnelly* showed that selective or special placement (interlocking of stones) will withstand larger ice shove forces as compared to randomly placed riprap. Figure 34 gives an example of special placement. Although special placement will increase construction costs, it is often an important factor for the erosion mitigation measure to maintain effectiveness throughout the design life of the project.

* D. Sodhi and C. J. Donnelly (unpublished manuscript, 1996), "Ice Effects on Riprap: Model Tests," U.S. Army Cold Regions Research and Engineering Laboratory, Hanover, NH.

Figure 33. Plots of cumulative probability of failure versus h/D_{50} for various slopes.

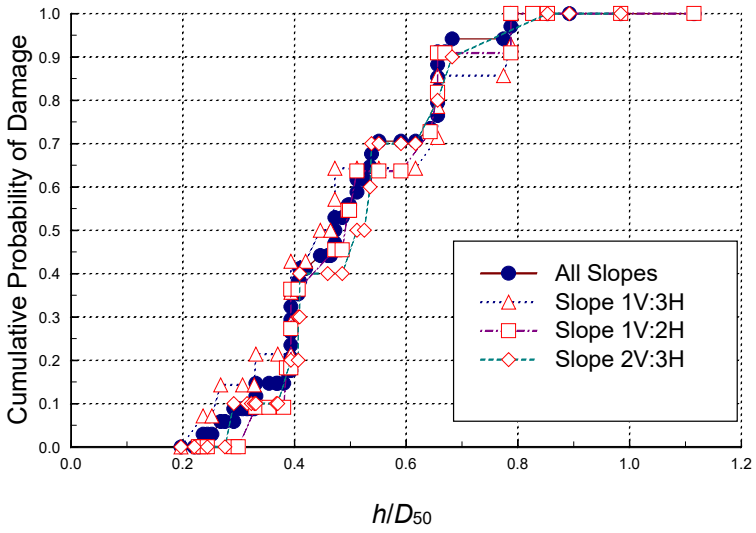

Figure 34. Special stone placement for a breakwater structure.

We should note that armoring of the shoreline with riprap is not the only erosion mitigation measure that has been shown to be effective. In many areas where significant ice thickness occurs, a potential cost-effective solution is to construct a breakwater-type structure. These structures are usually constructed for locations of significant erosion concern (e.g., critical

infrastructure near the shoreline). They are placed away from the shoreline into the waterbody and are designed with relatively low slopes on the water side of the structure (Figure 35). This promotes the ice to "ride up" onto the breakwater and fail with a bending force on the shoreline side. This method of failing the ice sheet is much less destructive when compared to crushing failure that occurs when the ice piles up against a relatively steep shoreline.

Figure 35. An example of a breakwater structure with special stone placement.

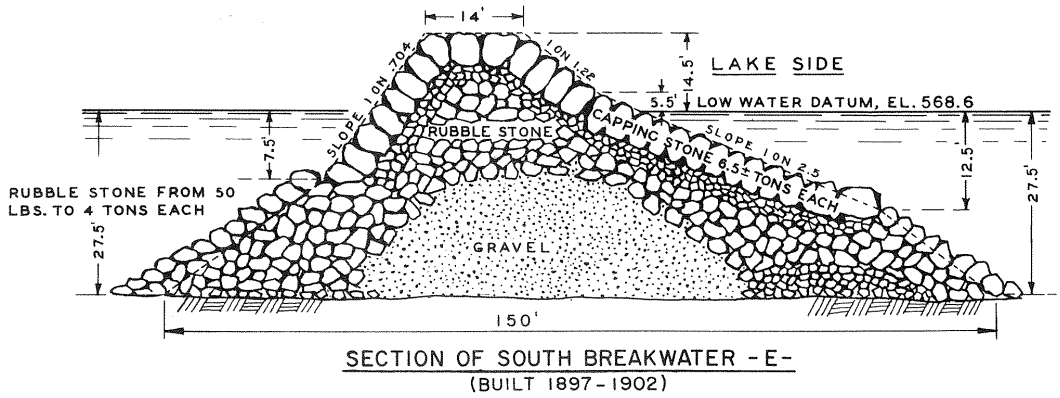

5 Summary

The combination of wind events and ice conditions for Lake Sharpe can vary drastically from year to year. This is reflected in both the range of wind speed magnitudes and the range of maximum annual ice thickness values. The wind speed frequency analysis indicated that relatively high 1-hour events are possible during the periods of ice cover. January and February wind speeds range from approximately 43 mph for the 10-year return period to approximately 47 mph for the 50-year return period. The wind speed magnitudes do increase in March and April to more than 50 mph for the 50-year return period. This is generally the timeframe for maximum ice thickness, which results in potentially large ice forces on many shoreline locations of Lake Sharpe. The shoreline locations near the treatment ponds for the LBST community have the compounding issue that both maximum wind speed and water velocity direction in the reservoir are coincident, thus resulting in an increase in potential environmental forces on the ice sheet and even greater erosion potential due to ice shove in these locations.

Because of the relatively low water velocity and small operating range of Lake Sharpe, the heat transfer mechanics are going to be the primary control for the ice formation processes. Although there were limited observations for ice thickness at Lake Sharpe, the available information from the LBST did help in the model validation. The average annual maximum ice thickness computed was approximately 18 in. The annual maximum date was between mid-February and mid-March, based on the model results.

The ice thickness estimates indicate that crushing strength of the ice is much greater than environmental forces that have been observed. Although the crushing strength of the ice decreases significantly in later winter when the maximum annual ice thickness occurs, the estimated strength is still much greater than the combined environmental forces. This results in the shoreline erosion being only a function of the environmental forces anytime when ice is present. Using the 50-year wind speed values, the combined (wind and water current) force for the Lake Sharpe shoreline ranges from approximately 100 lb_f/ft at RM 999.1 to 800 at RM992.5. The measures considered for Lake Sharpe will need to be evaluated by location based on this large range of ice forces.

Shoreline erosion mitigation measures should consider ice forces. The measures may consist of a combination of riprap and offshore breakwater structures, depending on the estimated ice forces and criticality of the infrastructure near the shoreline. The stone sizing criteria for ice shove that are based on laboratory experiments indicate that a D_{50} of 36–54 in. would result in a 15% chance of failure for the riprap. This design guidance should be combined with any information from current field installations in the region to develop a cost-effective, long-term solution.

References

AASHTO (American Association of State Highway and Transporatation Officials). 2012. *LRFD Bridge Design Specifications*. Washington, DC: American Association of State Highway and Transportation Officials.

Abdelnour, R. 2012. *Design of Oil City Allegheny River Ice Boom*. Kanata, Ontario: BMT Fleet Technology LTD.

Ashton, G. D. 1989. Thin Ice Growth. *Water Resources Research* 25 (3): 564–566.

Banke, E. G., and S. D. Smith. 1973. Wind Stress on Arctic Sea Ice. *Journal of Geophysical Research* 78 (33): 7871–7883.

Carslaw, D. 2018. *openair: Tools for the Analysis of Air Pollution Data*. R package version 2.2.3. http://davidcarslaw.github.io/openair/.

Foltyn, E. P., and A. M. Tuthill. 1996. *Design of Ice Booms*. Cold Regions Technical Digest 96-1. Hanover, NH: U.S. Army Cold Regions Research and Engineering Laboratory.

Hardwood, D. G. 1993. Processes and Rates of Shoreline Bluff Recession at Lake Sharpe, South Dakota. M.S. Thesis, Texas A&M University.

Justus, C. G., W. R. Hargraves, A. Mikhail, and D. Graber. 1977. Methods for Estimating Wind Speed Frequency Distributions. *Journal of Applied Meteorology* 17:350–353.

Louis Berger. 2017. *Shoreline Stablization Summary Report: Lower Brule Sioux Reservation, South Dakota*. Rapid City, SD: Louis Berger.

Millard, S. 2017. *EvnStats: Package for Enironmental Statistics, Including US EPA Guidance*. R package version 2.3.0. http://www.probstatinfo.com.

Nelson, M. 1988. *Big Bend Project Design Winds: Preliminary Study*. U.S. Army Corps of Engineers.

Palutikof, J. P., B. B. Brabson, D. H. Lister, and S. T. Adcock. 1999. A Review of Methods to Calculate Extreme Wind Speeds. *Meteorological Applications* 6:119–132.

Schlichting, H. 1979. *Boundary Layer Theory*. 7th ed. New York: Mcgraw-Hill.

Seers, B. 2017. *fetchR: Calculate Wind Fetch in R*. R package version 2.1-0. https://cran.r-project.org/package=fetchR.

Simiu, E., and N. A. Heckert. 1995. *Extreme Wind Distribution Tails: A 'Peaks Over Threshold' Approach*. NIST Building Science Series 174. Gaithersburg, MD: U.S. Department of Commerce, National Institue of Standards and Technology.

Thompson, R. F. 2013. *Nearshore Bathymetric Mapping along a 7-Mile Reach of Lake Sharpe Shoreline near Lower Brule, South Dakota*. Scientific Investigation Map 3307. Reston, VA: Department of the Interior, U.S. Geological Survey.

USACE (U.S. Army Corps of Engineers). 2006. *Engineering and Design: Ice Engineering*. EM 1110-2-1612, Washington, D.C.: Department of the Army, U.S. Army Corps of Engineers.

Appendix A: Ice Cover Data

MRBWM Freeze-up and Breakup Dates			
Big Bend Reservoir			
	Froze	Broke-Up	No. of Days
1962 - 1963	31 DEC.	18 MAR.	47
1963 - 1964	12 DEC.	23 MAR.	101
1964 - 1965	15 DEC.	19 APR.	124
1965 - 1966	31 DEC.	29 MAR.	88
1966 - 1967	11 DEC.	29 MAR.	108
1967 - 1968	21 DEC.	19 MAR.	88
1968 - 1969	14 DEC.	13 APR.	119
1969 - 1970	28 DEC.	8 APR.	100
1970 - 1971	14 DEC.	31 MAR.	107
1971 - 1972	17 DEC.	24 MAR.	97
1972 - 1973	7 DEC.	13 MAR.	86
1973 - 1974	16 DEC.	19 MAR.	93
1974 - 1975	24 DEC.	14 APR.	110
1975 - 1976	14 DEC.	19 MAR.	95
1976 - 1977	29 NOV.	1 APR.	122
1977 - 1978	7 DEC.	11 APR.	124
1978 - 1979	14 DEC.	17 APR.	123
1979 - 1980	1 FEB.	7 APR.	66
1980 - 1981	9 FEB.	18 MAR.	46
1981 - 1982	30 DEC.	8 APR.	98
1982 - 1983	Did not freeze over		
1983 - 1984	20 DEC.		–
1984 - 1985		3 APR.	–
1985 - 1986	1 DEC.	31 MAR.	120
1986 - 1987	23 DEC.	7 MAR.	84
1987 - 1988	25 DEC.	31 MAR.	96
1988 - 1989	26 DEC.	6 APR.	100
1989 - 1990	12 DEC.	21 MAR.	99
1990 - 1991	19 DEC.	2 APR.	103
1991 - 1992	4 DEC.	16 MAR.	102
1992 - 1993	20 DEC.	1 APR.	99
1993 - 1994	20 DEC.	7 APR.	107
1994 - 1995	18 DEC.	22 MAR.	95
1995 - 1996	9 DEC.	11 APR.	122
1996 - 1997	26 NOV.	3 APR.	128
1997 - 1998	4 JAN.	25 FEB	52
(Refroze)	28 FEB	22 MAR	23
Total			75
1998 - 1999	31 DEC	20 MAR	80
1999 - 2000	2 FEB	3 MAR	31
2000 - 2001	8 DEC	20 APR	133
2001 - 2002	25 DEC	7 APR	103
2002 - 2003	23 DEC	25 MAR	92
2003 - 2004	23 DEC	16 MAR	85
2004 - 2005	23 DEC	12 MAR	80
2005 - 2006	22 DEC	13 MAR	81
2006 - 2007	13 DEC	26 MAR	103
2007 - 2008	19 DEC	7 APR	109
2008 - 2009	18 DEC	6 APR	109
2009 - 2010	16 DEC	6 APR	111
2010 - 2011	14 DEC	7 APR	114
2011-2012	19-Jan	16-Mar	57
2012-2013	26-Dec	08-Apr	103
2013-2014	09-Dec	09-Apr	121
2014-2015	30-Dec	16-Mar	76
2015-2016	29-Dec	11-Mar	73
2016-2017	15-Dec	23-Mar	98

Tribe Freeze-up and Break-up Dates			
Ice Records on Lake Sharpe			
Rod Vaughn (formerly COE Park Ranger, Big Bend Office)			
12/14/2017 compiled by Joel Bich, Lower Brule Sioux Tribe			
Following observations were made on lower 15 miles of Lake Sharpe			
Dates are from 100% ice-up to 100% ice-out			
	Ice-Up	Ice-Out	Days of Ice Cover
	12/25/01	4/7/2002	104
	12/23/02	3/25/2003	92
	12/23/03	3/20/2004	87
	12/23/04	--	--
	11/30/05	3/13/2006	103
	01/02/07	3/26/2007	83
	12/15/08	4/6/2008	112
		4/6/2010	--
	12/07/10	4/9/2011	123
	01/13/12	3/16/2012	62
	12/24/12	4/15/2013	112
	12/07/13	4/10/2014	124
	11/30/14	3/17/2015	107
	12/28/15	3/13/2016	75
	12/15/16	--	--
	12/27/17		
Average	12/20	3/26	99

Appendix B: Ice Thickness and Strength Information

The following email correspondence was from Joel Bich, biologist, Lower Brule Sioux Tribe, Lower Brule, South Dakota, on 18 January 2018.

> Jeremy: I visited this morning with Jim Brouse who works for the Tribe in our construction enterprise; he has been living here and has been an avid ice fisherman since 1974 - he is a carpenter and a reliable source so I would trust his knowledge, by far the local ice expert. He shared the following with me which hopefully will be helpful along with the ice-up and ice-out data I previously sent.
>
> Since 1974 average ice depth: 24 inches
> In last 8-10 years, average ice depth: 18 inches
> Thinnest maximum ice depth since 1976: 12 inches
> Thickest maximum ice depth since 1976: 42 inches (1977)
>
> Jim also indicated that from 1976 through the mid-1990s (before ATVs), he and two other guys would routinely drive a caravan of 3 pickup trucks all the way from Lower Brule across the reservoir to a fishing spot near the east shoreline - they preferred at least 2 ft of ice to do this and were close to that every year. No comment on the wisdom of this activity…
>
> From my experience on the ice over the last 5 years, I would agree that it has averaged about 18 inches thick. Also, I have observed that as winter declines and spring approaches, the ice doesn't lose all that much of its thickness but rather becomes more porous. The factor that determines the latest safe ice for ice fishing is not the ice thickness, but the porosity or "rottenness" of the ice. We judge this by how fast melt water runs through the ice instead of pooling on top, by the "softness" of the ice while drilling through it with an ice auger, bubbles forming in the ice column, and by the color of the ice - it gets much darker as it weakens. For example, last year the last day of ice fishing was Feb. 16, the ice was still about 18 inches thick but very soft; ice-out was about an month later so presumably the ice had thinned but I am not sure how much. I have observed spring ice shove here when the ice was at least a foot thick in the spring.

Also, ice shove does not occur only in the spring, but also during the winter with temperature fluctuations and changes in ice and river flows - we continually see pressure ridges forming and changing as well as ice shoving up on the shoreline causing damage anytime during the winter. But, I would suggest that the majority of shoreline damage occurs in the late winter, early spring.

I imagine you need figures regarding ice weights, densities, etc. so if there is any data I can collect this year that would be helpful, please let me know and I would be glad to - always looking for an excuse to get outside. Right now the ice is from 8-10 inches thick.

Thanks, Joel

Appendix C: Pierre Wind Speed Summary Tables

Pierre, SD Regional Airport (1987-2016) 1.01 yr, 1 hr duration Maximum Wind (mph)													
Dir	Jan	Feb	Mar	Apr	May	Jun	Jul	Aug	Sep	Oct	Nov	Dec	Annual
N	12.7	11.2	16.2	14.3	14.8	13.5	15.9	14.0	13.7	11.8	11.6	8.9	20.7
NNE	5.3	6.0	9.8	13.1	10.3	12.5	11.8	10.5	9.0	9.3	4.5	4.5	19.4
NE	6.8	12.5	10.8	14.2	12.5	12.8	12.1	12.3	8.9	7.8	6.3	5.8	20.7
ENE	6.8	8.2	11.2	14.7	13.2	12.9	12.3	11.8	9.3	8.3	6.3	8.5	20.0
E	7.3	9.3	14.8	16.1	16.4	13.5	13.8	14.1	13.0	10.8	10.1	7.7	20.6
ESE	14.6	14.2	19.7	18.0	18.9	15.2	16.0	16.5	16.1	14.7	13.8	12.7	21.2
SE	9.7	10.3	14.0	16.8	20.2	14.1	17.1	17.5	17.3	15.0	13.7	7.7	25.0
SSE	6.2	7.2	12.4	12.7	14.4	14.8	15.0	16.4	18.1	9.8	6.0	5.5	21.6
S	6.2	4.9	3.0	7.1	8.1	10.6	10.8	9.0	9.3	6.7	5.6	4.0	16.5
SSW	6.7	5.9	4.3	6.7	5.6	8.3	6.5	7.5	5.0	7.6	6.0	5.9	17.0
SW	9.2	7.2	10.3	11.6	9.3	10.4	6.5	7.6	8.0	8.1	7.6	10.0	16.1
WSW	13.4	12.6	11.4	10.7	10.0	11.3	10.3	5.7	7.8	14.0	9.9	13.0	19.6
W	15.5	15.4	12.4	16.6	14.8	12.5	8.6	10.2	12.1	16.5	15.0	17.3	27.3
WNW	23.3	18.0	13.7	21.1	19.0	16.8	13.8	12.3	20.4	20.4	23.0	21.5	32.2
NW	20.1	18.9	21.7	20.5	18.0	16.0	16.5	16.1	17.9	19.6	18.5	22.2	32.1
NNW	18.1	14.7	16.2	18.9	17.5	13.6	11.3	16.9	16.9	16.6	10.7	12.2	27.0
All	23.3	21.3	24.2	24.3	22.6	21.3	21.8	21.1	24.1	25.4	24.1	24.0	32.7

Pierre, SD Regional Airport (1987-2016) 2 yr, 1 hr duration Maximum Wind (mph)													
Dir	Jan	Feb	Mar	Apr	May	Jun	Jul	Aug	Sep	Oct	Nov	Dec	Annual
N	20.3	21.7	24.7	26.5	22.2	22.4	23.0	23.3	22.4	21.7	19.5	19.8	31.0
NNE	13.2	18.6	22.1	23.1	20.5	20.9	19.0	19.8	18.1	18.4	14.6	14.3	30.2
NE	15.5	17.9	21.2	23.8	21.7	20.3	19.6	18.8	16.6	16.4	14.1	14.5	28.5
ENE	17.0	18.3	19.9	22.3	20.7	20.9	19.0	19.2	16.5	16.7	14.9	15.9	26.9
E	19.3	20.8	22.4	21.9	22.0	21.5	21.3	20.3	18.9	18.7	16.7	17.1	27.9
ESE	21.0	21.5	22.6	25.5	23.7	22.0	23.5	22.6	22.1	22.4	20.7	20.8	29.4
SE	19.7	21.2	22.8	26.2	25.2	23.7	22.9	24.3	24.3	24.2	20.7	20.1	30.4
SSE	15.1	16.5	22.0	24.7	25.6	23.0	23.3	24.1	26.0	21.6	19.6	14.6	30.6
S	9.3	11.0	13.7	17.4	17.9	16.6	18.0	18.7	18.1	16.0	12.3	10.9	25.9
SSW	10.9	11.7	12.6	15.2	16.0	14.8	14.5	15.7	15.6	14.5	12.8	11.4	22.9
SW	16.4	16.2	15.7	16.7	15.7	16.7	14.3	14.5	14.4	14.5	15.8	14.6	23.7
WSW	19.4	18.9	18.6	20.4	20.9	20.7	17.3	17.0	18.9	19.3	17.7	19.4	30.4
W	24.8	26.1	26.3	26.0	25.9	23.0	20.5	20.4	23.4	28.5	26.7	26.6	35.6
WNW	32.6	32.5	33.2	29.4	30.0	25.7	23.2	23.3	27.7	34.5	33.2	35.4	43.0
NW	34.0	33.2	32.4	31.0	28.9	24.8	23.8	23.5	29.2	33.9	32.3	32.4	40.2
NNW	28.1	24.9	29.9	27.9	25.8	23.2	23.3	21.3	25.1	26.3	26.5	27.2	35.6
All	36.7	34.9	36.1	35.6	33.9	32.3	29.7	30.9	32.6	37.4	35.7	37.3	43.8

Pierre, SD Regional Airport (1987-2016) 10 yr, 1 hr duration Maximum Wind (mph)													
Dir	Jan	Feb	Mar	Apr	May	Jun	Jul	Aug	Sep	Oct	Nov	Dec	Annual
N	29.4	27.8	29.2	35.6	29.3	29.5	30.3	31.9	27.7	31.7	27.1	29.1	38.9
NNE	22.8	22.6	30.2	33.5	30.1	28.9	24.2	26.9	24.2	26.9	21.9	24.4	37.9
NE	21.3	23.9	27.1	32.6	30.9	27.8	25.1	25.1	22.0	25.5	20.8	22.4	36.0
ENE	23.1	23.5	25.6	28.5	27.9	27.1	25.6	22.9	22.4	21.3	22.1	22.0	31.3
E	25.0	24.1	28.2	27.9	28.1	27.0	26.4	23.5	25.6	25.5	22.6	23.6	32.8
ESE	26.2	27.5	28.8	31.4	29.8	28.1	28.1	27.6	28.5	27.2	26.1	26.6	35.6
SE	26.3	27.2	29.7	33.8	30.1	29.5	27.8	28.9	31.0	31.6	26.5	26.6	36.5
SSE	21.2	21.7	31.2	34.2	31.4	28.4	27.9	30.1	32.4	31.3	26.2	23.7	37.0
S	14.7	16.7	22.5	24.5	25.9	24.4	25.9	27.0	28.8	22.2	19.3	18.8	33.6
SSW	15.0	18.5	21.7	21.8	24.2	21.2	18.3	22.2	21.3	22.1	18.4	15.6	28.4
SW	19.6	20.3	21.8	22.5	21.3	24.6	22.1	20.6	18.8	22.9	19.3	19.4	30.7
WSW	23.4	26.2	26.5	28.8	29.7	30.5	28.2	23.2	26.7	25.6	26.2	25.3	38.1
W	30.8	36.7	37.4	35.8	35.0	31.7	30.6	29.9	33.1	38.0	33.6	36.3	42.9
WNW	39.8	41.9	42.1	40.0	37.3	34.7	29.8	33.6	35.4	45.7	42.2	45.5	50.6
NW	41.8	40.5	40.8	38.1	35.8	33.0	30.7	33.9	35.8	43.2	40.6	40.7	46.5
NNW	37.3	33.5	37.2	34.7	32.9	31.8	32.6	29.3	29.7	32.5	33.5	32.9	41.6
All	43.3	42.9	44.3	44.7	39.6	38.5	36.2	39.8	39.4	46.3	43.3	46.0	50.8

Pierre, SD Regional Airport (1987-2016) 20 yr, 1 hr duration Maximum Wind (mph)													
Dir	Jan	Feb	Mar	Apr	May	Jun	Jul	Aug	Sep	Oct	Nov	Dec	Annual
N	33.3	29.5	30.4	38.4	32.0	31.9	33.0	35.0	29.3	35.4	30.0	32.3	41.5
NNE	26.7	23.1	32.5	37.6	33.7	31.9	25.8	29.2	26.0	29.9	23.9	28.0	40.3
NE	22.9	26.3	28.7	35.8	34.4	30.6	26.9	27.4	23.7	29.1	23.1	25.2	38.8
ENE	24.6	24.7	27.2	30.7	30.6	29.2	28.0	23.9	24.4	22.4	24.4	24.1	32.6
E	26.2	24.5	30.1	30.1	30.4	28.7	27.9	24.4	28.4	28.0	24.7	25.6	34.3
ESE	27.9	29.5	31.8	33.4	32.3	30.2	29.5	29.4	31.1	28.7	27.9	28.4	37.6
SE	28.2	28.6	32.0	36.4	31.9	31.1	29.5	30.3	33.5	34.1	28.6	28.1	38.9
SSE	23.0	23.0	34.6	37.3	32.8	30.1	29.1	32.1	34.5	34.6	27.4	27.0	39.1
S	17.3	18.8	24.9	26.5	28.6	27.8	29.0	29.8	33.3	24.0	21.9	22.0	36.3
SSW	16.5	21.3	25.2	23.8	26.8	23.6	19.2	24.3	22.6	25.0	20.3	16.9	30.4
SW	20.3	21.1	24.3	24.9	23.3	28.0	24.9	22.7	20.1	26.5	20.0	21.2	33.3
WSW	24.6	29.3	29.6	31.7	32.6	34.2	33.4	24.6	29.0	28.1	29.7	27.3	40.6
W	32.6	40.7	41.0	39.6	38.0	34.7	33.9	33.4	36.5	41.2	35.6	40.1	45.4
WNW	42.2	44.7	43.9	44.5	39.5	38.2	31.8	37.4	38.3	49.3	45.4	48.7	53.0
NW	43.9	42.3	43.6	40.3	37.8	36.0	33.2	38.5	37.5	46.0	42.9	43.5	48.6
NNW	40.7	36.5	39.1	37.0	35.3	34.9	35.6	33.1	31.0	34.3	34.9	33.9	43.6
All	45.0	45.1	46.8	47.8	41.1	40.3	38.4	42.9	41.8	49.3	45.5	48.7	52.9

Pierre, SD Regional Airport (1987-2016) 50 yr, 1 hr duration Maximum Wind (mph)													
Dir	Jan	Feb	Mar	Apr	May	Jun	Jul	Aug	Sep	Oct	Nov	Dec	Annual
N	38.6	31.2	31.7	41.8	35.4	34.8	36.6	39.0	31.0	40.3	33.6	36.1	44.7
NNE	32.1	23.4	35.1	42.9	38.1	35.7	27.8	32.0	28.1	33.8	26.0	32.6	43.1
NE	24.8	29.6	30.3	39.8	39.0	34.2	29.0	30.4	25.6	33.8	25.8	28.6	42.5
ENE	26.2	25.9	29.1	33.3	34.0	31.7	31.2	24.8	26.8	23.7	27.3	26.6	34.2
E	27.2	24.8	32.4	33.0	33.6	30.7	29.7	25.4	32.0	31.0	27.3	27.7	36.0
ESE	30.0	32.0	36.1	35.8	35.7	33.0	31.0	31.5	34.4	30.3	30.1	30.6	40.0
SE	30.3	30.1	34.8	39.5	34.3	33.0	31.6	32.0	36.7	37.1	31.1	29.5	42.0
SSE	24.9	24.3	38.9	41.0	34.3	32.0	30.5	34.5	37.2	38.4	28.5	31.2	41.6
S	21.2	21.3	27.5	28.7	31.7	32.5	33.2	33.3	39.5	25.9	25.3	26.2	39.6
SSW	18.5	25.1	29.7	26.2	29.6	26.7	20.0	26.8	23.8	29.0	22.6	18.5	33.0
SW	20.9	21.9	27.7	28.1	25.8	32.8	28.6	25.4	21.6	31.7	20.6	23.5	36.6
WSW	26.0	33.4	33.8	35.2	36.1	39.1	41.1	25.9	31.6	31.5	34.2	30.0	43.5
W	34.7	45.9	45.3	44.7	41.8	38.4	37.9	37.8	40.7	45.1	37.7	45.0	48.7
WNW	45.3	47.5	45.5	50.7	42.0	42.2	34.2	42.2	42.1	52.8	48.1	51.7	55.9
NW	46.2	44.2	47.0	42.9	40.2	39.9	36.4	45.0	39.5	49.1	45.5	47.0	51.2
NNW	44.9	40.2	41.1	39.7	38.3	38.8	39.1	38.7	32.4	36.4	36.1	34.8	45.8
All	46.7	47.5	49.8	51.6	42.7	42.2	41.1	47.0	44.6	52.8	48.1	51.7	55.3

Pierre, SD Regional Airport (1987-2016) 100 yr, 1 hr duration Maximum Wind (mph)													
Dir	Jan	Feb	Mar	Apr	May	Jun	Jul	Aug	Sep	Oct	Nov	Dec	Annual
N	42.8	32.3	32.6	44.1	37.9	36.9	39.4	42.0	32.2	44.1	36.4	38.8	46.6
NNE	36.2	23.5	36.7	45.1	41.4	38.5	29.1	33.9	29.5	36.7	27.4	35.9	45.1
NE	25.9	32.1	31.3	42.8	42.5	37.0	30.5	32.7	26.9	37.4	27.8	31.0	45.2
ENE	27.1	26.6	30.4	35.2	35.2	33.5	33.6	25.4	28.5	24.4	29.3	28.4	35.2
E	27.8	24.9	34.0	35.3	36.0	32.1	30.9	26.0	34.9	33.2	29.3	29.2	37.2
ESE	31.5	33.8	39.7	37.5	38.4	35.0	32.0	33.0	36.9	31.5	31.7	32.0	41.7
SE	31.6	31.0	36.7	41.8	36.0	34.2	33.2	33.2	39.1	39.3	33.0	30.3	44.3
SSE	26.1	25.1	42.2	43.3	35.3	33.3	31.3	36.3	39.1	41.2	29.0	34.3	43.3
S	24.6	23.2	29.0	30.2	34.0	36.4	36.4	35.7	42.0	27.2	27.9	29.4	42.0
SSW	20.0	28.1	33.2	27.8	31.6	29.0	20.4	28.5	24.4	32.0	24.2	19.6	34.9
SW	21.3	22.3	30.4	30.6	27.7	36.6	31.4	27.3	22.5	36.0	20.9	25.4	39.1
WSW	27.0	36.6	37.1	37.8	38.5	42.9	43.1	26.6	33.3	34.2	37.8	31.9	45.5
W	36.1	49.0	48.3	48.5	43.7	41.0	40.7	41.0	43.7	47.8	39.0	48.8	51.1
WNW	47.5	49.0	46.4	54.3	43.7	43.4	35.8	45.8	44.9	55.3	49.9	53.8	57.9
NW	47.6	45.3	49.5	44.6	41.7	42.7	38.9	49.9	40.8	51.2	47.1	49.5	53.0
NNW	47.7	42.9	42.3	41.7	40.6	41.6	41.5	43.3	33.3	37.8	36.7	35.2	47.7
All	47.8	49.0	51.9	54.3	43.7	43.4	43.1	49.9	46.7	55.3	49.9	53.8	56.9

Appendix D: Outlier Test

Results of Outlier Test

Test Method: Rosner's Test for Outliers
Hypothesized Distribution: Normal
Data: df
Sample Size: 30
Test Statistics: R.1 = 3.209165
R.2 = 2.893218
R.3 = 2.499541
Test Statistic Parameter: k = 3

Alternative Hypothesis: Up to 3 observations are not from the same Distribution.

Type I Error: 5%

Number of Outliers Detected: 2

	i	Mean.i	SD.i	Value	Obs.Num	R.i+1	lambda.i+1	Outlier
1	159.1855	58.82824	347.9750	13	3.209165	2.908473		TRUE
2	152.6755	47.61887	290.4472	28	2.893218	2.892705		TRUE
3	147.7551	40.29182	248.4661	19	2.499541	2.876209		FALSE

Appendix E: Summary Tables for Ice Thickness Probabilities

Lake Sharpe Genaralized Frequency Analysis Annual Maximum Ice Thickness (in.)			
		Confidence Limits	
Percent Chance Exceedance	Computed Curve	0.05	0.95
0.2	35.5	41.5	31.6
0.5	33.8	39.1	30.2
1	32.4	37.2	29.1
2	30.7	35.0	27.7
5	28.2	31.8	25.7
10	25.9	28.9	23.8
20	23.2	25.5	21.4
50	18.1	19.5	16.9
80	13.5	14.6	12.3
90	11.4	12.4	10.1
95	9.7	10.8	8.5
99	7.1	8.2	5.9

Lake Sharpe Genaralized Frequency Analysis December Maximum Ice Thickness (in.)			
		Confidence Limits	
Percent Chance Exceedance	Computed Curve	0.05	0.95
0.2	22.2	29.1	18.0
0.5	21.1	27.4	17.2
1	20.0	25.8	16.4
2	18.8	24.0	15.5
5	16.7	21.0	13.9
10	14.7	18.2	12.4
20	12.2	14.8	10.4
50	7.8	9.1	6.7
80	4.3	5.0	3.5
90	2.9	3.5	2.3
95	2.0	2.5	1.5
99	0.9	1.3	0.6

Lake Sharpe Genaralized Frequency Analysis January Maximum Ice Thickness (in.)			
		Confidence Limits	
Percent Chance Exceedance	Computed Curve	0.05	0.95
0.2	27.9	32.2	25.0
0.5	27.0	30.9	24.3
1	26.1	29.8	23.5
2	25.1	28.4	22.7
5	23.4	26.3	21.3
10	21.8	24.2	20.0
20	19.7	21.7	18.2
50	15.6	16.8	14.5
80	11.6	12.5	10.6
90	9.6	10.6	8.6
95	8.1	9.1	7.1
99	5.7	6.7	4.7

Lake Sharpe Genaralized Frequency Analysis February Maximum Ice Thickness (in.)			
		Confidence Limits	
Percent Chance Exceedance	Computed Curve	0.05	0.95
0.2	35.9	42.5	31.7
0.5	34.0	39.8	30.1
1	32.4	37.6	28.8
2	30.6	35.2	27.4
5	27.8	31.6	25.1
10	25.4	28.4	23.1
20	22.4	24.8	20.6
50	17.2	18.6	15.9
80	12.5	13.6	11.3
90	10.4	11.5	9.2
95	8.8	9.8	7.6
99	6.3	7.3	5.2

Lake Sharpe Genaralized Frequency Analysis March Maximum Ice Thickness (in.)			
		Confidence Limits	
Percent Chance Exceedance	Computed Curve	0.05	0.95
0.2	36.2	46.1	29.9
0.5	35.0	44.3	29.1
1	33.8	42.6	28.1
2	32.2	40.4	27.0
5	29.4	36.4	24.8
10	26.6	32.4	22.6
20	22.7	27.2	19.5
50	15.0	17.4	13.1
80	8.3	9.7	7.0
90	5.7	6.8	4.6
95	4.0	4.9	3.0
99	1.9	2.5	1.2

Lake Sharpe Genaralized Frequency Analysis April Maximum Ice Thickness (in.)			
		Confidence Limits	
Percent Chance Exceedance	Computed Curve	0.05	0.95
0.2	53.0	103.8	31.7
0.5	42.3	80.0	25.9
1	34.6	63.5	21.7
2	27.4	48.5	17.6
5	18.7	31.3	12.4
10	12.9	20.5	8.9
20	7.9	11.8	5.6
50	2.7	3.7	2.0
80	0.7	1.1	0.5
90	0.4	0.5	0.2
95	0.2	0.3	0.1
99	0.0	0.1	0.0

Appendix F: Reservoir Velocity Information

The following email correspondence was from Email Correspondence from Roger Kay, chief of the Hydraulics Section, USACE Omaha District, Omaha, Nebraska, on 14 December 2017.

> Jeremy,
>
> I thought I had already replied to this, my apologies. Fortunately, I still had velocity values written on a sticky on my desk, so I don't have to go hunting again.
>
> The following values represent average velocity in the reservoir between R.M. 1000.6 and R.M. 993.8:
>
> 25kcfs - 0.1 fps
> 60kcfs - 0.2-0.3 fps
> 100kcfs - 0.2-0.4 fps
> 200kcfs - 0.5-0.8 fps
> 300kcfs - 0.7-1.3 fps
> 400kcfs - 0.9-1.6 fps
>
> I realize you probably aren't interested in velocities for discharge greater than Oahe powerplant release (~60kcfs), but just in case, here they are. These are based on a pool of 1420, and they won't vary with minor fluctuations in pool that we typically see. If you require any additional information, please let me know.
>
> Roger

Appendix G: Summary of Ice Force Variables Used in Calculations

Lake Sharpe Drag Coefficients used in Force Calculation

	December						January						February						March						April					
Return Period	**1.01-yr**	**2-yr**	**10-yr**	**20-yr**	**50-yr**	**100-yr**	**1.01-yr**	**2-yr**	**10-yr**	**20-yr**	**50-yr**	**100-yr**	**1.01-yr**	**2-yr**	**10-yr**	**20-yr**	**50-yr**	**100-yr**	**1.01-yr**	**2-yr**	**10-yr**	**20-yr**	**50-yr**	**100-yr**	**1.01-yr**	**2-yr**	**10-yr**	**20-yr**	**50-yr**	**100-yr**
Percent Chance Exceedance	**0.9901**	**0.5**	**0.1**	**0.05**	**0.02**	**0.01**	**0.9901**	**0.5**	**0.1**	**0.05**	**0.02**	**0.01**	**0.9901**	**0.5**	**0.1**	**0.05**	**0.02**	**0.01**	**0.9901**	**0.5**	**0.1**	**0.05**	**0.02**	**0.01**	**0.9901**	**0.5**	**0.1**	**0.05**	**0.02**	**0.01**
RM992.1	0.0022	0.0022	0.0022	0.0022	0.0022	0.0022	0.0022	0.0022	0.0022	0.0022	0.0022	0.0022	0.0022	0.0022	0.0022	0.0022	0.0022	0.0022	0.0022	0.0022	0.0022	0.0022	0.0022	0.0022	0.0022	0.0022	0.0022	0.0022	0.0022	0.0022
RM992.3	0.0022	0.0022	0.0022	0.0022	0.0022	0.0022	0.0022	0.0022	0.0022	0.0022	0.0022	0.0022	0.0022	0.0022	0.0022	0.0022	0.0022	0.0022	0.0022	0.0022	0.0022	0.0022	0.0022	0.0022	0.0022	0.0022	0.0022	0.0022	0.0022	0.0022
RM992.5	0.0022	0.0022	0.0022	0.0022	0.0022	0.0022	0.0022	0.0022	0.0022	0.0022	0.0022	0.0022	0.0022	0.0022	0.0022	0.0022	0.0022	0.0022	0.0022	0.0022	0.0022	0.0022	0.0022	0.0022	0.0022	0.0022	0.0022	0.0022	0.0022	0.0022
RM992.6	0.0022	0.0022	0.0022	0.0022	0.0022	0.0022	0.0022	0.0022	0.0022	0.0022	0.0022	0.0022	0.0022	0.0022	0.0022	0.0022	0.0022	0.0022	0.0022	0.0022	0.0022	0.0022	0.0022	0.0022	0.0022	0.0022	0.0022	0.0022	0.0022	0.0022
RM992.7	0.0022	0.0022	0.0022	0.0022	0.0022	0.0022	0.0022	0.0022	0.0022	0.0022	0.0022	0.0022	0.0022	0.0022	0.0022	0.0022	0.0022	0.0022	0.0022	0.0022	0.0022	0.0022	0.0022	0.0022	0.0022	0.0022	0.0022	0.0022	0.0022	0.0022
RM992.9	0.0022	0.0022	0.0022	0.0022	0.0022	0.0022	0.0022	0.0022	0.0022	0.0022	0.0022	0.0022	0.0022	0.0022	0.0022	0.0022	0.0022	0.0022	0.0022	0.0022	0.0022	0.0022	0.0022	0.0022	0.0022	0.0022	0.0022	0.0022	0.0022	0.0022
RM993.2	0.0022	0.0022	0.0022	0.0022	0.0022	0.0022	0.0022	0.0022	0.0022	0.0022	0.0022	0.0022	0.0022	0.0022	0.0022	0.0022	0.0022	0.0022	0.0022	0.0022	0.0022	0.0022	0.0022	0.0022	0.0022	0.0022	0.0022	0.0022	0.0022	0.0022
RM993.3	0.0022	0.0022	0.0022	0.0022	0.0022	0.0022	0.0022	0.0022	0.0022	0.0022	0.0022	0.0022	0.0022	0.0022	0.0022	0.0022	0.0022	0.0022	0.0022	0.0022	0.0022	0.0022	0.0022	0.0022	0.0022	0.0022	0.0022	0.0022	0.0022	0.0022
RM993.6	0.0022	0.0022	0.0022	0.0022	0.0022	0.0022	0.0022	0.0022	0.0022	0.0022	0.0022	0.0022	0.0022	0.0022	0.0022	0.0022	0.0022	0.0022	0.0022	0.0022	0.0022	0.0022	0.0022	0.0022	0.0022	0.0022	0.0022	0.0022	0.0022	0.0022
RM993.8	0.0022	0.0022	0.0022	0.0022	0.0022	0.0022	0.0022	0.0022	0.0022	0.0022	0.0022	0.0022	0.0022	0.0022	0.0022	0.0022	0.0022	0.0022	0.0022	0.0022	0.0022	0.0022	0.0022	0.0022	0.0022	0.0022	0.0022	0.0022	0.0022	0.0022
RM994.1	0.0022	0.0022	0.0022	0.0022	0.0022	0.0022	0.0022	0.0022	0.0022	0.0022	0.0022	0.0022	0.0022	0.0022	0.0022	0.0022	0.0022	0.0022	0.0022	0.0022	0.0022	0.0022	0.0022	0.0022	0.0022	0.0022	0.0022	0.0022	0.0022	0.0022
RM994.3	0.0022	0.0022	0.0022	0.0022	0.0022	0.0022	0.0022	0.0022	0.0022	0.0022	0.0022	0.0022	0.0022	0.0022	0.0022	0.0022	0.0022	0.0022	0.0022	0.0022	0.0022	0.0022	0.0022	0.0022	0.0022	0.0022	0.0022	0.0022	0.0022	0.0022
RM994.5	0.0022	0.0022	0.0022	0.0022	0.0022	0.0022	0.0022	0.0022	0.0022	0.0022	0.0022	0.0022	0.0022	0.0022	0.0022	0.0022	0.0022	0.0022	0.0022	0.0022	0.0022	0.0022	0.0022	0.0022	0.0022	0.0022	0.0022	0.0022	0.0022	0.0022
RM994.8	0.0022	0.0022	0.0022	0.0022	0.0022	0.0022	0.0022	0.0022	0.0022	0.0022	0.0022	0.0022	0.0022	0.0022	0.0022	0.0022	0.0022	0.0022	0.0022	0.0022	0.0022	0.0022	0.0022	0.0022	0.0022	0.0022	0.0022	0.0022	0.0022	0.0022
RM995.1	0.0022	0.0022	0.0022	0.0022	0.0022	0.0022	0.0022	0.0022	0.0022	0.0022	0.0022	0.0022	0.0022	0.0022	0.0022	0.0022	0.0022	0.0022	0.0022	0.0022	0.0022	0.0022	0.0022	0.0022	0.0022	0.0022	0.0022	0.0022	0.0022	0.0022
RM995.3	0.0022	0.0022	0.0022	0.0022	0.0022	0.0022	0.0022	0.0022	0.0022	0.0022	0.0022	0.0022	0.0022	0.0022	0.0022	0.0022	0.0022	0.0022	0.0022	0.0022	0.0022	0.0022	0.0022	0.0022	0.0022	0.0022	0.0022	0.0022	0.0022	0.0022
RM995.4	0.0022	0.0022	0.0022	0.0022	0.0022	0.0022	0.0022	0.0022	0.0022	0.0022	0.0022	0.0022	0.0022	0.0022	0.0022	0.0022	0.0022	0.0022	0.0022	0.0022	0.0022	0.0022	0.0022	0.0022	0.0022	0.0022	0.0022	0.0022	0.0022	0.0022
RM995.7	0.0022	0.0022	0.0022	0.0022	0.0022	0.0022	0.0022	0.0022	0.0022	0.0022	0.0022	0.0022	0.0022	0.0022	0.0022	0.0022	0.0022	0.0022	0.0022	0.0022	0.0022	0.0022	0.0022	0.0022	0.0022	0.0022	0.0022	0.0022	0.0022	0.0022
RM995.9	0.0022	0.0022	0.0022	0.0022	0.0022	0.0022	0.0022	0.0022	0.0022	0.0022	0.0022	0.0022	0.0022	0.0022	0.0022	0.0022	0.0022	0.0022	0.0022	0.0022	0.0022	0.0022	0.0022	0.0022	0.0022	0.0022	0.0022	0.0022	0.0022	0.0022
RM996.1	0.0022	0.0022	0.0022	0.0022	0.0022	0.0022	0.0022	0.0022	0.0022	0.0022	0.0022	0.0022	0.0022	0.0022	0.0022	0.0022	0.0022	0.0022	0.0022	0.0022	0.0022	0.0022	0.0022	0.0022	0.0022	0.0022	0.0022	0.0022	0.0022	0.0022
RM996.3	0.0022	0.0022	0.0022	0.0022	0.0022	0.0022	0.0022	0.0022	0.0022	0.0022	0.0022	0.0022	0.0022	0.0022	0.0022	0.0022	0.0022	0.0022	0.0022	0.0022	0.0022	0.0022	0.0022	0.0022	0.0022	0.0022	0.0022	0.0022	0.0022	0.0022
RM996.5	0.0022	0.0022	0.0022	0.0022	0.0022	0.0022	0.0022	0.0022	0.0022	0.0022	0.0022	0.0022	0.0022	0.0022	0.0022	0.0022	0.0022	0.0022	0.0022	0.0022	0.0022	0.0022	0.0022	0.0022	0.0022	0.0022	0.0022	0.0022	0.0022	0.0022
RM996.7	0.0022	0.0022	0.0022	0.0022	0.0022	0.0022	0.0022	0.0022	0.0022	0.0022	0.0022	0.0022	0.0022	0.0022	0.0022	0.0022	0.0022	0.0022	0.0022	0.0022	0.0022	0.0022	0.0022	0.0022	0.0022	0.0022	0.0022	0.0022	0.0022	0.0022
RM997.4	0.0022	0.0022	0.0022	0.0022	0.0022	0.0022	0.0022	0.0022	0.0022	0.0022	0.0022	0.0022	0.0022	0.0022	0.0022	0.0022	0.0022	0.0022	0.0022	0.0022	0.0022	0.0022	0.0022	0.0022	0.0022	0.0022	0.0022	0.0022	0.0022	0.0022
RM997.9	0.0022	0.0022	0.0022	0.0022	0.0022	0.0022	0.0022	0.0022	0.0022	0.0022	0.0022	0.0022	0.0022	0.0022	0.0022	0.0022	0.0022	0.0022	0.0022	0.0022	0.0022	0.0022	0.0022	0.0022	0.0022	0.0022	0.0022	0.0022	0.0022	0.0022
RM997	0.0022	0.0022	0.0022	0.0022	0.0022	0.0022	0.0022	0.0022	0.0022	0.0022	0.0022	0.0022	0.0022	0.0022	0.0022	0.0022	0.0022	0.0022	0.0022	0.0022	0.0022	0.0022	0.0022	0.0022	0.0022	0.0022	0.0022	0.0022	0.0022	0.0022
RM998.3	0.0022	0.0022	0.0022	0.0022	0.0022	0.0022	0.0022	0.0022	0.0022	0.0022	0.0022	0.0022	0.0022	0.0022	0.0022	0.0022	0.0022	0.0022	0.0022	0.0022	0.0022	0.0022	0.0022	0.0022	0.0022	0.0022	0.0022	0.0022	0.0022	0.0022
RM998.6	0.0022	0.0022	0.0022	0.0022	0.0022	0.0022	0.0022	0.0022	0.0022	0.0022	0.0022	0.0022	0.0022	0.0022	0.0022	0.0022	0.0022	0.0022	0.0022	0.0022	0.0022	0.0022	0.0022	0.0022	0.0022	0.0022	0.0022	0.0022	0.0022	0.0022
RM998.9	0.0022	0.0022	0.0022	0.0022	0.0022	0.0022	0.0022	0.0022	0.0022	0.0022	0.0022	0.0022	0.0022	0.0022	0.0022	0.0022	0.0022	0.0022	0.0022	0.0022	0.0022	0.0022	0.0022	0.0022	0.0022	0.0022	0.0022	0.0022	0.0022	0.0022
RM999.1	0.0022	0.0022	0.0022	0.0022	0.0022	0.0022	0.0022	0.0022	0.0022	0.0022	0.0022	0.0022	0.0022	0.0022	0.0022	0.0022	0.0022	0.0022	0.0022	0.0022	0.0022	0.0022	0.0022	0.0022	0.0022	0.0022	0.0022	0.0022	0.0022	0.0022
RM999.4	0.0022	0.0022	0.0022	0.0022	0.0022	0.0022	0.0022	0.0022	0.0022	0.0022	0.0022	0.0022	0.0022	0.0022	0.0022	0.0022	0.0022	0.0022	0.0022	0.0022	0.0022	0.0022	0.0022	0.0022	0.0022	0.0022	0.0022	0.0022	0.0022	0.0022
RM999.7	0.0022	0.0022	0.0022	0.0022	0.0022	0.0022	0.0022	0.0022	0.0022	0.0022	0.0022	0.0022	0.0022	0.0022	0.0022	0.0022	0.0022	0.0022	0.0022	0.0022	0.0022	0.0022	0.0022	0.0022	0.0022	0.0022	0.0022	0.0022	0.0022	0.0022
RM1000.1	0.0022	0.0022	0.0022	0.0022	0.0022	0.0022	0.0022	0.0022	0.0022	0.0022	0.0022	0.0022	0.0022	0.0022	0.0022	0.0022	0.0022	0.0022	0.0022	0.0022	0.0022	0.0022	0.0022	0.0022	0.0022	0.0022	0.0022	0.0022	0.0022	0.0022
RM1000.5	0.0022	0.0022	0.0022	0.0022	0.0022	0.0022	0.0022	0.0022	0.0022	0.0022	0.0022	0.0022	0.0022	0.0022	0.0022	0.0022	0.0022	0.0022	0.0022	0.0022	0.0022	0.0022	0.0022	0.0022	0.0022	0.0022	0.0022	0.0022	0.0022	0.0022
RM1000.8	0.0022	0.0022	0.0022	0.0022	0.0022	0.0022	0.0022	0.0022	0.0022	0.0022	0.0022	0.0022	0.0022	0.0022	0.0022	0.0022	0.0022	0.0022	0.0022	0.0022	0.0022	0.0022	0.0022	0.0022	0.0022	0.0022	0.0022	0.0022	0.0022	0.0022
RM1001.2	0.0022	0.0022	0.0022	0.0022	0.0022	0.0022	0.0022	0.0022	0.0022	0.0022	0.0022	0.0022	0.0022	0.0022	0.0022	0.0022	0.0022	0.0022	0.0022	0.0022	0.0022	0.0022	0.0022	0.0022	0.0022	0.0022	0.0022	0.0022	0.0022	0.0022
RM1017.9	0.0022	0.0022	0.0022	0.0022	0.0022	0.0022	0.0022	0.0022	0.0022	0.0022	0.0022	0.0022	0.0022	0.0022	0.0022	0.0022	0.0022	0.0022	0.0022	0.0022	0.0022	0.0022	0.0022	0.0022	0.0022	0.0022	0.0022	0.0022	0.0022	0.0022

Lake Sharpe Air Densiy [kg/m3] used in Force Calculation

	December						January						February						March						April					
Return Period	**1.01-yr**	**2-yr**	**10-yr**	**20-yr**	**50-yr**	**100-yr**	**1.01-yr**	**2-yr**	**10-yr**	**20-yr**	**50-yr**	**100-yr**	**1.01-yr**	**2-yr**	**10-yr**	**20-yr**	**50-yr**	**100-yr**	**1.01-yr**	**2-yr**	**10-yr**	**20-yr**	**50-yr**	**100-yr**	**1.01-yr**	**2-yr**	**10-yr**	**20-yr**	**50-yr**	**100-yr**
Percent Chance Exceedance	**0.9901**	**0.5**	**0.1**	**0.05**	**0.02**	**0.01**	**0.9901**	**0.5**	**0.1**	**0.05**	**0.02**	**0.01**	**0.9901**	**0.5**	**0.1**	**0.05**	**0.02**	**0.01**	**0.9901**	**0.5**	**0.1**	**0.05**	**0.02**	**0.01**	**0.9901**	**0.5**	**0.1**	**0.05**	**0.02**	**0.01**
RM992.1	1.315	1.315	1.315	1.315	1.315	1.315	1.328	1.328	1.328	1.328	1.328	1.328	1.312	1.312	1.312	1.312	1.312	1.312	1.287	1.287	1.287	1.287	1.287	1.287	1.258	1.258	1.258	1.258	1.258	1.258
RM992.3	1.315	1.315	1.315	1.315	1.315	1.315	1.328	1.328	1.328	1.328	1.328	1.328	1.312	1.312	1.312	1.312	1.312	1.312	1.287	1.287	1.287	1.287	1.287	1.287	1.258	1.258	1.258	1.258	1.258	1.258
RM992.5	1.315	1.315	1.315	1.315	1.315	1.315	1.328	1.328	1.328	1.328	1.328	1.328	1.312	1.312	1.312	1.312	1.312	1.312	1.287	1.287	1.287	1.287	1.287	1.287	1.258	1.258	1.258	1.258	1.258	1.258
RM992.6	1.315	1.315	1.315	1.315	1.315	1.315	1.328	1.328	1.328	1.328	1.328	1.328	1.312	1.312	1.312	1.312	1.312	1.312	1.287	1.287	1.287	1.287	1.287	1.287	1.258	1.258	1.258	1.258	1.258	1.258
RM992.7	1.315	1.315	1.315	1.315	1.315	1.315	1.328	1.328	1.328	1.328	1.328	1.328	1.312	1.312	1.312	1.312	1.312	1.312	1.287	1.287	1.287	1.287	1.287	1.287	1.258	1.258	1.258	1.258	1.258	1.258
RM992.9	1.315	1.315	1.315	1.315	1.315	1.315	1.328	1.328	1.328	1.328	1.328	1.328	1.312	1.312	1.312	1.312	1.312	1.312	1.287	1.287	1.287	1.287	1.287	1.287	1.258	1.258	1.258	1.258	1.258	1.258
RM993.2	1.315	1.315	1.315	1.315	1.315	1.315	1.328	1.328	1.328	1.328	1.328	1.328	1.312	1.312	1.312	1.312	1.312	1.312	1.287	1.287	1.287	1.287	1.287	1.287	1.258	1.258	1.258	1.258	1.258	1.258
RM993.3	1.315	1.315	1.315	1.315	1.315	1.315	1.328	1.328	1.328	1.328	1.328	1.328	1.312	1.312	1.312	1.312	1.312	1.312	1.287	1.287	1.287	1.287	1.287	1.287	1.258	1.258	1.258	1.258	1.258	1.258
RM993.6	1.315	1.315	1.315	1.315	1.315	1.315	1.328	1.328	1.328	1.328	1.328	1.328	1.312	1.312	1.312	1.312	1.312	1.312	1.287	1.287	1.287	1.287	1.287	1.287	1.258	1.258	1.258	1.258	1.258	1.258
RM993.8	1.315	1.315	1.315	1.315	1.315	1.315	1.328	1.328	1.328	1.328	1.328	1.328	1.312	1.312	1.312	1.312	1.312	1.312	1.287	1.287	1.287	1.287	1.287	1.287	1.258	1.258	1.258	1.258	1.258	1.258
RM994.1	1.315	1.315	1.315	1.315	1.315	1.315	1.328	1.328	1.328	1.328	1.328	1.328	1.312	1.312	1.312	1.312	1.312	1.312	1.287	1.287	1.287	1.287	1.287	1.287	1.258	1.258	1.258	1.258	1.258	1.258
RM994.3	1.315	1.315	1.315	1.315	1.315	1.315	1.328	1.328	1.328	1.328	1.328	1.328	1.312	1.312	1.312	1.312	1.312	1.312	1.287	1.287	1.287	1.287	1.287	1.287	1.258	1.258	1.258	1.258	1.258	1.258
RM994.5	1.315	1.315	1.315	1.315	1.315	1.315	1.328	1.328	1.328	1.328	1.328	1.328	1.312	1.312	1.312	1.312	1.312	1.312	1.287	1.287	1.287	1.287	1.287	1.287	1.258	1.258	1.258	1.258	1.258	1.258
RM994.8	1.315	1.315	1.315	1.315	1.315	1.315	1.328	1.328	1.328	1.328	1.328	1.328	1.312	1.312	1.312	1.312	1.312	1.312	1.287	1.287	1.287	1.287	1.287	1.287	1.258	1.258	1.258	1.258	1.258	1.258
RM995.1	1.315	1.315	1.315	1.315	1.315	1.315	1.328	1.328	1.328	1.328	1.328	1.328	1.312	1.312	1.312	1.312	1.312	1.312	1.287	1.287	1.287	1.287	1.287	1.287	1.258	1.258	1.258	1.258	1.258	1.258
RM995.3	1.315	1.315	1.315	1.315	1.315	1.315	1.328	1.328	1.328	1.328	1.328	1.328	1.312	1.312	1.312	1.312	1.312	1.312	1.287	1.287	1.287	1.287	1.287	1.287	1.258	1.258	1.258	1.258	1.258	1.258
RM995.4	1.315	1.315	1.315	1.315	1.315	1.315	1.328	1.328	1.328	1.328	1.328	1.328	1.312	1.312	1.312	1.312	1.312	1.312	1.287	1.287	1.287	1.287	1.287	1.287	1.258	1.258	1.258	1.258	1.258	1.258
RM995.7	1.315	1.315	1.315	1.315	1.315	1.315	1.328	1.328	1.328	1.328	1.328	1.328	1.312	1.312	1.312	1.312	1.312	1.312	1.287	1.287	1.287	1.287	1.287	1.287	1.258	1.258	1.258	1.258	1.258	1.258
RM995.9	1.315	1.315	1.315	1.315	1.315	1.315	1.328	1.328	1.328	1.328	1.328	1.328	1.312	1.312	1.312	1.312	1.312	1.312	1.287	1.287	1.287	1.287	1.287	1.287	1.258	1.258	1.258	1.258	1.258	1.258
RM996.1	1.315	1.315	1.315	1.315	1.315	1.315	1.328	1.328	1.328	1.328	1.328	1.328	1.312	1.312	1.312	1.312	1.312	1.312	1.287	1.287	1.287	1.287	1.287	1.287	1.258	1.258	1.258	1.258	1.258	1.258
RM996.3	1.315	1.315	1.315	1.315	1.315	1.315	1.328	1.328	1.328	1.328	1.328	1.328	1.312	1.312	1.312	1.312	1.312	1.312	1.287	1.287	1.287	1.287	1.287	1.287	1.258	1.258	1.258	1.258	1.258	1.258
RM996.5	1.315	1.315	1.315	1.315	1.315	1.315	1.328	1.328	1.328	1.328	1.328	1.328	1.312	1.312	1.312	1.312	1.312	1.312	1.287	1.287	1.287	1.287	1.287	1.287	1.258	1.258	1.258	1.258	1.258	1.258
RM996.7	1.315	1.315	1.315	1.315	1.315	1.315	1.328	1.328	1.328	1.328	1.328	1.328	1.312	1.312	1.312	1.312	1.312	1.312	1.287	1.287	1.287	1.287	1.287	1.287	1.258	1.258	1.258	1.258	1.258	1.258
RM997.4	1.315	1.315	1.315	1.315	1.315	1.315	1.328	1.328	1.328	1.328	1.328	1.328	1.312	1.312	1.312	1.312	1.312	1.312	1.287	1.287	1.287	1.287	1.287	1.287	1.258	1.258	1.258	1.258	1.258	1.258
RM997.9	1.315	1.315	1.315	1.315	1.315	1.315	1.328	1.328	1.328	1.328	1.328	1.328	1.312	1.312	1.312	1.312	1.312	1.312	1.287	1.287	1.287	1.287	1.287	1.287	1.258	1.258	1.258	1.258	1.258	1.258
RM997	1.315	1.315	1.315	1.315	1.315	1.315	1.328	1.328	1.328	1.328	1.328	1.328	1.312	1.312	1.312	1.312	1.312	1.312	1.287	1.287	1.287	1.287	1.287	1.287	1.258	1.258	1.258	1.258	1.258	1.258
RM998.3	1.315	1.315	1.315	1.315	1.315	1.315	1.328	1.328	1.328	1.328	1.328	1.328	1.312	1.312	1.312	1.312	1.312	1.312	1.287	1.287	1.287	1.287	1.287	1.287	1.258	1.258	1.258	1.258	1.258	1.258
RM998.6	1.315	1.315	1.315	1.315	1.315	1.315	1.328	1.328	1.328	1.328	1.328	1.328	1.312	1.312	1.312	1.312	1.312	1.312	1.287	1.287	1.287	1.287	1.287	1.287	1.258	1.258	1.258	1.258	1.258	1.258
RM998.9	1.315	1.315	1.315	1.315	1.315	1.315	1.328	1.328	1.328	1.328	1.328	1.328	1.312	1.312	1.312	1.312	1.312	1.312	1.287	1.287	1.287	1.287	1.287	1.287	1.258	1.258	1.258	1.258	1.258	1.258
RM999.1	1.315	1.315	1.315	1.315	1.315	1.315	1.328	1.328	1.328	1.328	1.328	1.328	1.312	1.312	1.312	1.312	1.312	1.312	1.287	1.287	1.287	1.287	1.287	1.287	1.258	1.258	1.258	1.258	1.258	1.258
RM999.4	1.315	1.315	1.315	1.315	1.315	1.315	1.328	1.328	1.328	1.328	1.328	1.328	1.312	1.312	1.312	1.312	1.312	1.312	1.287	1.287	1.287	1.287	1.287	1.287	1.258	1.258	1.258	1.258	1.258	1.258
RM999.7	1.315	1.315	1.315	1.315	1.315	1.315	1.328	1.328	1.328	1.328	1.328	1.328	1.312	1.312	1.312	1.312	1.312	1.312	1.287	1.287	1.287	1.287	1.287	1.287	1.258	1.258	1.258	1.258	1.258	1.258
RM1000.1	1.315	1.315	1.315	1.315	1.315	1.315	1.328	1.328	1.328	1.328	1.328	1.328	1.312	1.312	1.312	1.312	1.312	1.312	1.287	1.287	1.287	1.287	1.287	1.287	1.258	1.258	1.258	1.258	1.258	1.258
RM1000.5	1.315	1.315	1.315	1.315	1.315	1.315	1.328	1.328	1.328	1.328	1.328	1.328	1.312	1.312	1.312	1.312	1.312	1.312	1.287	1.287	1.287	1.287	1.287	1.287	1.258	1.258	1.258	1.258	1.258	1.258
RM1000.8	1.315	1.315	1.315	1.315	1.315	1.315	1.328	1.328	1.328	1.328	1.328	1.328	1.312	1.312	1.312	1.312	1.312	1.312	1.287	1.287	1.287	1.287	1.287	1.287	1.258	1.258	1.258	1.258	1.258	1.258
RM1001.2	1.315	1.315	1.315	1.315	1.315	1.315	1.328	1.328	1.328	1.328	1.328	1.328	1.312	1.312	1.312	1.312	1.312	1.312	1.287	1.287	1.287	1.287	1.287	1.287	1.258	1.258	1.258	1.258	1.258	1.258
RM1017.9	1.315	1.315	1.315	1.315	1.315	1.315	1.328	1.328	1.328	1.328	1.328	1.328	1.312	1.312	1.312	1.312	1.312	1.312	1.287	1.287	1.287	1.287	1.287	1.287	1.258	1.258	1.258	1.258	1.258	1.258

Lake Sharpe Wind Speed (meters/second) Used in Force Calculation

	December						January						February						March						April					
Return Period	**1.01-yr**	**2-yr**	**10-yr**	**20-yr**	**50-yr**	**100-yr**	**1.01-yr**	**2-yr**	**10-yr**	**20-yr**	**50-yr**	**100-yr**	**1.01-yr**	**2-yr**	**10-yr**	**20-yr**	**50-yr**	**100-yr**	**1.01-yr**	**2-yr**	**10-yr**	**20-yr**	**50-yr**	**100-yr**	**1.01-yr**	**2-yr**	**10-yr**	**20-yr**	**50-yr**	**100-yr**
Percent Chance Exceedance	**0.9901**	**0.5**	**0.1**	**0.05**	**0.02**	**0.01**	**0.9901**	**0.5**	**0.1**	**0.05**	**0.02**	**0.01**	**0.9901**	**0.5**	**0.1**	**0.05**	**0.02**	**0.01**	**0.9901**	**0.5**	**0.1**	**0.05**	**0.02**	**0.01**	**0.9901**	**0.5**	**0.1**	**0.05**	**0.02**	**0.01**
RM992.1	9.92	12.17	14.72	15.17	15.55	22.13	8.09	12.58	16.69	18.18	20.07	21.35	6.58	11.12	14.97	16.31	17.97	19.17	7.26	13.35	16.64	17.49	18.37	18.92	8.46	12.46	15.52	16.53	17.76	18.63
RM992.3	9.92	12.17	14.72	15.17	15.55	15.74	8.09	12.58	16.69	18.18	20.07	21.35	6.58	11.12	14.97	16.31	17.97	19.17	7.26	13.35	16.64	17.49	18.37	18.92	8.46	12.46	15.52	16.53	17.76	18.63
RM992.5	3.98	8.85	13.02	14.43	16.14	17.35	5.69	9.06	13.16	14.89	17.26	19.15	5.00	9.68	12.43	13.17	13.96	14.46	7.25	11.04	13.07	13.61	14.19	14.56	6.39	11.86	15.89	17.17	18.67	19.70
RM992.6	3.46	7.63	10.55	11.42	12.40	13.06	3.26	8.62	11.17	11.70	12.17	12.43	4.16	9.30	10.76	10.95	11.08	11.13	6.60	10.02	12.61	13.45	14.48	15.20	7.21	9.81	12.46	13.46	14.77	15.76
RM992.7	3.98	8.85	13.02	14.43	16.14	17.35	5.69	9.06	13.16	14.89	17.26	19.15	5.00	9.68	12.43	13.17	13.96	14.46	7.25	11.04	13.07	13.61	14.19	14.56	6.39	11.86	15.89	17.17	18.67	19.70
RM992.9	5.68	8.85	13.02	14.43	16.14	17.35	5.69	9.06	13.16	14.89	17.26	19.15	5.00	9.68	12.43	13.17	13.96	14.46	7.25	11.04	13.07	13.61	14.19	14.56	6.39	11.86	15.89	17.17	18.67	19.70
RM993.2	5.68	8.85	13.02	14.43	16.14	17.35	5.69	9.06	13.16	14.89	17.26	19.15	6.34	9.68	12.43	13.17	13.96	14.46	8.82	11.04	13.07	13.61	14.19	17.76	8.06	11.86	15.89	17.17	18.67	19.70
RM993.3	5.68	9.31	13.02	14.43	16.14	17.35	6.51	9.41	13.16	14.89	17.26	19.15	6.34	9.68	12.43	13.19	14.30	15.10	8.82	11.04	13.07	14.20	16.14	17.76	8.06	11.86	15.89	17.17	18.67	19.70
RM993.6	5.68	9.31	11.89	12.71	13.66	14.32	6.51	9.41	11.70	12.47	17.26	19.15	6.34	9.63	12.29	13.19	14.30	15.10	8.82	10.09	12.87	14.20	16.14	17.76	8.06	11.42	14.04	14.92	15.99	16.75
RM993.8	5.68	9.31	11.89	12.71	13.66	14.32	6.51	9.41	11.70	12.47	13.41	16.20	6.34	9.63	12.29	13.19	14.30	15.10	8.82	10.09	12.87	14.20	16.14	17.76	8.06	11.42	14.04	16.79	19.17	20.16
RM994.1	5.68	9.31	11.89	12.71	13.66	16.04	6.51	9.41	11.70	12.47	13.41	16.20	6.34	9.63	12.29	13.19	14.30	15.10	8.82	10.09	12.87	14.20	16.14	17.76	8.06	11.42	14.04	16.79	19.17	20.16
RM994.3	5.68	9.31	11.89	12.71	13.66	16.04	6.51	9.41	11.70	12.47	13.41	16.20	6.34	9.63	12.29	13.19	14.30	15.10	8.82	10.09	12.87	14.20	16.14	17.76	8.06	11.42	14.04	16.79	19.17	20.16
RM994.5	5.68	9.31	11.89	12.71	13.66	16.04	6.51	9.41	11.70	12.47	13.41	16.20	6.34	9.63	12.29	13.19	14.30	15.10	8.82	10.09	12.87	14.20	16.14	17.76	8.06	11.42	14.04	16.79	19.17	20.16
RM994.8	5.68	8.98	10.89	12.52	14.56	16.04	6.51	8.83	11.76	11.95	14.33	16.20	6.34	9.49	12.14	12.80	13.47	13.88	8.82	9.88	13.52	14.55	15.68	16.41	7.50	11.70	14.99	16.79	19.17	20.16
RM995.1	5.68	8.98	11.90	12.52	14.56	16.04	6.51	8.83	11.76	12.60	14.33	16.20	4.59	9.49	12.14	12.80	13.47	13.88	8.82	10.18	13.52	14.55	15.68	16.41	7.50	11.70	14.99	16.79	19.17	20.16
RM995.3	5.68	8.98	11.90	12.55	14.56	16.04	6.51	8.83	11.76	12.60	14.33	16.20	4.59	9.49	12.14	12.80	13.47	13.88	6.25	10.18	13.52	14.55	15.68	16.42	7.50	11.70	15.10	16.79	19.17	20.16
RM995.4	5.68	8.98	11.90	12.55	14.56	16.04	4.33	8.83	11.76	12.60	13.53	16.20	4.59	9.49	12.14	12.80	13.47	13.88	6.25	10.18	13.27	14.29	15.54	16.42	7.50	11.70	15.10	16.25	19.17	20.16
RM995.7	3.42	8.98	11.90	12.55	13.18	13.54	4.33	8.83	11.76	12.60	13.53	14.14	4.59	9.49	12.14	12.80	13.47	13.88	6.25	10.18	13.27	14.29	15.54	16.42	7.50	11.70	15.10	16.25	17.66	18.68
RM995.9	3.42	8.98	11.90	12.55	13.18	13.54	4.33	8.83	11.76	12.60	13.53	14.14	4.59	9.49	12.14	12.80	13.47	13.88	6.25	10.18	13.27	14.29	15.54	16.42	7.50	11.70	15.10	16.25	17.66	18.68
RM996.1	5.68	8.98	10.60	12.08	13.95	15.32	6.51	8.83	10.19	11.95	14.33	16.20	5.60	8.31	9.72	10.30	10.88	11.23	5.55	9.84	13.94	15.46	17.40	18.86	7.50	11.04	15.28	16.67	18.34	19.35
RM996.3	5.68	6.53	10.60	12.08	13.95	15.32	6.51	6.76	9.48	10.26	11.11	11.66	5.60	7.39	9.72	10.30	10.88	11.23	5.55	9.84	13.94	15.46	17.40	18.86	5.66	11.04	15.28	16.67	18.34	19.35
RM996.5	5.68	6.53	10.60	12.08	13.95	15.32	6.51	6.76	9.48	10.26	11.11	11.66	5.60	7.39	9.72	10.30	10.88	11.23	5.55	9.84	13.94	15.46	17.40	18.86	5.66	11.04	15.28	16.67	18.34	19.35
RM996.7	5.68	6.53	10.60	12.08	13.95	15.32	6.51	6.76	9.48	10.26	11.11	11.66	5.60	7.39	9.72	10.30	10.88	11.23	5.55	9.84	13.94	15.46	17.40	18.86	5.66	11.04	15.28	16.67	18.34	19.35
RM997.4	5.68	6.53	10.60	12.08	13.95	15.32	6.51	6.76	9.48	10.26	11.11	11.66	5.60	7.39	9.72	10.30	10.88	11.23	5.55	9.84	13.94	15.46	17.40	18.86	5.66	11.04	15.28	16.67	18.34	19.35
RM997.9	5.68	9.31	10.60	12.08	13.95	15.32	6.51	9.41	11.76	12.60	13.53	14.14	5.60	9.49	10.69	11.77	13.22	14.35	8.82	9.84	13.94	15.46	17.40	18.86	8.06	11.04	15.28	16.67	18.34	19.35
RM997	5.68	6.53	10.60	12.08	13.95	15.32	6.51	6.76	9.48	10.26	11.11	11.66	5.60	7.39	9.72	10.30	10.88	11.23	5.55	9.84	13.94	15.46	17.40	18.86	5.66	11.04	15.28	16.67	18.34	19.35
RM998.3	5.68	8.98	8.43	9.84	11.71	13.16	6.51	9.41	11.76	7.72	9.47	10.98	6.34	9.49	7.49	8.40	9.54	10.37	8.82	9.84	10.04	11.12	12.27	12.98	8.06	7.79	10.96	11.86	12.85	13.48
RM998.6	5.68	8.98	8.43	9.84	11.71	13.16	6.51	8.83	11.76	7.72	9.47	10.98	6.34	9.49	7.49	8.40	9.54	10.37	8.82	6.14	10.04	11.12	12.27	12.98	7.50	7.79	10.96	11.86	12.85	13.48
RM998.9	5.68	9.31	10.89	12.52	14.56	16.04	6.51	9.41	10.19	11.95	14.33	16.20	6.34	8.31	10.09	13.19	13.22	14.35	8.82	9.88	13.52	14.55	15.68	16.41	8.06	10.33	14.99	16.79	19.17	20.16
RM999.1	5.68	9.31	11.90	12.55	13.66	14.32	6.51	9.41	11.76	12.60	13.53	14.14	6.34	9.49	12.14	13.19	14.30	15.10	8.82	10.18	13.27	14.29	16.14	17.76	8.06	11.70	15.10	16.25	17.66	19.15
RM999.4	5.68	8.85	13.02	14.43	16.14	17.35	5.69	9.06	13.16	14.89	17.26	19.15	5.00	9.68	12.43	13.17	13.96	14.46	7.25	11.04	13.07	13.61	14.19	14.56	6.39	11.86	15.89	17.17	18.67	19.70
RM999.7	5.68	8.85	13.02	14.43	16.14	17.35	5.69	9.06	13.16	14.89	17.26	19.15	6.34	9.68	12.43	13.17	13.96	14.46	7.25	11.04	13.07	13.61	15.54	16.42	7.50	11.86	15.89	17.17	18.67	19.70
RM1000.1	5.68	8.98	11.90	12.55	13.18	13.54	6.51	8.83	11.76	12.60	13.53	14.14	6.34	9.49	12.14	12.80	13.47	13.88	8.82	10.18	13.27	14.29	15.54	16.42	7.50	11.70	15.10	16.25	17.66	18.68
RM1000.5	5.68	8.98	10.60	12.08	13.95	15.32	6.51	8.83	13.16	14.89	17.26	19.15	6.34	9.49	12.14	12.80	13.47	13.88	8.82	9.84	13.94	15.46	17.40	18.86	7.50	11.04	15.28	16.67	18.34	19.35
RM1000.8	9.92	14.48	18.19	19.45	21.01	22.13	8.99	15.19	18.68	19.62	20.64	21.29	8.43	14.86	18.12	18.93	19.76	20.27	9.71	14.47	18.22	19.47	21.01	22.11	9.16	13.85	17.03	18.02	19.16	19.94
RM1001.2	9.92	14.48	18.19	19.45	21.01	22.13	8.99	15.19	18.68	19.62	20.64	21.29	8.43	14.86	18.12	18.93	19.76	20.27	9.71	14.47	18.22	19.47	21.01	22.11	9.16	13.85	17.03	18.02	19.16	19.94
RM1017.9	9.59	15.82	20.34	21.76	23.12	24.04	10.43	14.58	17.79	18.89	20.24	21.22	8.06	14.52	18.74	19.98	21.22	21.91	9.71	14.84	18.81	19.61	20.34	20.72	9.43	13.13	17.88	19.89	22.66	24.28

Lake Sharpe Fetch Length (meters) Used in Force Calculation

	December						January						February						March						April					
Return Period	**1.01-yr**	**2-yr**	**10-yr**	**20-yr**	**50-yr**	**100-yr**	**1.01-yr**	**2-yr**	**10-yr**	**20-yr**	**50-yr**	**100-yr**	**1.01-yr**	**2-yr**	**10-yr**	**20-yr**	**50-yr**	**100-yr**	**1.01-yr**	**2-yr**	**10-yr**	**20-yr**	**50-yr**	**100-yr**	**1.01-yr**	**2-yr**	**10-yr**	**20-yr**	**50-yr**	**100-yr**
Percent Chance Exceedance	**0.9901**	**0.5**	**0.1**	**0.05**	**0.02**	**0.01**	**0.9901**	**0.5**	**0.1**	**0.05**	**0.02**	**0.01**	**0.9901**	**0.5**	**0.1**	**0.05**	**0.02**	**0.01**	**0.9901**	**0.5**	**0.1**	**0.05**	**0.02**	**0.01**	**0.9901**	**0.5**	**0.1**	**0.05**	**0.02**	**0.01**
RM992.1	3917.3	7628.5	7628.5	7628.5	7628.5	3917.3	7628.5	7628.5	7628.5	7628.5	7628.5	7628.5	7628.5	7628.5	7628.5	7628.5	7628.5	7628.5	7628.5	7628.5	7628.5	7628.5	7628.5	7628.5	7628.5	7628.5	7628.5	7628.5	7628.5	7628.5
RM992.3	3356.6	6919.8	6919.8	6919.8	6919.8	6919.8	6919.8	6919.8	6919.8	6919.8	6919.8	6919.8	6919.8	6919.8	6919.8	6919.8	6919.8	6919.8	6919.8	6919.8	6919.8	6919.8	6919.8	6919.8	6919.8	6919.8	6919.8	6919.8	6919.8	6919.8
RM992.5	14792.3	14792.3	14792.3	14792.3	14792.3	14792.3	14792.3	14792.3	14792.3	14792.3	14792.3	14792.3	14792.3	14792.3	14792.3	14792.3	14792.3	14792.3	14792.3	14792.3	14792.3	14792.3	14792.3	14792.3	14792.3	14792.3	14792.3	14792.3	14792.3	14792.3
RM992.6	8089.7	8089.7	8089.7	8089.7	8089.7	8089.7	8089.7	8089.7	8089.7	8089.7	8089.7	8089.7	8089.7	8089.7	8089.7	8089.7	8089.7	8089.7	8089.7	8089.7	8089.7	8089.7	8089.7	8089.7	8089.7	8089.7	8089.7	8089.7	8089.7	8089.7
RM992.7	15043.4	15043.4	15043.4	15043.4	15043.4	15043.4	15043.4	15043.4	15043.4	15043.4	15043.4	15043.4	15043.4	15043.4	15043.4	15043.4	15043.4	15043.4	15043.4	15043.4	15043.4	15043.4	15043.4	15043.4	15043.4	15043.4	15043.4	15043.4	15043.4	15043.4
RM992.9	5602.0	9754.0	9754.0	9754.0	9754.0	9754.0	9754.0	9754.0	9754.0	9754.0	9754.0	9754.0	9754.0	9754.0	9754.0	9754.0	9754.0	9754.0	9754.0	9754.0	9754.0	9754.0	9754.0	9754.0	9754.0	9754.0	9754.0	9754.0	9754.0	9754.0
RM993.2	6414.1	9074.0	9074.0	9074.0	9074.0	9074.0	9074.0	9074.0	9074.0	9074.0	9074.0	9074.0	6414.1	9074.0	9074.0	9074.0	9074.0	9074.0	6414.1	9074.0	9074.0	9074.0	9074.0	6414.1	6414.1	9074.0	9074.0	9074.0	9074.0	9074.0
RM993.3	7704.7	7704.7	7647.3	7647.3	7647.3	7647.3	7704.7	7704.7	7647.3	7647.3	7647.3	7647.3	7704.7	7647.3	7647.3	7704.7	7704.7	7704.7	7704.7	7647.3	7647.3	7704.7	7704.7	7704.7	7704.7	7647.3	7647.3	7647.3	7647.3	7647.3
RM993.6	8965.0	8965.0	8965.0	8965.0	8965.0	8965.0	8965.0	8965.0	8965.0	8965.0	5959.4	5959.4	8965.0	8965.0	8965.0	8965.0	8965.0	8965.0	8965.0	8965.0	8965.0	8965.0	8965.0	8965.0	8965.0	8965.0	8965.0	8965.0	8965.0	8965.0
RM993.8	11641.4	11641.4	11641.4	11641.4	11641.4	11641.4	11641.4	11641.4	11641.4	11641.4	11641.4	9197.4	11641.4	11641.4	11641.4	11641.4	11641.4	11641.4	11641.4	11641.4	11641.4	11641.4	11641.4	11641.4	11641.4	11641.4	11641.4	9197.4	9197.4	9197.4
RM994.1	11837.5	11837.5	11837.5	11837.5	11837.5	9506.6	11837.5	11837.5	11837.5	11837.5	11837.5	9506.6	11837.5	11837.5	11837.5	11837.5	11837.5	11837.5	11837.5	11837.5	11837.5	11837.5	11837.5	11837.5	11837.5	11837.5	11837.5	9506.6	9506.6	9506.6
RM994.3	11563.8	11563.8	11563.8	11563.8	11563.8	9608.7	11563.8	11563.8	11563.8	11563.8	11563.8	9608.7	11563.8	11563.8	11563.8	11563.8	11563.8	11563.8	11563.8	11563.8	11563.8	11563.8	11563.8	11563.8	11563.8	11563.8	11563.8	9608.7	9608.7	9608.7
RM994.5	11299.7	11299.7	11299.7	11299.7	11299.7	9549.9	11299.7	11299.7	11299.7	11299.7	11299.7	9549.9	11299.7	11299.7	11299.7	11299.7	11299.7	11299.7	11299.7	11299.7	11299.7	11299.7	11299.7	11299.7	11299.7	11299.7	11299.7	9549.9	9549.9	9549.9
RM994.8	5560.3	7586.2	9310.6	9310.6	9310.6	9310.6	5560.3	7586.2	7586.2	9310.6	9310.6	9310.6	5560.3	7586.2	7586.2	7586.2	7586.2	7586.2	5560.3	9310.6	9310.6	9310.6	9310.6	9310.6	7586.2	7586.2	9310.6	9310.6	9310.6	9310.6
RM995.1	4520.8	8762.1	8762.1	9044.5	9044.5	9044.5	4520.8	8762.1	8762.1	8762.1	9044.5	9044.5	8762.1	8762.1	8762.1	8762.1	8762.1	8762.1	4520.8	8762.1	9044.5	9044.5	9044.5	9044.5	8762.1	8762.1	9044.5	9044.5	9044.5	9044.5
RM995.3	4360.2	9061.7	9061.7	9061.7	8990.3	8990.3	4360.2	9061.7	9061.7	9061.7	8990.3	8990.3	9061.7	9061.7	9061.7	9061.7	9061.7	9061.7	9061.7	9061.7	8990.3	8990.3	8990.3	9061.7	9061.7	9061.7	9061.7	8990.3	8990.3	8990.3
RM995.4	3879.7	9726.9	9726.9	9726.9	8624.3	8624.3	9726.9	9726.9	9726.9	9726.9	9726.9	8624.3	9726.9	9726.9	9726.9	9726.9	9726.9	9726.9	9726.9	9726.9	9726.9	9726.9	9726.9	9726.9	9726.9	9726.9	9726.9	8624.3	8624.3	8624.3
RM995.7	10386.1	10386.1	10386.1	10386.1	10386.1	10386.1	10386.1	10386.1	10386.1	10386.1	10386.1	10386.1	10386.1	10386.1	10386.1	10386.1	10386.1	10386.1	10386.1	10386.1	10386.1	10386.1	10386.1	10386.1	10386.1	10386.1	10386.1	10386.1	10386.1	10386.1
RM995.9	11205.4	11205.4	11205.4	11205.4	11205.4	11205.4	11205.4	11205.4	11205.4	11205.4	11205.4	11205.4	11205.4	11205.4	11205.4	11205.4	11205.4	11205.4	11205.4	11205.4	11205.4	11205.4	11205.4	11205.4	11205.4	11205.4	11205.4	11205.4	11205.4	11205.4
RM996.1	2370.7	4945.1	8217.0	8217.0	8217.0	8217.0	2370.7	4945.1	7272.0	7272.0	7272.0	7272.0	4998.0	7272.0	8217.0	8217.0	8217.0	8217.0	8217.0	8217.0	8217.0	8217.0	8217.0	8217.0	4945.1	8217.0	8217.0	8217.0	8217.0	8217.0
RM996.3	2295.6	8882.6	8882.6	8882.6	8882.6	8882.6	2295.6	8882.6	8882.6	8882.6	8882.6	8882.6	4878.3	8882.6	8882.6	8882.6	8882.6	8882.6	8882.6	8882.6	8882.6	8882.6	8882.6	8882.6	8882.6	8882.6	8882.6	8882.6	8882.6	8882.6
RM996.5	2204.7	9559.2	9559.2	9559.2	9559.2	9559.2	2204.7	9559.2	9559.2	9559.2	9559.2	9559.2	4634.7	9559.2	9559.2	9559.2	9559.2	9559.2	9559.2	9559.2	9559.2	9559.2	9559.2	9559.2	9559.2	9559.2	9559.2	9559.2	9559.2	9559.2
RM996.7	2313.9	10100.0	10100.0	10100.0	10100.0	10100.0	2313.9	10100.0	10100.0	10100.0	10100.0	10100.0	4489.8	10100.0	10100.0	10100.0	10100.0	10100.0	10100.0	10100.0	10100.0	10100.0	10100.0	10100.0	10100.0	10100.0	10100.0	10100.0	10100.0	10100.0
RM997.4	2421.4	11239.2	11239.2	11239.2	11239.2	11239.2	2421.4	11239.2	11239.2	11239.2	11239.2	11239.2	3950.8	11239.2	11239.2	11239.2	11239.2	11239.2	11239.2	11239.2	11239.2	11239.2	11239.2	11239.2	11239.2	11239.2	11239.2	11239.2	11239.2	11239.2
RM997.9	2618.3	2618.3	3995.9	3995.9	3995.9	3995.9	2618.3	2618.3	2736.7	2736.7	2736.7	2736.7	3727.3	2736.7	3727.3	3727.3	3727.3	3727.3	2618.3	3995.9	3995.9	3995.9	3995.9	3995.9	2618.3	3995.9	3995.9	3995.9	3995.9	3995.9
RM997	2456.3	10770.8	10770.8	10770.8	10770.8	10770.8	2456.3	10770.8	10770.8	10770.8	10770.8	10770.8	4292.5	10770.8	10770.8	10770.8	10770.8	10770.8	10770.8	10770.8	10770.8	10770.8	10770.8	10770.8	10770.8	10770.8	10770.8	10770.8	10770.8	10770.8
RM998.3	2530.1	2788.8	8949.6	8949.6	8949.6	8949.6	2530.1	2530.1	2788.8	8949.6	8949.6	8949.6	2530.1	2788.8	8949.6	8949.6	8949.6	8949.6	2530.1	3623.8	8949.6	8949.6	8949.6	8949.6	2530.1	8949.6	8949.6	8949.6	8949.6	8949.6
RM998.6	2607.1	3110.1	9518.2	9518.2	9518.2	9518.2	2607.1	3110.1	3110.1	9518.2	9518.2	9518.2	2607.1	3110.1	9518.2	9518.2	9518.2	9518.2	2607.1	9518.2	9518.2	9518.2	9518.2	9518.2	3110.1	9518.2	9518.2	9518.2	9518.2	9518.2
RM998.9	2163.7	2163.7	3243.6	3243.6	3243.6	3243.6	2163.7	2163.7	3243.6	3243.6	3243.6	3243.6	2163.7	3243.6	3243.6	2163.7	2545.2	2545.2	2163.7	3243.6	3243.6	3243.6	3243.6	3243.6	2163.7	3243.6	3243.6	3243.6	3243.6	3243.6
RM999.1	2474.6	2474.6	2618.8	2618.8	2474.6	2474.6	2474.6	2474.6	2618.8	2618.8	2618.8	2618.8	2474.6	2618.8	2618.8	2474.6	2474.6	2474.6	2474.6	2618.8	2618.8	2618.8	2474.6	2474.6	2474.6	2618.8	2618.8	2618.8	2618.8	2534.6
RM999.4	2207.0	4210.7	4210.7	4210.7	4210.7	4210.7	4210.7	4210.7	4210.7	4210.7	4210.7	4210.7	4210.7	4210.7	4210.7	4210.7	4210.7	4210.7	4210.7	4210.7	4210.7	4210.7	4210.7	4210.7	4210.7	4210.7	4210.7	4210.7	4210.7	4210.7
RM999.7	2435.3	3815.6	3815.6	3815.6	3815.6	3815.6	3815.6	3815.6	3815.6	3815.6	3815.6	3815.6	2435.3	3815.6	3815.6	3815.6	3815.6	3815.6	3815.6	3815.6	3815.6	3815.6	3253.0	3253.0	3253.0	3815.6	3815.6	3815.6	3815.6	3815.6
RM1000.1	2516.1	3255.8	3255.8	3255.8	3255.8	3255.8	2516.1	3255.8	3255.8	3255.8	3255.8	3255.8	2516.1	3255.8	3255.8	3255.8	3255.8	3255.8	2516.1	3255.8	3255.8	3255.8	3255.8	3255.8	3255.8	3255.8	3255.8	3255.8	3255.8	3255.8
RM1000.5	2514.1	3399.3	4693.0	4693.0	4693.0	4693.0	2514.1	3399.3	2744.9	2744.9	2744.9	2744.9	2514.1	3399.3	3399.3	3399.3	3399.3	3399.3	2514.1	4693.0	4693.0	4693.0	4693.0	4693.0	3399.3	4693.0	4693.0	4693.0	4693.0	4693.0
RM1000.8	5499.2	5499.2	5499.2	5499.2	5499.2	5499.2	5499.2	5499.2	5499.2	5499.2	5499.2	5499.2	5499.2	5499.2	5499.2	5499.2	5499.2	5499.2	5499.2	5499.2	5499.2	5499.2	5499.2	5499.2	5499.2	5499.2	5499.2	5499.2	5499.2	5499.2
RM1001.2	5264.3	5264.3	5264.3	5264.3	5264.3	5264.3	5264.3	5264.3	5264.3	5264.3	5264.3	5264.3	5264.3	5264.3	5264.3	5264.3	5264.3	5264.3	5264.3	5264.3	5264.3	5264.3	5264.3	5264.3	5264.3	5264.3	5264.3	5264.3	5264.3	5264.3
RM1017.9	7030.5	7030.5	7030.5	7030.5	7030.5	7030.5	7030.5	7030.5	7030.5	7030.5	7030.5	7030.5	7030.5	7030.5	7030.5	7030.5	7030.5	7030.5	2804.4	7030.5	7030.5	7030.5	7030.5	7030.5	7030.5	7030.5	7030.5	7030.5	7030.5	7030.5

Lake Sharpe Ice Force(kN/m) Calculation

	December						January						February						March						April					
Return Period	**1.01-yr**	**2-yr**	**10-yr**	**20-yr**	**50-yr**	**100-yr**	**1.01-yr**	**2-yr**	**10-yr**	**20-yr**	**50-yr**	**100-yr**	**1.01-yr**	**2-yr**	**10-yr**	**20-yr**	**50-yr**	**100-yr**	**1.01-yr**	**2-yr**	**10-yr**	**20-yr**	**50-yr**	**100-yr**	**1.01-yr**	**2-yr**	**10-yr**	**20-yr**	**50-yr**	**100-yr**
Percent Chance Exceedance	**0.9901**	**0.5**	**0.1**	**0.05**	**0.02**	**0.01**	**0.9901**	**0.5**	**0.1**	**0.05**	**0.02**	**0.01**	**0.9901**	**0.5**	**0.1**	**0.05**	**0.02**	**0.01**	**0.9901**	**0.5**	**0.1**	**0.05**	**0.02**	**0.01**	**0.9901**	**0.5**	**0.1**	**0.05**	**0.02**	**0.01**
RM992.1	1.12	3.27	4.78	5.08	5.34	5.55	1.46	3.52	6.20	7.36	8.98	10.15	0.95	2.72	4.94	5.86	7.11	8.10	1.14	3.85	5.98	6.61	7.29	7.73	1.51	3.28	5.09	5.77	6.66	7.33
RM992.3	0.96	2.96	4.34	4.61	4.84	4.96	1.32	3.20	5.63	6.68	8.15	9.21	0.87	2.47	4.48	5.31	6.45	7.34	1.03	3.49	5.43	5.99	6.61	7.01	1.37	2.97	4.61	5.23	6.04	6.65
RM992.5	0.68	3.35	7.26	8.91	11.15	12.89	1.40	3.54	7.49	9.58	12.87	15.84	1.07	4.00	6.60	7.40	8.32	8.93	2.20	5.11	7.15	7.76	8.43	8.88	1.67	5.76	10.34	12.07	14.27	15.89
RM992.6	0.28	1.36	2.61	3.05	3.60	3.99	0.25	1.76	2.95	3.23	3.50	3.65	0.40	2.02	2.71	2.80	2.87	2.89	1.00	2.30	3.64	4.14	4.80	5.29	1.16	2.15	3.47	4.06	4.89	5.56
RM992.7	0.69	3.41	7.38	9.06	11.34	13.10	1.42	3.60	7.61	9.74	13.09	16.11	1.09	4.07	6.71	7.53	8.46	9.08	2.24	5.19	7.27	7.89	8.57	9.03	1.70	5.86	10.52	12.27	14.51	16.16
RM992.9	0.52	2.21	4.78	5.88	7.35	8.50	0.92	2.34	4.94	6.32	8.48	10.45	0.71	2.64	4.35	4.88	5.49	5.89	1.45	3.37	4.72	5.11	5.56	5.85	1.10	3.80	6.82	7.96	9.41	10.48
RM993.2	0.60	2.06	4.45	5.47	6.84	7.90	0.86	2.17	4.59	5.88	7.89	9.72	0.74	2.46	4.05	4.54	5.10	5.48	1.41	3.13	4.39	4.76	5.17	5.72	1.15	3.53	6.34	7.40	8.75	9.75
RM993.3	0.72	1.93	3.75	4.61	5.76	6.66	0.95	1.99	3.87	4.95	6.65	8.19	0.89	2.07	3.41	3.87	4.55	5.07	1.70	2.64	3.70	4.40	5.68	6.88	1.38	2.98	5.35	6.24	7.38	8.22
RM993.6	0.84	2.25	3.67	4.19	4.84	5.32	1.11	2.32	3.58	4.07	5.18	6.38	1.04	2.40	3.91	4.50	5.29	5.90	1.97	2.58	4.20	5.12	6.61	8.00	1.61	3.23	4.89	5.52	6.34	6.97
RM993.8	1.09	2.92	4.77	5.44	6.29	6.91	1.44	3.01	4.65	5.28	6.11	7.05	1.35	3.11	5.07	5.85	6.87	7.67	2.56	3.36	5.45	6.64	8.58	10.39	2.09	4.20	6.35	7.18	9.36	10.35
RM994.1	1.11	2.97	4.85	5.53	6.39	7.08	1.47	3.06	4.73	5.37	6.21	7.29	1.37	3.17	5.16	5.95	6.99	7.80	2.61	3.41	5.55	6.76	8.73	10.56	2.13	4.27	6.46	7.42	9.67	10.70
RM994.3	1.08	2.90	4.73	5.40	6.24	7.16	1.43	2.99	4.62	5.25	6.07	7.37	1.34	3.09	5.04	5.81	6.83	7.61	2.55	3.33	5.42	6.60	8.53	10.32	2.08	4.17	6.31	7.50	9.78	10.81
RM994.5	1.06	2.84	4.63	5.28	6.10	7.11	1.40	2.92	4.52	5.13	5.93	7.32	1.31	3.02	4.93	5.68	6.67	7.44	2.49	3.26	5.29	6.45	8.33	10.08	2.03	4.08	6.17	7.46	9.72	10.75
RM994.8	0.52	1.77	3.19	4.22	5.71	6.93	0.69	1.73	3.06	3.89	5.59	7.14	0.64	1.97	3.23	3.59	3.97	4.22	1.22	2.57	4.81	5.58	6.48	7.10	1.18	2.88	5.79	7.27	9.47	10.48
RM995.1	0.42	2.04	3.59	4.10	5.55	6.74	0.56	1.99	3.54	4.06	5.43	6.94	0.53	2.28	3.73	4.14	4.59	4.87	1.00	2.57	4.68	5.42	6.29	6.90	1.37	3.32	5.62	7.06	9.20	10.18
RM995.3	0.41	2.11	3.71	4.13	5.52	6.70	0.54	2.06	3.66	4.20	5.39	6.89	0.55	2.36	3.85	4.28	4.75	5.04	1.00	2.66	4.65	5.39	6.26	6.92	1.41	3.44	5.72	7.02	9.15	10.12
RM995.4	0.36	2.27	3.98	4.43	5.29	6.42	0.53	2.21	3.93	4.51	5.20	6.61	0.59	2.53	4.14	4.60	5.09	5.41	1.08	2.85	4.85	5.62	6.65	7.42	1.52	3.69	6.14	7.11	8.77	9.70
RM995.7	0.35	2.42	4.25	4.74	5.22	5.51	0.57	2.36	4.19	4.81	5.55	6.07	0.63	2.70	4.42	4.91	5.44	5.77	1.15	3.05	5.17	6.00	7.10	7.93	1.62	3.94	6.55	7.59	8.97	10.03
RM995.9	0.38	2.61	4.59	5.11	5.63	5.94	0.61	2.55	4.53	5.19	5.99	6.54	0.68	2.91	4.77	5.30	5.87	6.23	1.24	3.29	5.58	6.48	7.66	8.55	1.75	4.25	7.07	8.19	9.68	10.82
RM996.1	0.22	1.15	2.67	3.47	4.63	5.58	0.29	1.13	2.21	3.03	4.36	5.58	0.45	1.45	2.24	2.52	2.81	2.99	0.72	2.25	4.52	5.56	7.04	8.27	0.77	2.77	5.31	6.32	7.65	8.52
RM996.3	0.21	1.10	2.89	3.75	5.00	6.03	0.28	1.19	2.33	2.73	3.20	3.53	0.44	1.40	2.42	2.72	3.04	3.24	0.77	2.44	4.89	6.01	7.61	8.94	0.79	2.99	5.74	6.84	8.27	9.21
RM996.5	0.21	1.18	3.11	4.04	5.38	6.49	0.27	1.28	2.51	2.94	3.45	3.80	0.42	1.51	2.61	2.93	3.27	3.48	0.83	2.62	5.26	6.47	8.19	9.62	0.85	3.22	6.18	7.36	8.90	9.91
RM996.7	0.22	1.25	3.28	4.27	5.69	6.86	0.29	1.35	2.65	3.11	3.64	4.01	0.41	1.59	2.76	3.09	3.45	3.68	0.88	2.77	5.56	6.83	8.66	10.17	0.89	3.40	6.53	7.77	9.40	10.47
RM997.4	0.23	1.39	3.65	4.75	6.33	7.63	0.30	1.50	2.95	3.46	4.05	4.47	0.36	1.77	3.07	3.44	3.84	4.10	0.98	3.08	6.19	7.60	9.63	11.31	1.00	3.79	7.27	8.65	10.46	11.65
RM997.9	0.24	0.66	1.30	1.69	2.25	2.71	0.32	0.68	1.11	1.27	1.46	1.60	0.34	0.71	1.23	1.49	1.88	2.22	0.58	1.10	2.20	2.70	3.43	4.02	0.47	1.35	2.58	3.08	3.72	4.14
RM997	0.23	1.33	3.50	4.55	6.06	7.31	0.30	1.44	2.83	3.31	3.88	4.28	0.39	1.70	2.94	3.30	3.68	3.92	0.94	2.95	5.93	7.29	9.23	10.84	0.95	3.63	6.96	8.29	10.03	11.17
RM998.3	0.24	0.65	1.84	2.51	3.55	4.48	0.31	0.65	1.13	1.56	2.34	3.15	0.29	0.72	1.45	1.82	2.35	2.78	0.56	0.99	2.55	3.13	3.82	4.27	0.45	1.50	2.97	3.48	4.09	4.50
RM998.6	0.24	0.72	1.96	2.66	3.78	4.77	0.32	0.71	1.26	1.66	2.49	3.35	0.30	0.81	1.54	1.94	2.50	2.95	0.57	1.02	2.72	3.33	4.06	4.54	0.48	1.60	3.16	3.70	4.35	4.79
RM998.9	0.20	0.54	1.11	1.47	1.99	2.42	0.27	0.56	0.98	1.35	1.95	2.49	0.25	0.65	0.95	1.09	1.28	1.51	0.48	0.90	1.68	1.94	2.26	2.47	0.39	0.96	2.02	2.53	3.30	3.65
RM999.1	0.23	0.62	1.07	1.19	1.34	1.47	0.31	0.64	1.06	1.21	1.40	1.53	0.29	0.68	1.11	1.24	1.46	1.63	0.54	0.77	1.30	1.51	1.82	2.21	0.44	0.99	1.65	1.91	2.26	2.57
RM999.4	0.21	0.95	2.07	2.54	3.17	3.67	0.40	1.01	2.13	2.73	3.66	4.51	0.30	1.14	1.88	2.11	2.37	2.54	0.63	1.45	2.04	2.21	2.40	2.53	0.48	1.64	2.94	3.43	4.06	4.52
RM999.7	0.23	0.86	1.87	2.30	2.88	3.32	0.36	0.91	1.93	2.47	3.32	4.09	0.28	1.03	1.70	1.91	2.15	2.30	0.57	1.32	1.85	2.00	2.22	2.48	0.51	1.49	2.67	3.11	3.68	4.10
RM1000.1	0.24	0.76	1.33	1.48	1.64	1.73	0.31	0.74	1.31	1.51	1.74	1.90	0.29	0.85	1.38	1.54	1.71	1.81	0.55	0.96	1.62	1.88	2.22	2.49	0.51	1.23	2.05	2.38	2.81	3.14
RM1000.5	0.24	0.79	1.53	1.98	2.64	3.19	0.31	0.77	1.39	1.78	2.39	2.94	0.29	0.88	1.45	1.61	1.78	1.89	0.55	1.29	2.58	3.17	4.02	4.72	0.53	1.58	3.03	3.61	4.37	4.87
RM1000.8	1.57	3.34	5.26	6.02	7.02	7.79	1.30	3.70	5.61	6.19	6.84	7.28	1.13	3.50	5.21	5.69	6.20	6.52	1.47	3.26	5.17	5.90	6.87	7.61	1.28	2.92	4.42	4.94	5.59	6.05
RM1001.2	1.50	3.19	5.04	5.76	6.72	7.46	1.24	3.55	5.37	5.92	6.55	6.97	1.08	3.35	4.99	5.45	5.94	6.24	1.41	3.12	4.95	5.65	6.58	7.29	1.22	2.80	4.23	4.73	5.35	5.80
RM1017.9	1.87	5.09	8.41	9.63	10.87	11.75	2.24	4.37	6.50	7.32	8.41	9.25	1.32	4.28	7.13	8.10	9.14	9.75	0.75	4.38	7.04	7.65	8.23	8.55	1.73	3.35	6.22	7.70	9.99	11.47

Lake Sharpe Direction (deg) Used in Force Calculation

	December						January						February						March						April					
Return Period	**1.01-yr**	**2-yr**	**10-yr**	**20-yr**	**50-yr**	**100-yr**	**1.01-yr**	**2-yr**	**10-yr**	**20-yr**	**50-yr**	**100-yr**	**1.01-yr**	**2-yr**	**10-yr**	**20-yr**	**50-yr**	**100-yr**	**1.01-yr**	**2-yr**	**10-yr**	**20-yr**	**50-yr**	**100-yr**	**1.01-yr**	**2-yr**	**10-yr**	**20-yr**	**50-yr**	**100-yr**
Percent Chance Exceedance	**0.9901**	**0.5**	**0.1**	**0.05**	**0.02**	**0.01**	**0.9901**	**0.5**	**0.1**	**0.05**	**0.02**	**0.01**	**0.9901**	**0.5**	**0.1**	**0.05**	**0.02**	**0.01**	**0.9901**	**0.5**	**0.1**	**0.05**	**0.02**	**0.01**	**0.9901**	**0.5**	**0.1**	**0.05**	**0.02**	**0.01**
RM992.1	315.0	337.5	337.5	337.5	337.5	315.0	337.5	337.5	337.5	337.5	337.5	337.5	337.5	337.5	337.5	337.5	337.5	337.5	337.5	337.5	337.5	337.5	337.5	337.5	337.5	337.5	337.5	337.5	337.5	337.5
RM992.3	315.0	337.5	337.5	337.5	337.5	337.5	337.5	337.5	337.5	337.5	337.5	337.5	337.5	337.5	337.5	337.5	337.5	337.5	337.5	337.5	337.5	337.5	337.5	337.5	337.5	337.5	337.5	337.5	337.5	337.5
RM992.5	0.0	0.0	0.0	0.0	0.0	0.0	0.0	0.0	0.0	0.0	0.0	0.0	0.0	0.0	0.0	0.0	0.0	0.0	0.0	0.0	0.0	0.0	0.0	0.0	0.0	0.0	0.0	0.0	0.0	0.0
RM992.6	90.0	90.0	90.0	90.0	90.0	90.0	90.0	90.0	90.0	90.0	90.0	90.0	90.0	90.0	90.0	90.0	90.0	90.0	90.0	90.0	90.0	90.0	90.0	90.0	90.0	90.0	90.0	90.0	90.0	90.0
RM992.7	0.0	0.0	0.0	0.0	0.0	0.0	0.0	0.0	0.0	0.0	0.0	0.0	0.0	0.0	0.0	0.0	0.0	0.0	0.0	0.0	0.0	0.0	0.0	0.0	0.0	0.0	0.0	0.0	0.0	0.0
RM992.9	112.5	0.0	0.0	0.0	0.0	0.0	0.0	0.0	0.0	0.0	0.0	0.0	0.0	0.0	0.0	0.0	0.0	0.0	0.0	0.0	0.0	0.0	0.0	0.0	0.0	0.0	0.0	0.0	0.0	0.0
RM993.2	112.5	0.0	0.0	0.0	0.0	0.0	0.0	0.0	0.0	0.0	0.0	0.0	112.5	0.0	0.0	0.0	0.0	0.0	112.5	0.0	0.0	0.0	0.0	112.5	112.5	0.0	0.0	0.0	0.0	0.0
RM993.3	112.5	112.5	0.0	0.0	0.0	0.0	112.5	112.5	0.0	0.0	0.0	0.0	112.5	0.0	0.0	112.5	112.5	112.5	112.5	0.0	0.0	112.5	112.5	112.5	112.5	0.0	0.0	0.0	0.0	0.0
RM993.6	112.5	112.5	112.5	112.5	112.5	112.5	112.5	112.5	112.5	112.5	0.0	0.0	112.5	112.5	112.5	112.5	112.5	112.5	112.5	112.5	112.5	112.5	112.5	112.5	112.5	112.5	112.5	112.5	112.5	112.5
RM993.8	112.5	112.5	112.5	112.5	112.5	112.5	112.5	112.5	112.5	112.5	112.5	22.5	112.5	112.5	112.5	112.5	112.5	112.5	112.5	112.5	112.5	112.5	112.5	112.5	112.5	112.5	112.5	22.5	22.5	22.5
RM994.1	112.5	112.5	112.5	112.5	112.5	22.5	112.5	112.5	112.5	112.5	112.5	22.5	112.5	112.5	112.5	112.5	112.5	112.5	112.5	112.5	112.5	112.5	112.5	112.5	112.5	112.5	112.5	22.5	22.5	22.5
RM994.3	112.5	112.5	112.5	112.5	112.5	22.5	112.5	112.5	112.5	112.5	112.5	22.5	112.5	112.5	112.5	112.5	112.5	112.5	112.5	112.5	112.5	112.5	112.5	112.5	112.5	112.5	112.5	22.5	22.5	22.5
RM994.5	112.5	112.5	112.5	112.5	112.5	22.5	112.5	112.5	112.5	112.5	112.5	22.5	112.5	112.5	112.5	112.5	112.5	112.5	112.5	112.5	112.5	112.5	112.5	112.5	112.5	112.5	112.5	22.5	22.5	22.5
RM994.8	112.5	135.0	22.5	22.5	22.5	22.5	112.5	135.0	135.0	22.5	22.5	22.5	112.5	135.0	135.0	135.0	135.0	135.0	112.5	22.5	22.5	22.5	22.5	22.5	135.0	135.0	22.5	22.5	22.5	22.5
RM995.1	112.5	135.0	135.0	22.5	22.5	22.5	112.5	135.0	135.0	135.0	22.5	22.5	135.0	135.0	135.0	135.0	135.0	135.0	112.5	135.0	22.5	22.5	22.5	22.5	135.0	135.0	22.5	22.5	22.5	22.5
RM995.3	112.5	135.0	135.0	135.0	22.5	22.5	112.5	135.0	135.0	135.0	22.5	22.5	135.0	135.0	135.0	135.0	135.0	135.0	135.0	135.0	22.5	22.5	22.5	135.0	135.0	135.0	135.0	22.5	22.5	22.5
RM995.4	112.5	135.0	135.0	135.0	22.5	22.5	135.0	135.0	135.0	135.0	135.0	22.5	135.0	135.0	135.0	135.0	135.0	135.0	135.0	135.0	135.0	135.0	135.0	135.0	135.0	135.0	135.0	135.0	22.5	22.5
RM995.7	135.0	135.0	135.0	135.0	135.0	135.0	135.0	135.0	135.0	135.0	135.0	135.0	135.0	135.0	135.0	135.0	135.0	135.0	135.0	135.0	135.0	135.0	135.0	135.0	135.0	135.0	135.0	135.0	135.0	135.0
RM995.9	135.0	135.0	135.0	135.0	135.0	135.0	135.0	135.0	135.0	135.0	135.0	135.0	135.0	135.0	135.0	135.0	135.0	135.0	135.0	135.0	135.0	135.0	135.0	135.0	135.0	135.0	135.0	135.0	135.0	135.0
RM996.1	112.5	135.0	157.5	157.5	157.5	157.5	112.5	135.0	22.5	22.5	22.5	22.5	45.0	22.5	157.5	157.5	157.5	157.5	157.5	157.5	157.5	157.5	157.5	157.5	135.0	157.5	157.5	157.5	157.5	157.5
RM996.3	112.5	157.5	157.5	157.5	157.5	157.5	112.5	157.5	157.5	157.5	157.5	157.5	45.0	157.5	157.5	157.5	157.5	157.5	157.5	157.5	157.5	157.5	157.5	157.5	157.5	157.5	157.5	157.5	157.5	157.5
RM996.5	112.5	157.5	157.5	157.5	157.5	157.5	112.5	157.5	157.5	157.5	157.5	157.5	45.0	157.5	157.5	157.5	157.5	157.5	157.5	157.5	157.5	157.5	157.5	157.5	157.5	157.5	157.5	157.5	157.5	157.5
RM996.7	112.5	157.5	157.5	157.5	157.5	157.5	112.5	157.5	157.5	157.5	157.5	157.5	45.0	157.5	157.5	157.5	157.5	157.5	157.5	157.5	157.5	157.5	157.5	157.5	157.5	157.5	157.5	157.5	157.5	157.5
RM997.4	112.5	157.5	157.5	157.5	157.5	157.5	112.5	157.5	157.5	157.5	157.5	157.5	45.0	157.5	157.5	157.5	157.5	157.5	157.5	157.5	157.5	157.5	157.5	157.5	157.5	157.5	157.5	157.5	157.5	157.5
RM997.9	112.5	112.5	157.5	157.5	157.5	157.5	112.5	112.5	135.0	135.0	135.0	135.0	45.0	135.0	45.0	45.0	45.0	45.0	112.5	157.5	157.5	157.5	157.5	157.5	112.5	157.5	157.5	157.5	157.5	157.5
RM997	112.5	157.5	157.5	157.5	157.5	157.5	112.5	157.5	157.5	157.5	157.5	157.5	45.0	157.5	157.5	157.5	157.5	157.5	157.5	157.5	157.5	157.5	157.5	157.5	157.5	157.5	157.5	157.5	157.5	157.5
RM998.3	112.5	135.0	180.0	180.0	180.0	180.0	112.5	112.5	135.0	180.0	180.0	180.0	112.5	135.0	180.0	180.0	180.0	180.0	112.5	157.5	180.0	180.0	180.0	180.0	112.5	180.0	180.0	180.0	180.0	180.0
RM998.6	112.5	135.0	180.0	180.0	180.0	180.0	112.5	135.0	135.0	180.0	180.0	180.0	112.5	135.0	180.0	180.0	180.0	180.0	112.5	180.0	180.0	180.0	180.0	180.0	135.0	180.0	180.0	180.0	180.0	180.0
RM998.9	112.5	112.5	22.5	22.5	22.5	22.5	112.5	112.5	22.5	22.5	22.5	22.5	112.5	22.5	22.5	112.5	45.0	45.0	112.5	22.5	22.5	22.5	22.5	22.5	112.5	22.5	22.5	22.5	22.5	22.5
RM999.1	112.5	112.5	135.0	135.0	112.5	112.5	112.5	112.5	135.0	135.0	135.0	135.0	112.5	135.0	135.0	112.5	112.5	112.5	112.5	135.0	135.0	135.0	112.5	112.5	112.5	135.0	135.0	135.0	135.0	45.0
RM999.4	112.5	0.0	0.0	0.0	0.0	0.0	0.0	0.0	0.0	0.0	0.0	0.0	0.0	0.0	0.0	0.0	0.0	0.0	0.0	0.0	0.0	0.0	0.0	0.0	0.0	0.0	0.0	0.0	0.0	0.0
RM999.7	112.5	0.0	0.0	0.0	0.0	0.0	0.0	0.0	0.0	0.0	0.0	0.0	112.5	0.0	0.0	0.0	0.0	0.0	0.0	0.0	0.0	0.0	135.0	135.0	135.0	0.0	0.0	0.0	0.0	0.0
RM1000.1	112.5	135.0	135.0	135.0	135.0	135.0	112.5	135.0	135.0	135.0	135.0	135.0	112.5	135.0	135.0	135.0	135.0	135.0	112.5	135.0	135.0	135.0	135.0	135.0	135.0	135.0	135.0	135.0	135.0	135.0
RM1000.5	112.5	135.0	157.5	157.5	157.5	157.5	112.5	135.0	0.0	0.0	0.0	0.0	112.5	135.0	135.0	135.0	135.0	135.0	112.5	157.5	157.5	157.5	157.5	157.5	135.0	157.5	157.5	157.5	157.5	157.5
RM1000.8	315.0	315.0	315.0	315.0	315.0	315.0	315.0	315.0	315.0	315.0	315.0	315.0	315.0	315.0	315.0	315.0	315.0	315.0	315.0	315.0	315.0	315.0	315.0	315.0	315.0	315.0	315.0	315.0	315.0	315.0
RM1001.2	315.0	315.0	315.0	315.0	315.0	315.0	315.0	315.0	315.0	315.0	315.0	315.0	315.0	315.0	315.0	315.0	315.0	315.0	315.0	315.0	315.0	315.0	315.0	315.0	315.0	315.0	315.0	315.0	315.0	315.0
RM1017.9	292.5	292.5	292.5	292.5	292.5	292.5	292.5	292.5	292.5	292.5	292.5	292.5	292.5	292.5	292.5	292.5	292.5	292.5	315.0	292.5	292.5	292.5	292.5	292.5	292.5	292.5	292.5	292.5	292.5	292.5

Appendix H: Ice Force Maps

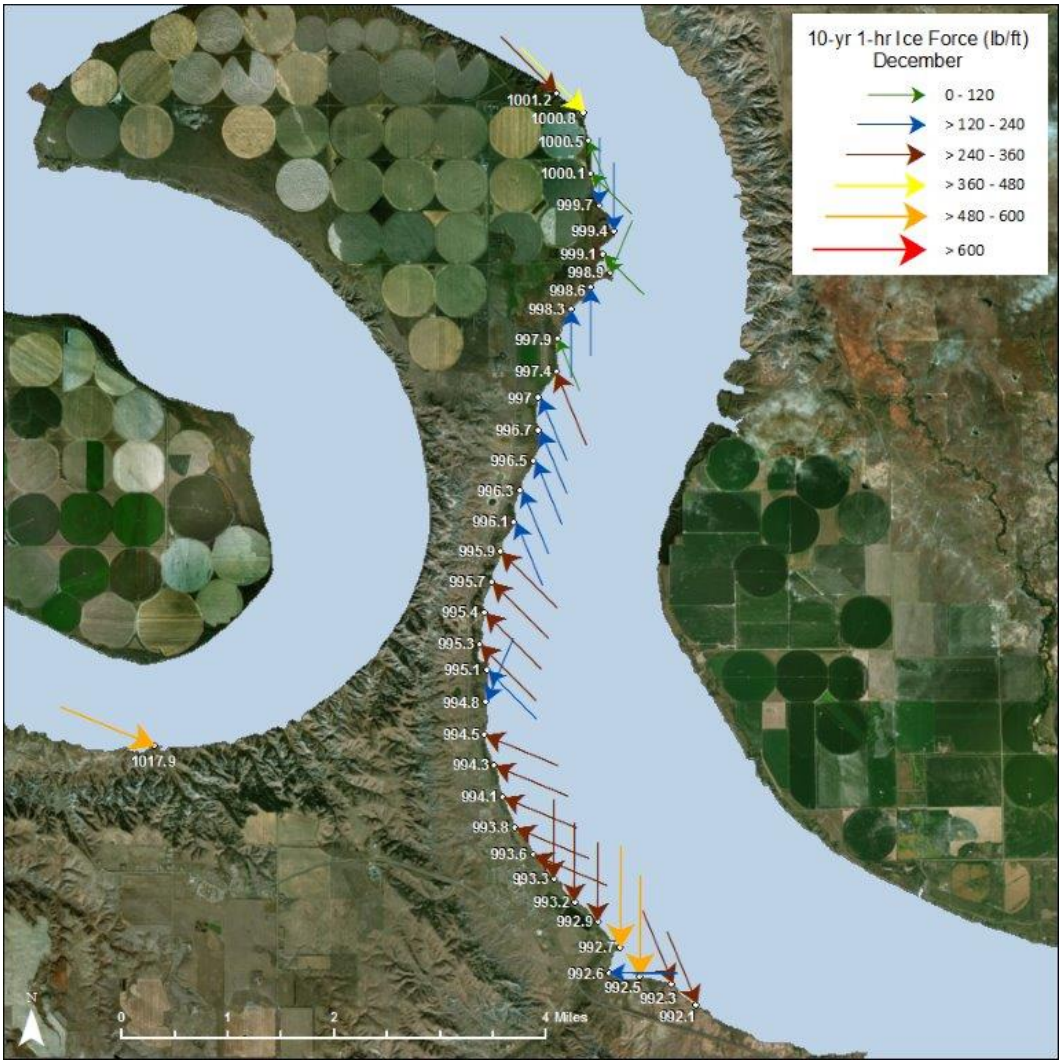

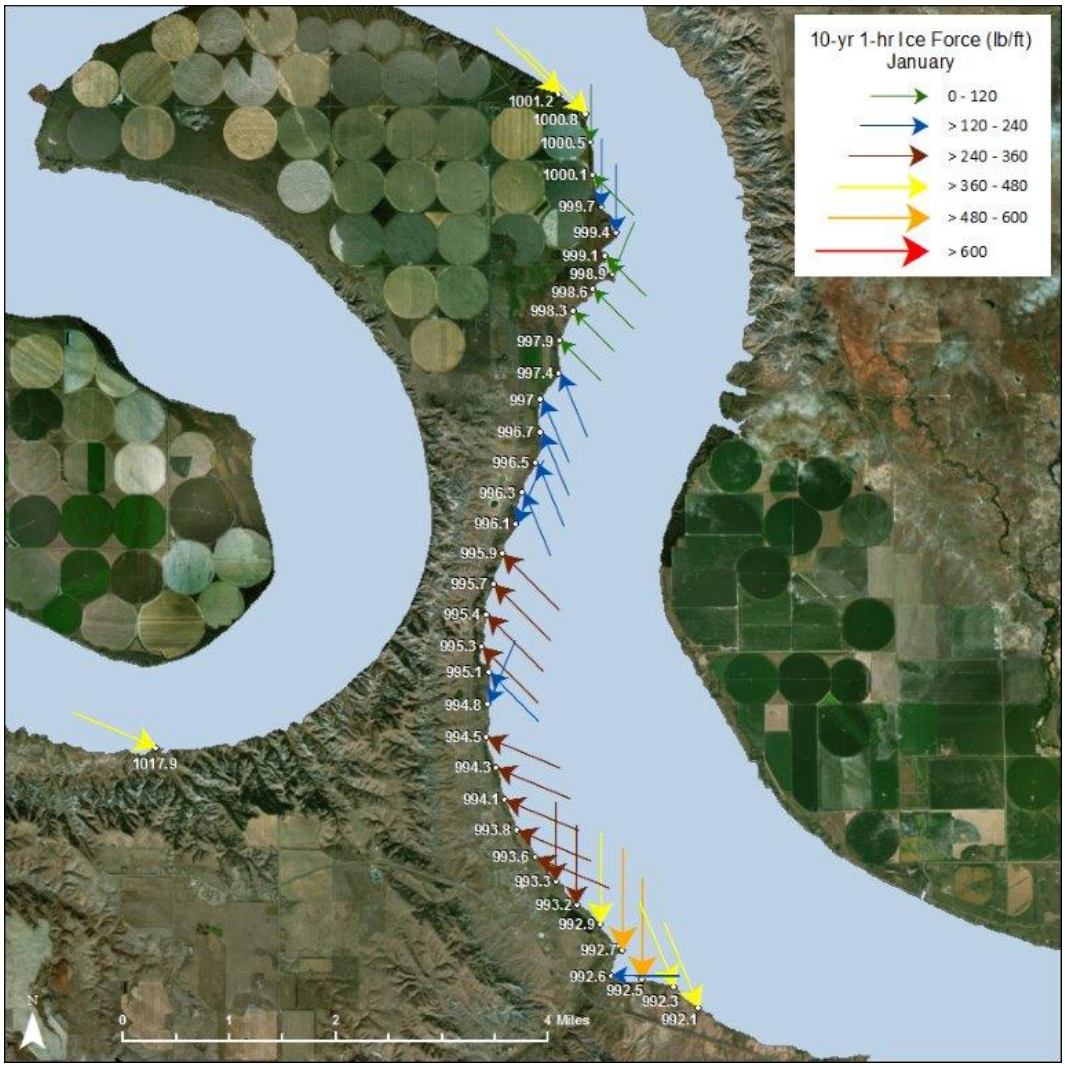
10-yr 1-hr Ice Force (lb/ft)
January
0 - 120
> 120 - 240
> 240 - 360
> 360 - 480
> 480 - 600
> 600
1001.2
1000.8
1000.5
1000.1
999.7
999.4
999.1
998.9
998.6
998.3
997.9
997.4
997
996.7
996.5
996.3
996.1
995.9
995.7
995.4
995.3
995.1
994.8
994.5
994.3
994.1
993.8
993.6
993.3
993.2
992.9
992.7
992.6
992.5
992.3
992.1
1017.9
N
0
1
2
4 Miles

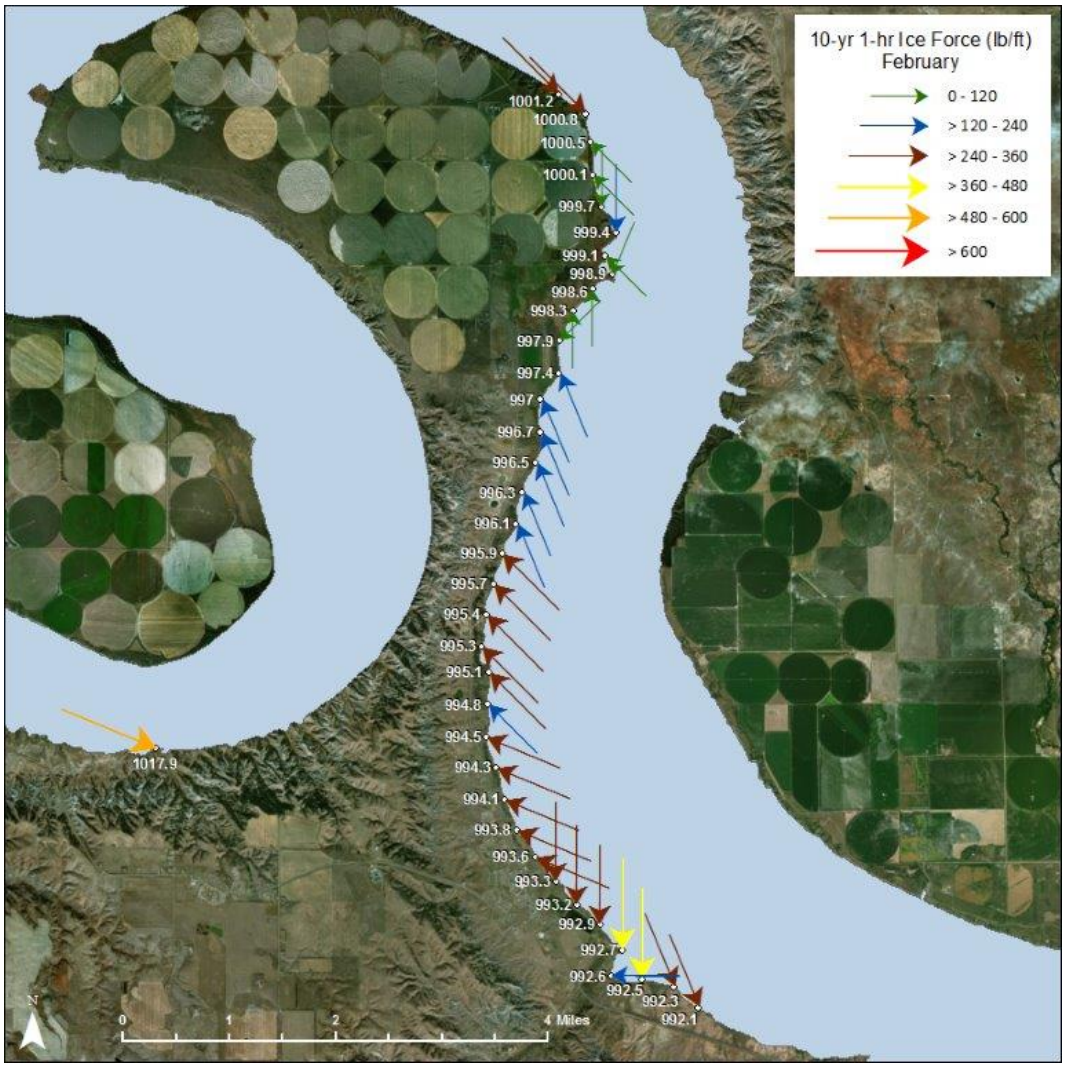
10-yr 1-hr Ice Force (lb/ft)
February
0 - 120
> 120 - 240
> 240 - 360
> 360 - 480
> 480 - 600
> 600
1001.2
1000.8
1000.5
1000.1
999.7
999.4
999.1
998.9
998.6
998.3
997.9
997.4
997
996.7
996.5
996.3
996.1
995.9
995.7
995.4
995.3
995.1
994.8
994.5
994.3
994.1
993.8
993.6
993.3
993.2
992.9
992.7
992.6
992.5
992.3
992.1
1017.9
N
0
1
2
4 Miles

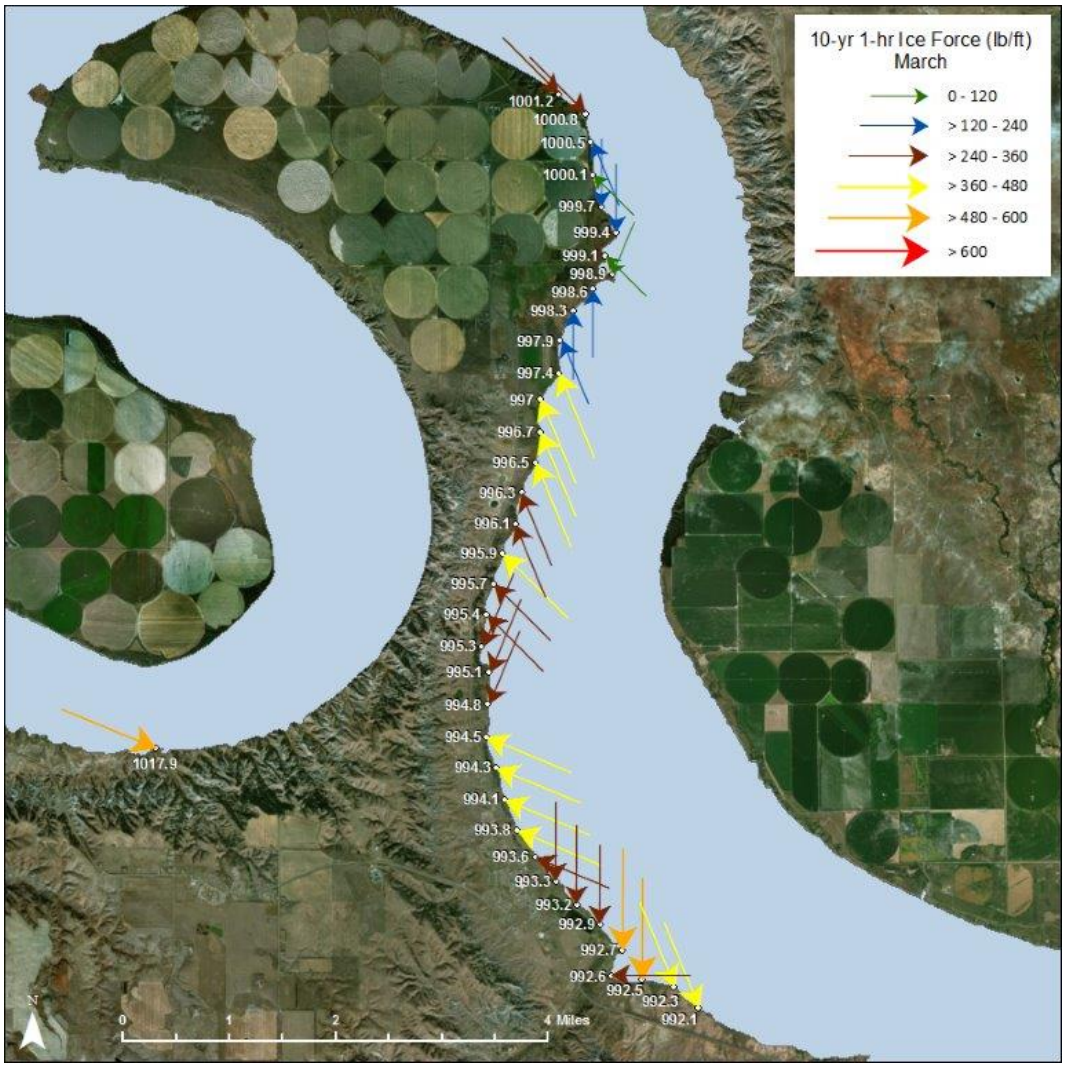
10-yr 1-hr Ice Force (lb/ft)
March
0 - 120
> 120 - 240
> 240 - 360
> 360 - 480
> 480 - 600
> 600
1001.2
1000.8
1000.5
1000.1
999.7
999.4
999.1
998.9
998.6
998.3
997.9
997.4
997
996.7
996.5
996.3
996.1
995.9
995.7
995.4
995.3
995.1
994.8
994.5
994.3
994.1
993.8
993.6
993.3
993.2
992.9
992.7
992.6
992.5
992.3
992.1
1017.9
N
0
1
2
4 Miles

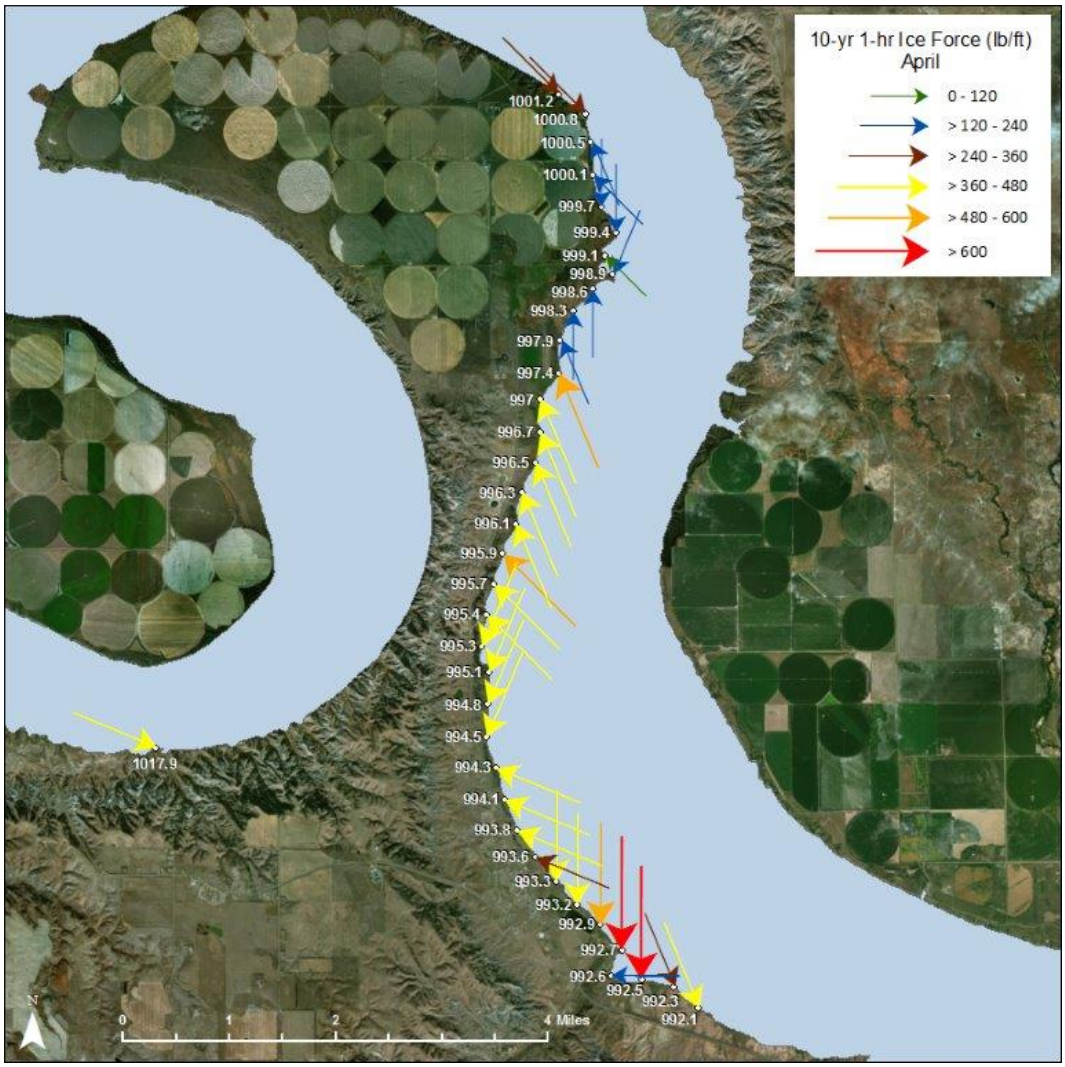
10-yr 1-hr Ice Force (lb/ft)
April
0 - 120
> 120 - 240
> 240 - 360
> 360 - 480
> 480 - 600
> 600
1001.2
1000.8
1000.5
1000.1
999.7
999.4
999.1
998.9
998.6
998.3
997.9
997.4
997
996.7
996.5
996.3
996.1
995.9
995.7
995.4
995.3
995.1
994.8
994.5
994.3
994.1
993.8
993.6
993.3
993.2
992.9
992.7
992.6
992.5
992.3
992.1
1017.9
N
0
1
2
4 Miles

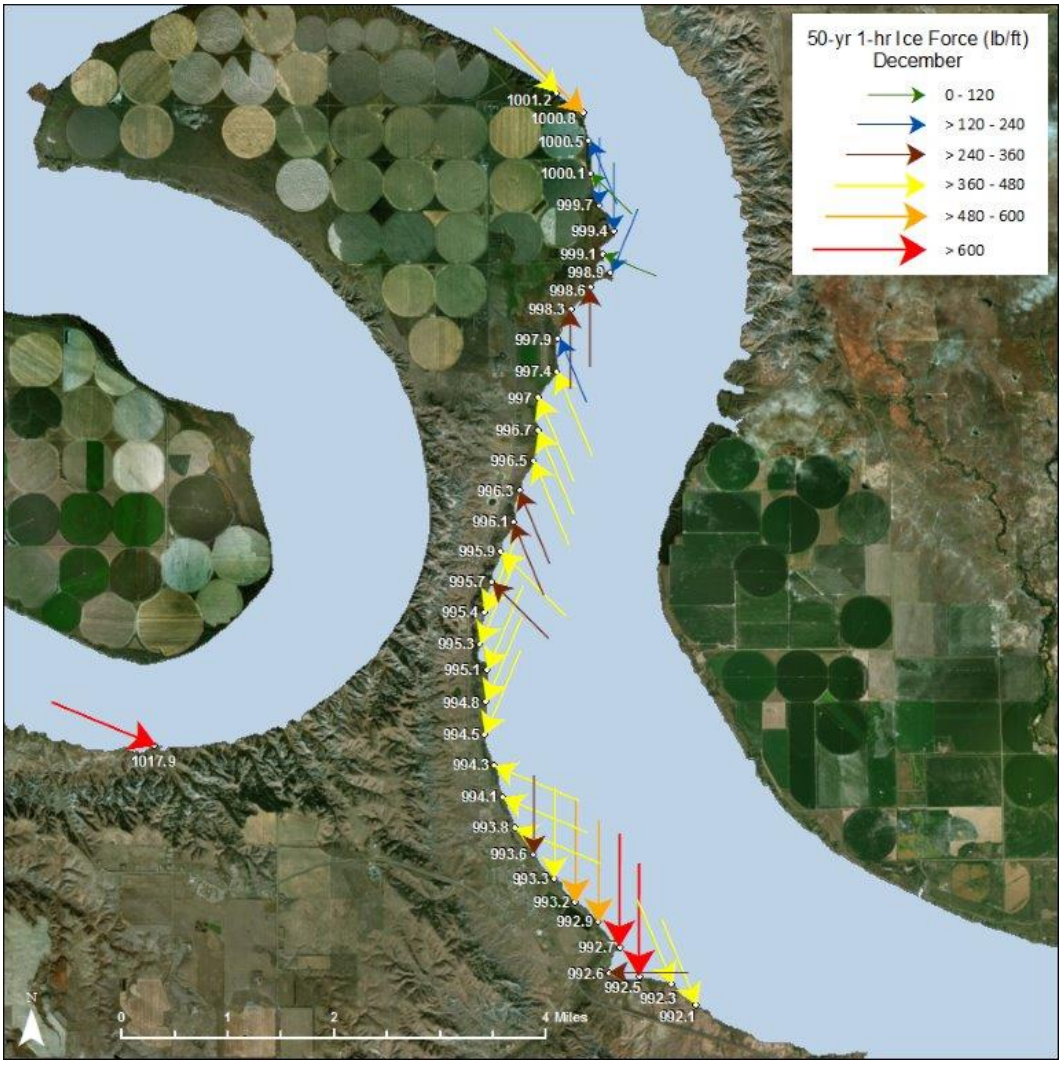
50-yr 1-hr Ice Force (lb/ft)
December
0 - 120
> 120 - 240
> 240 - 360
> 360 - 480
> 480 - 600
> 600
1001.2
1000.8
1000.5
1000.1
999.7
999.4
999.1
998.9
998.6
998.3
997.9
997.4
997
996.7
996.5
996.3
996.1
995.9
995.7
995.4
995.3
995.1
994.8
994.5
994.3
994.1
993.8
993.6
993.3
993.2
992.9
992.7
992.6
992.5
992.3
992.1
1017.9
N
0
1
2
4 Miles

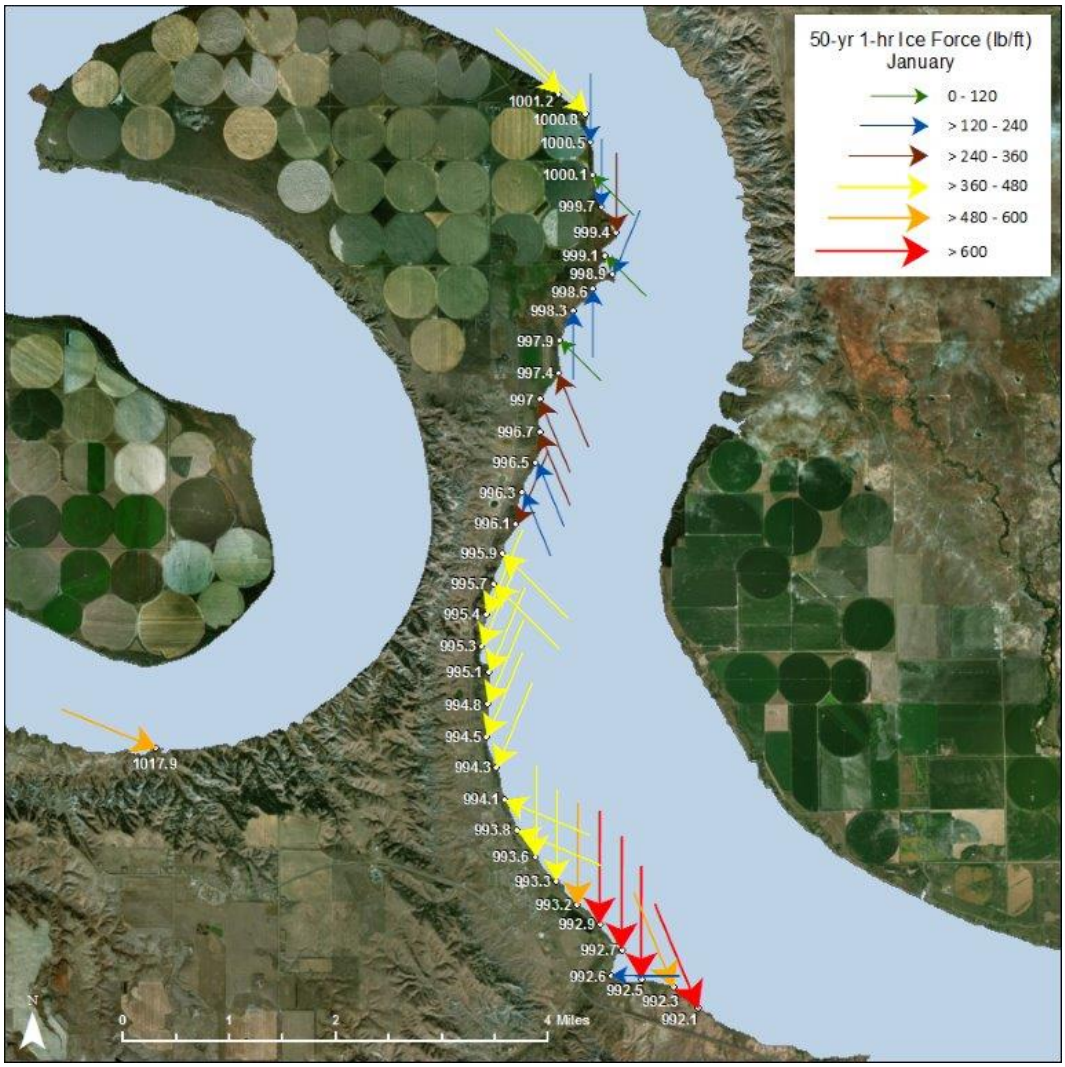
50-yr 1-hr Ice Force (lb/ft)
January
0 - 120
> 120 - 240
> 240 - 360
> 360 - 480
> 480 - 600
> 600
1001.2
1000.8
1000.5
1000.1
999.7
999.4
999.1
998.9
998.6
998.3
997.9
997.4
997
996.7
996.5
996.3
996.1
995.9
995.7
995.4
995.3
995.1
994.8
994.5
994.3
994.1
993.8
993.6
993.3
993.2
992.9
992.7
992.6
992.5
992.3
992.1
1017.9
N
0
1
2
4 Miles

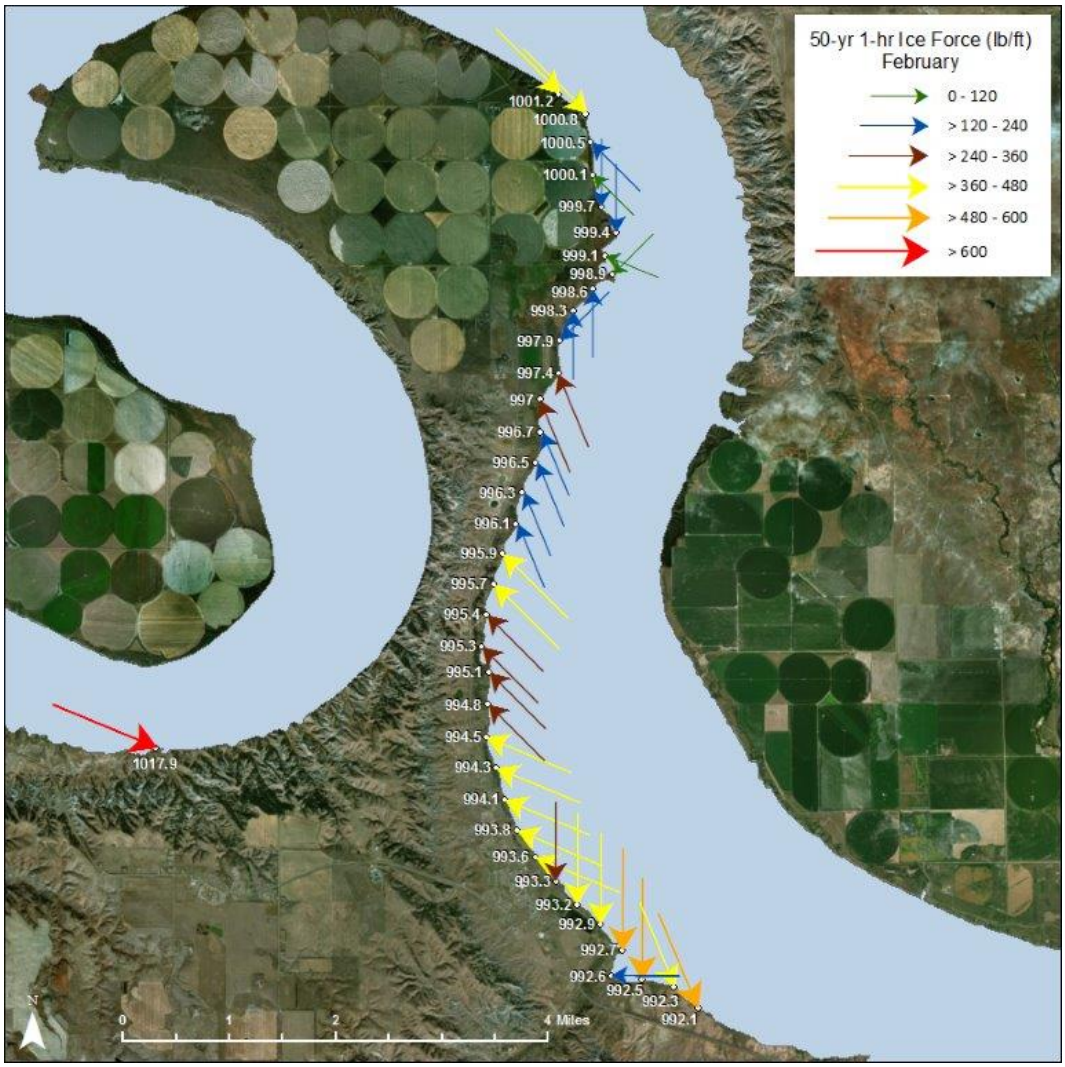
50-yr 1-hr Ice Force (lb/ft)
February
0 - 120
> 120 - 240
> 240 - 360
> 360 - 480
> 480 - 600
> 600
1001.2
1000.8
1000.5
1000.1
999.7
999.4
999.1
998.9
998.6
998.3
997.9
997.4
997
996.7
996.5
996.3
996.1
995.9
995.7
995.4
995.3
995.1
994.8
994.5
994.3
994.1
993.8
993.6
993.3
993.2
992.9
992.7
992.6
992.5
992.3
992.1
1017.9
N
0
1
2
4 Miles

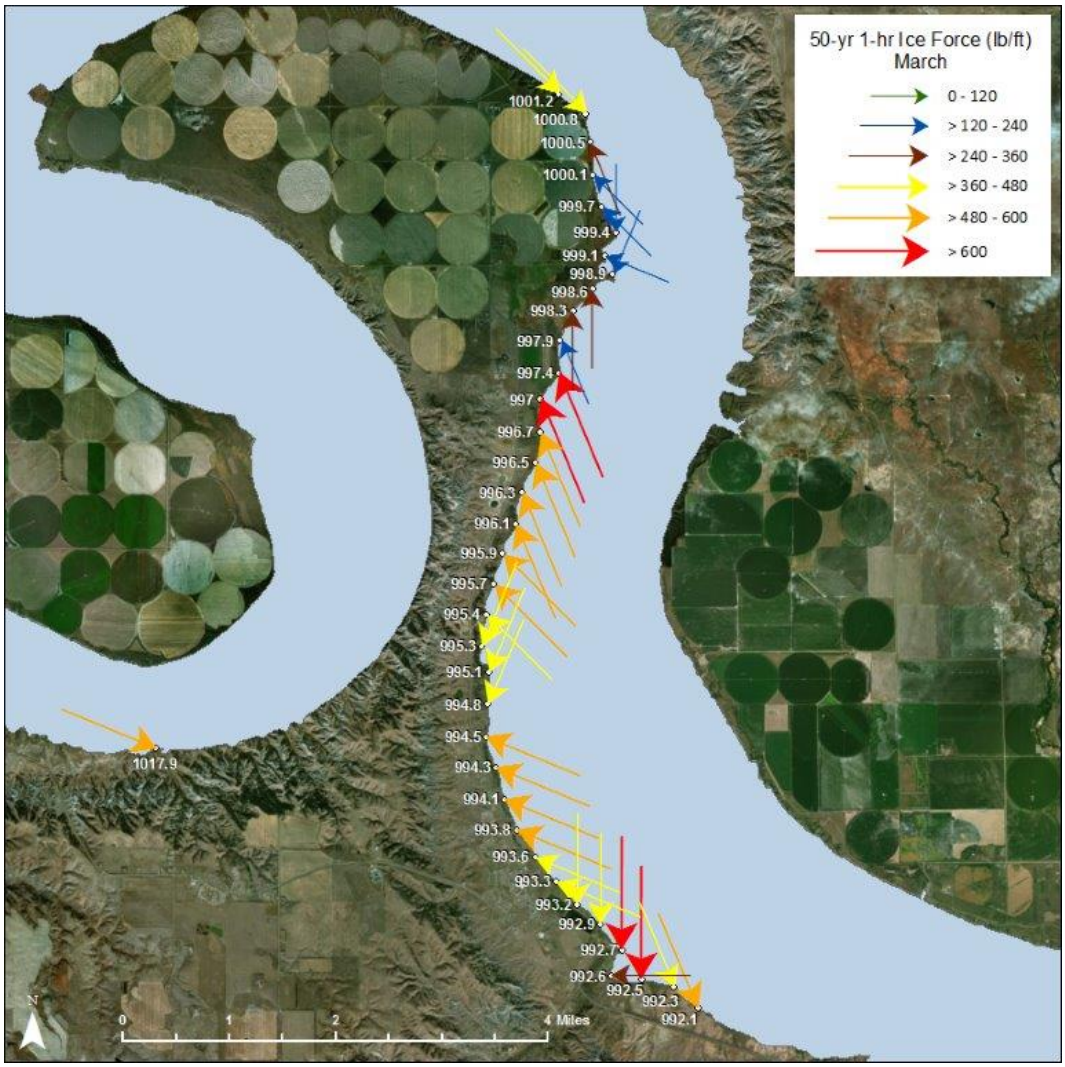
50-yr 1-hr Ice Force (lb/ft)
March
0 - 120
> 120 - 240
> 240 - 360
> 360 - 480
> 480 - 600
> 600
1001.2
1000.8
1000.5
1000.1
999.7
999.4
999.1
998.9
998.6
998.3
997.9
997.4
997
996.7
996.5
996.3
996.1
995.9
995.7
995.4
995.3
995.1
994.8
994.5
994.3
994.1
993.8
993.6
993.3
993.2
992.9
992.7
992.6
992.5
992.3
992.1
1017.9
N
0
1
2
4 Miles

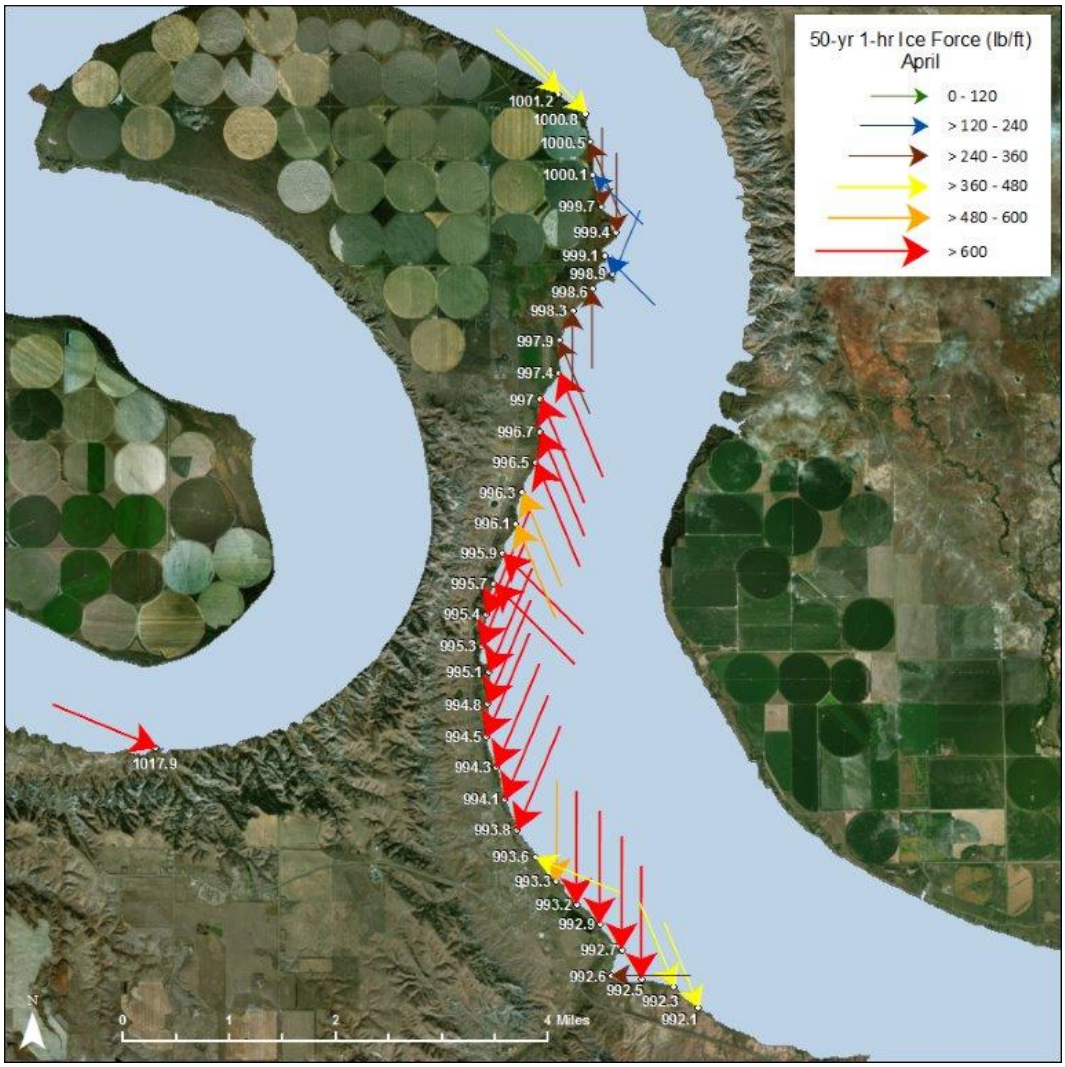
50-yr 1-hr Ice Force (lb/ft)
April
0 - 120
> 120 - 240
> 240 - 360
> 360 - 480
> 480 - 600
> 600
1001.2
1000.8
1000.5
1000.1
999.7
999.4
999.1
998.9
998.6
998.3
997.9
997.4
997
996.7
996.5
996.3
996.1
995.9
995.7
995.4
995.3
995.1
994.8
994.5
994.3
994.1
993.8
993.6
993.3
993.2
992.9
992.7
992.6
992.5
992.3
992.1
1017.9
N
0
1
2
4 Miles

REPORT DOCUMENTATION PAGE

Form Approved
OMB No. 0704-0188

1. REPORT DATE *(DD-MM-YYYY)*	2. REPORT TYPE	3. DATES COVERED *(From - To)*
July 2018	Technical Report/Final	

4. TITLE AND SUBTITLE

Ice Forces along the Missouri River Shoreline of the Lower Brule Sioux Tribe Lands

5a. CONTRACT NUMBER

5b. GRANT NUMBER
3121

5c. PROGRAM ELEMENT NUMBER

6. AUTHOR(S)

Jeremy Giovando, Robert B. Haehnel, Timothy Baldwin, and Steven F. Daly

5d. PROJECT NUMBER

5e. TASK NUMBER

5f. WORK UNIT NUMBER

7. PERFORMING ORGANIZATION NAME(S) AND ADDRESS(ES)

U.S. Army Engineer Research and Development Center (ERDC)
Cold Regions Research and Engineering Laboratory (CRREL)
72 Lyme Road
Hanover, NH 03755-1290

8. PERFORMING ORGANIZATION REPORT NUMBER

ERDC/CRREL TR-18-12

9. SPONSORING / MONITORING AGENCY NAME(S) AND ADDRESS(ES)

U.S. Army Corps of Engineers, Omaha District
1616 Capitol Ave., Ste. 9000
Omaha, NE 68102

10. SPONSOR/MONITOR'S ACRONYM(S)
USACE

11. SPONSOR/MONITOR'S REPORT NUMBER(S)

12. DISTRIBUTION / AVAILABILITY STATEMENT
Approved for public release; distribution is unlimited.

13. SUPPLEMENTARY NOTES

14. ABSTRACT

Significant erosion along Lake Sharpe reservoir has occurred since the reservoir was formed in the 1960s. A major contributor to the shoreline erosion is ice shove, which is most severe when thick ice cover on the reservoir is combined with large wind events. One of the areas of highest concern for erosion induced by ice shove is located on the Lower Brule Sioux Reservation in South Dakota. Critical infrastructure is at risk for the Lower Brule Sioux Tribe as continual erosion occurs. This analysis estimates the ice shove forces due to wind and the water current along 10 miles of shoreline adjacent to the reservation. Additionally, this report discusses shoreline erosion mitigation measures.

15. SUBJECT TERMS
Ice on rivers, lakes, etc--Missouri River; Erosion--Lower Brule Sioux Tribe of the Lower Brule Reservation, South Dakota; Shorelines--Sharpe, Lake (S.D.); Ice shoves

16. SECURITY CLASSIFICATION OF:			17. LIMITATION OF ABSTRACT	18. NUMBER OF PAGES	19a. NAME OF RESPONSIBLE PERSON
a. REPORT	b. ABSTRACT	c. THIS PAGE			19b. TELEPHONE NUMBER *(include area code)*
Unclassified	Unclassified	Unclassified	SAR	95	